NATIONAL TECHNICAL UNIVERSITY OF ATHENS (NTUA)
SCHOOL OF MECHANICAL ENGINEERING
PARALLEL CFD & OPTIMIZATION UNIT (PCOpt/NTUA)

Multi-Disciplinary Analysis & Optimisation

Dr. Kyriakos C. Giannakoglou, Professor NTUA

Dr. Varvara Asouti, Adjunct Lecturer NTUA

Contributors:

Dr. X. Trompoukis

Dr. M. Kontou

Dr. M. Monfaredi

Dr. K. Gkaragkounis

D. Pallas

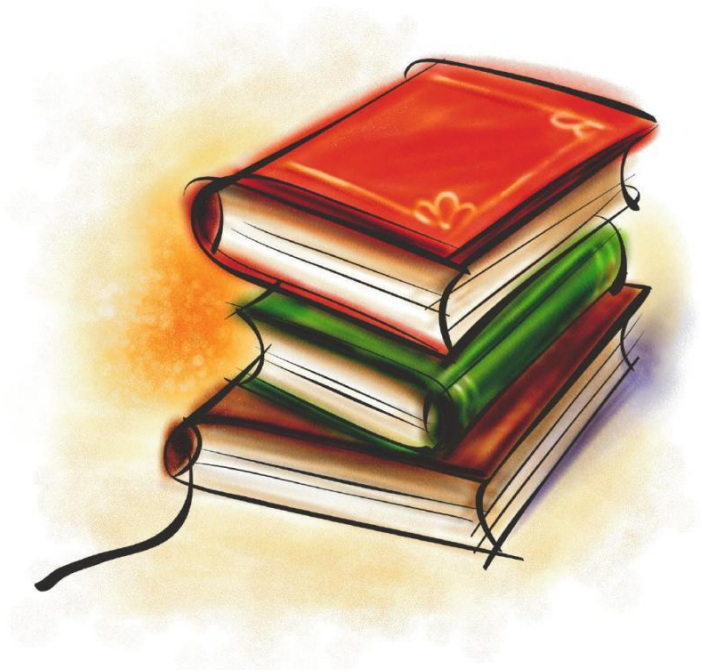

Introduction

Prof. K.C. Giannakoglou, kgianna@mail.ntua.gr, Dr. V.G. Asouti, vasouti@mail.ntua.gr

Introduction

Why Multi-Disciplinary Analysis and Optimisation?

- ✓ **Most real-world / engineering systems involve several disciplines:**
  - **Aircraft (aerodynamics, propulsion, structures, etc.).**
  - **Car (aerodynamics, structures, electrochemistry, etc.).**
  - **Wind turbines (aerodynamics, structures, acoustics, etc.).**

- ✓ **Computing the overall system performance requires the coupled analysis of all sub-systems; Multi-Disciplinary Analysis (MDA).**

- ✓ **Multi-Disciplinary Optimisation (MDO):**
  - **Avoid the difficulties and local optimal solutions of sequentially/iteratively optimising each discipline.**

MDA/MDO- Examples

- ✓ Aerostructural Analysis (aerodynamic loading and structural deformation; CFD – CSM models):
  - Aircraft wings, fuselage, empennage.
  - Wind, hydraulic turbines (hydrostructural analysis).
  - etc.
- ✓ Aeroacoustic Analysis (flow-induced noise, i.e. sound generated from a body inside a fluid flow; CFD – acoustic models):
  - Aircraft engine, airframe noise.
  - Wind turbines noise.
  - Automotive noise.
- ✓ Aerothermal Analysis (CFD – Heat Conduction models):
  - Thermal turbomachines.
  - Heat exchangers.
  - etc.
- ✓ CFD – electrochemical models:
  - Proton-Exchange Membrane Fuel Cells.
  - Redox Batteries.
  - etc.

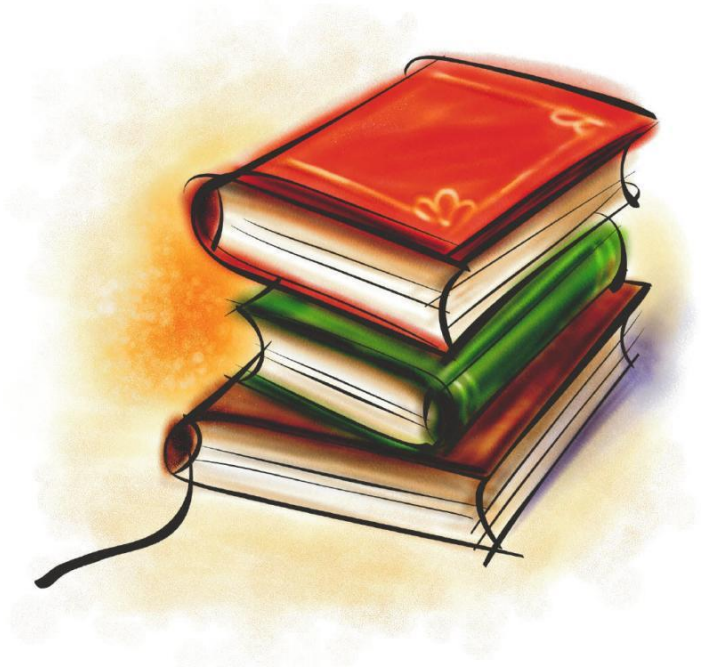

MDA/MDO Architectures

Prof. K.C. Giannakoglou, kgianna@mail.ntua.gr, Dr. V.G. Asouti, vasouti@mail.ntua.gr

MDO Architectures

MDO architecture: The way of organising numerical analysis models from different disciplines, as well as the optimisation algorithm.

- **Monolithic Architectures**
- **Distributed (or Bi-level) Architectures**

eXtended Design Structure Matrix (XDSM)

System components are placed on the main diagonal of a matrix.

Inputs to each component placed in the same column and the outputs from each component placed in the same row.

External inputs and outputs (if any) are placed on the outside edges of the diagram.

Shapes as in flowchart syntax, i.e. rectangles for processes, parallelograms for data input and output, etc.

The numbering system (1, 2, 3...) indicates the order of execution, with lines depicting the flow path

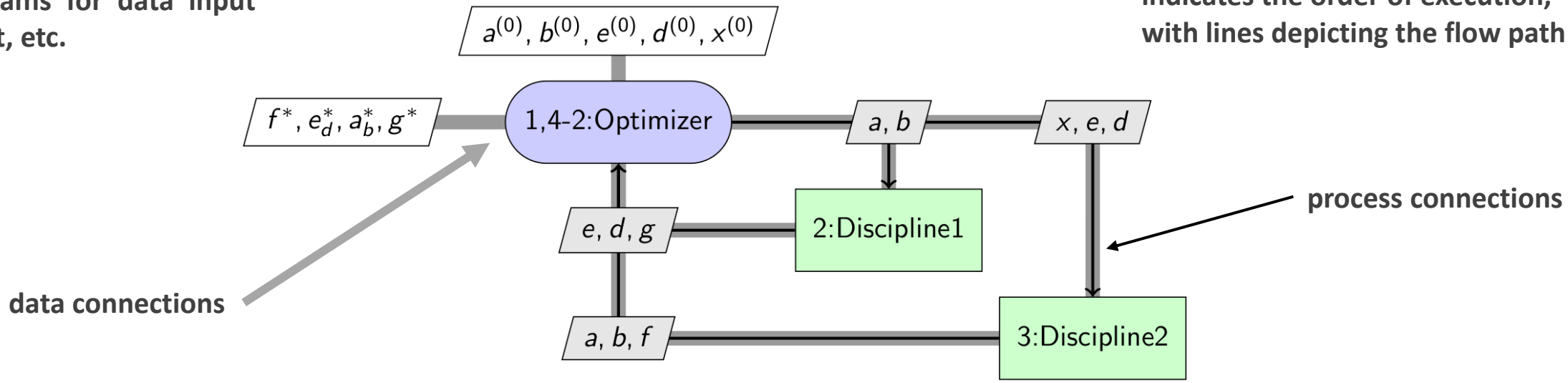

J.R.R.A. Martins, A. Ning. Engineering Design Optimization. Cambridge University Press; 2021.

XDSM Example - Sellar's Problem

Min.

$$f = x^2 + z_2 + y_1 + e^{-y_2}$$

subject to

$$g_1 = 3.16 - y_1 \leq 0$$
$$g_2 = y_2 - 24 \leq 0$$

Disciplinary eqs.

$$y_1 = z_1^2 + z_2 + x - 0.2y_2$$
$$y_2 = \sqrt{y_1} + z_1 + z_2$$

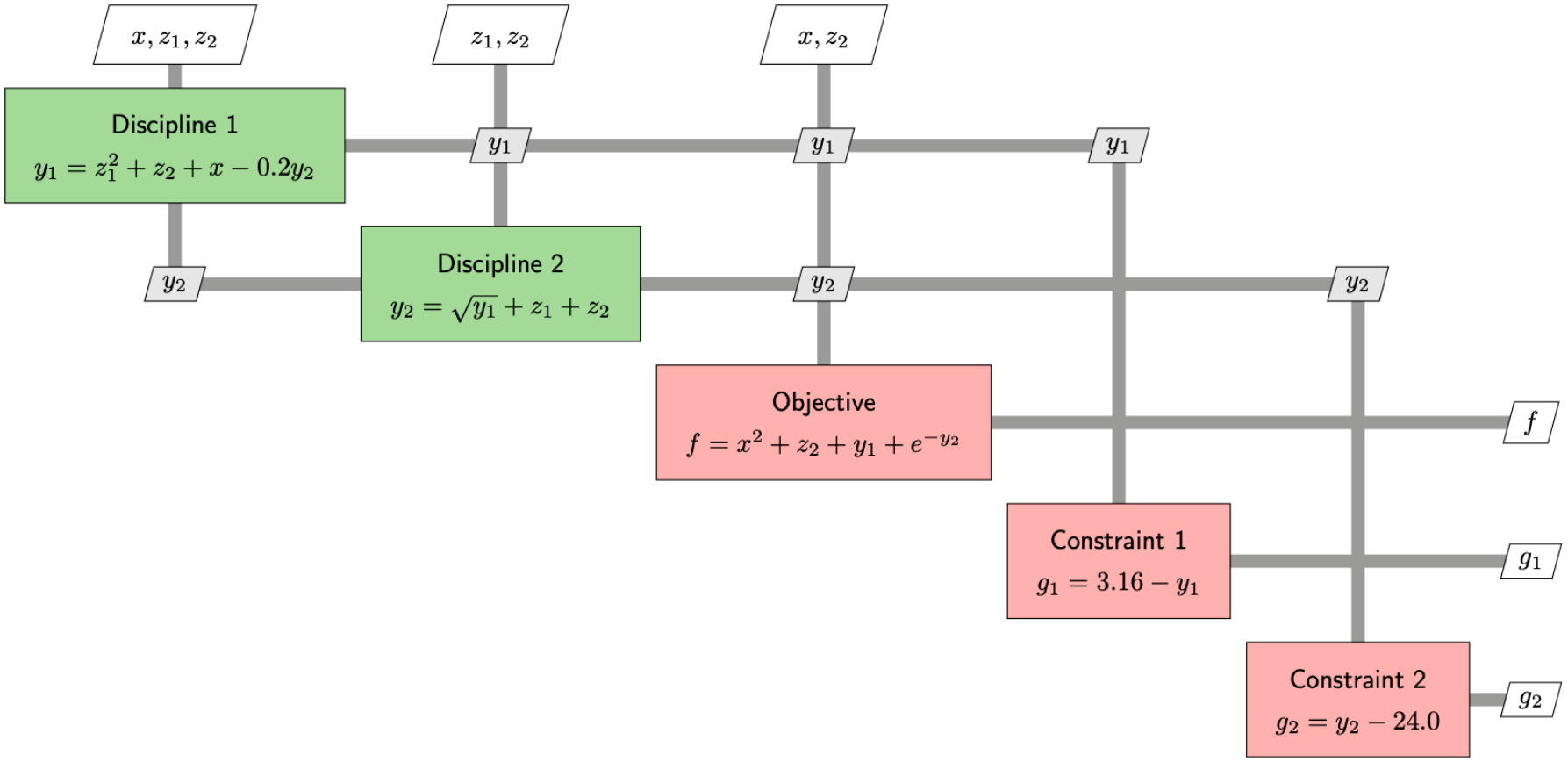

Design variables:

z_1, z_2 **(shared) and** x **(local)**

Coupling/output variables:

y_1, y_2

Monolithic MDO Architectures (1/3)

Solve the MDO problem by casting it as a single (centralised) optimisation problem which simultaneously considers all disciplines, design variables and constraints.

All-at-Once (AAO) and/or Simultaneous Analysis and Design (SAND): The optimiser controls all variables. Residuals of the disciplinary eqs. are imposed as (equality) constraints.

- **Increased problem size; all state variables and disciplinary equations on board.**
- **Premature termination of the optimiser may result in an infeasible solution.**
- **Residuals of the disciplinary eqs. must be available to the optimiser; not the case in 'black-box' s/w.**

Min. $f = x^2 + z_2 + y_1 + e^{-y_2}$

with respect to x, z_1, z_2, y_1, y_2

subject to
$$g_1 = 3.16 - y_1 \leq 0$$
$$g_2 = y_2 - 24 \leq 0$$
$$R_1 = y_1 - (z_1^2 + z_2 + x - 0.2y_2) = 0$$
$$R_2 = y_2 - (\sqrt{y_1} + z_1 + z_2) = 0$$

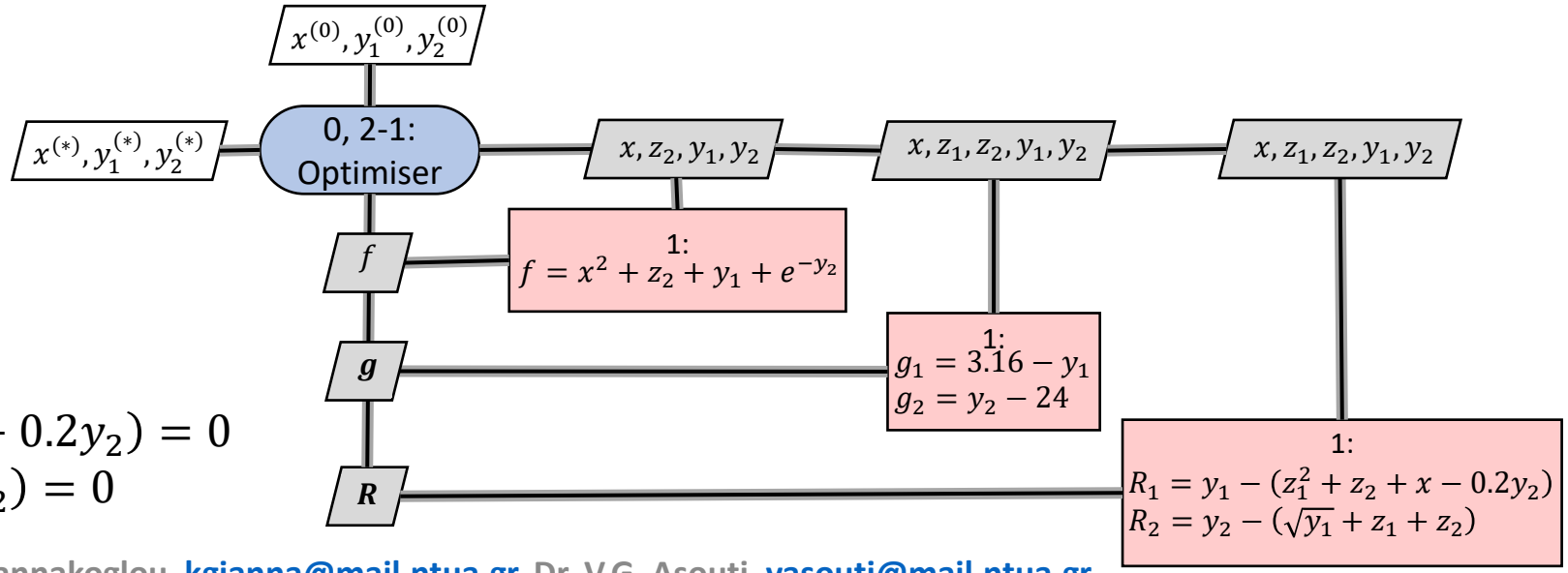

Monolithic MDO Architectures (2/3)

Individual Discipline Feasible (IDF): Coupling variables are set as (consistency) constraints to the optimiser.

- **+ Disciplines can be simulated in parallel.**
- **- Consistency constraints guarantee the disciplines feasibility only at the end of the optimisation**
- **- With a large number of coupling variables, the problem cannot be solved efficiently.**

Min. $f = x^2 + z_2 + y_1^t + e^{-y_2^t}$

with respect to $x, z_1, z_2, y_1^t, y_2^t$ **target variables**

subject to
$$g_1 = 3.16 - y_1^t \leq 0$$
$$g_2 = y_2^t - 24 \leq 0$$

Consistency constraints
$$h_1^t = y_1^t - y_1 = 0$$
$$h_2^t = y_2^t - y_2 = 0$$

while satisfying
$$R_1 = y_1 - (z_1^2 + z_2 + x - 0.2y_2^t)$$
$$R_2 = y_2 - \left(\sqrt{y_1^t} + z_1 + z_2\right)$$

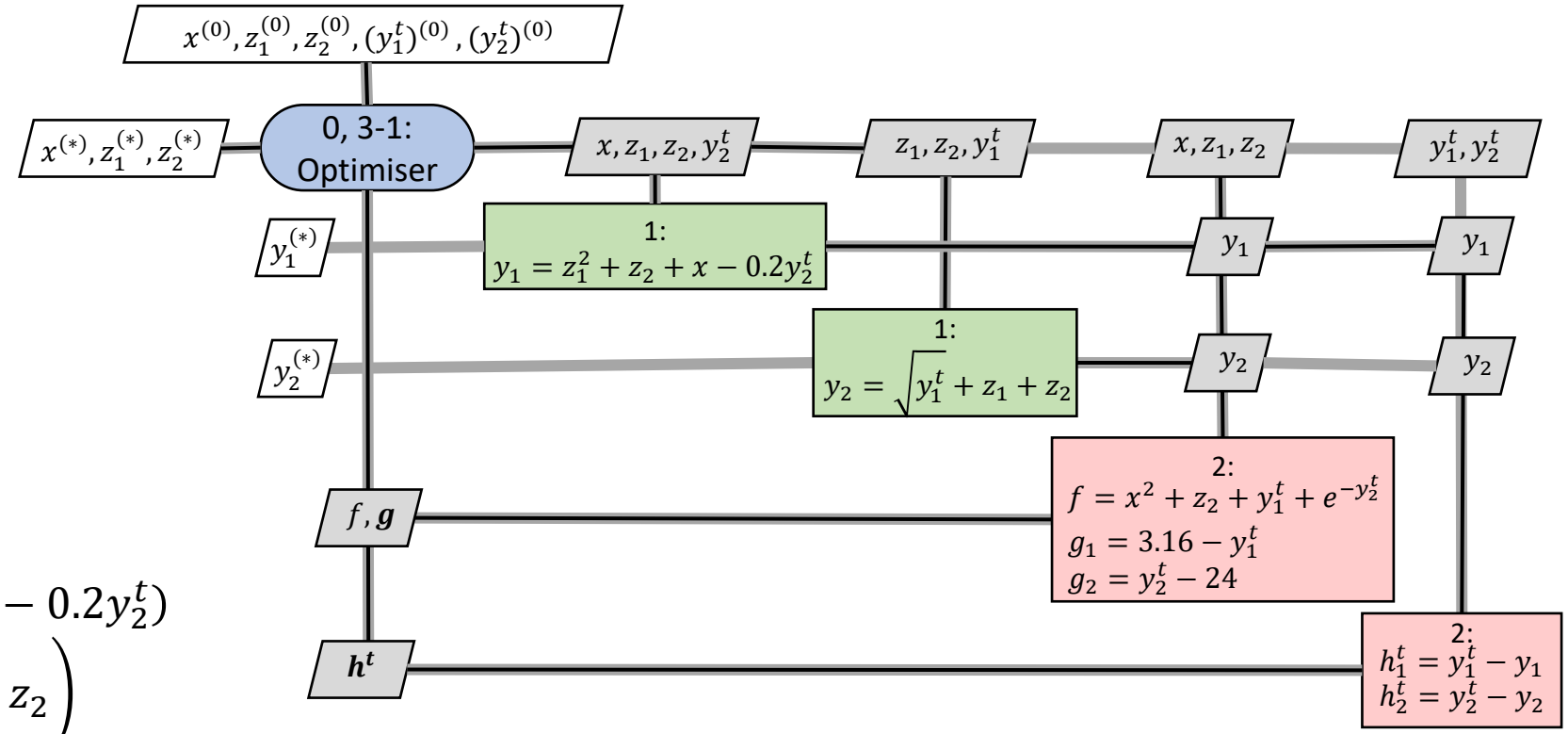

Monolithic MDO Architectures (3/3)

Multidisciplinary Feasible (MDF): A full MDA is performed during each optimisation cycle to converge the coupling variables across disciplines to their equilibrium values.

- **+ Small problem; the optimiser controls only the design variables, the objectives and constraints.**
- **+ The solution at the end of an optimisation cycle always satisfies all disciplines; MDA till convergence.**

Min. $f = x^2 + z_2 + y_1 + e^{-y_2}$

with respect to x, z_1, z_2

subject to $g_1 = 3.16 - y_1 \leq 0$

$g_2 = y_2 - 24 \leq 0$

while satisfying $R_1 = y_1 - (z_1^2 + z_2 + x - 0.2y_2)$

$R_2 = y_2 - (\sqrt{y_1} + z_1 + z_2)$

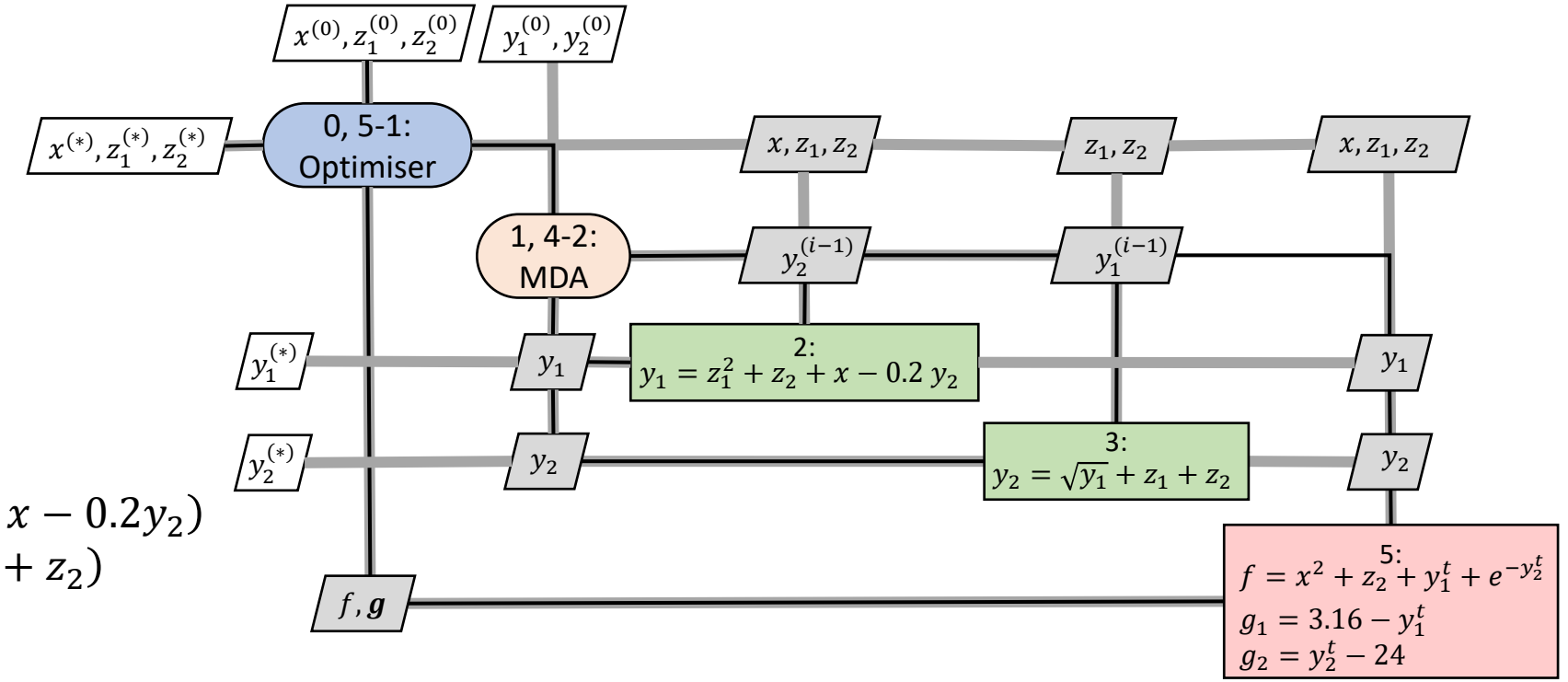

Distributed or Bi-Level MDO Architectures (1/5)

Decompose the MDO problem into a set of smaller optimisation problems (subproblems) which must be solved.

- ✓ **Distributed IDF:**
  - **Collaborative Optimisation (CO)**
- ✓ **Distributed MDF:**
  - **Bilevel Integrated System Synthesis (BLISS)**
  - **Concurrent Subspace Optimisation (CSSO)**

Distributed or Bi-Level MDO Architectures (2/5)

Collaborative Optimisation (CO): Discipline optimisation subproblems are running independent of each other by using copies of the coupling and shared variables.

- **+ Easy organisation of the MDO problem.**
- **+ The formulation is mathematically equivalent to that of IDF → equivalent to the 'original' MDO.**
- **- Poor performance; if more equality constraints than variables then the subproblem is infeasible.**
- **- Discipline feasibility is guaranteed only at the end of it.**
- **- Poor convergence of gradient-based optimisers; constraint gradients become zero at an optimal.**

Discipline1 subproblem

Min. $J_1 = \left(x^t - x\right)^2 + \left(z_{1,1}^t - z_1\right)^2 + \left(z_{2,1}^t - z_1\right)^2 + \left(y_1^t - y_1\right)^2$

w.r.t. $x, z_{1,1}^t, z_{2,1}^t$

while satisfying

$R_1 = y_1 - \left(\left(z_{1,1}^t\right)^2 + z_{2,1}^t + x - 0.2y_2^t\right) = 0$

System-level problem

Min. $f = x^2 + z_2 + y_1^t + e^{-y_2^t}$

w.r.t. $z_1, z_2, x^t, y_1^t, y_2^t$

subject to $g_1 = 3.16 - y_1^t \le 0$

$g_2 = y_2^t - 24 \le 0$

while satisfying

$J_1^* = 0$

$J_2^* = 0$

Discipline2 subproblem

Min. $J_2 = \left(z_{1,2}^t - z_1\right)^2 + \left(z_{2,2}^t - z_1\right)^2 + \left(y_2^t - y_2\right)^2$

w.r.t. $z_{1,2}^t, z_{2,2}^t$

while satisfying

$R_2 = y_2 - \left(\sqrt{y_1} + z_{1,2}^t + z_{2,2}^t\right) = 0$

Distributed or Bi-Level MDO Architectures – CO by Example (3/5)

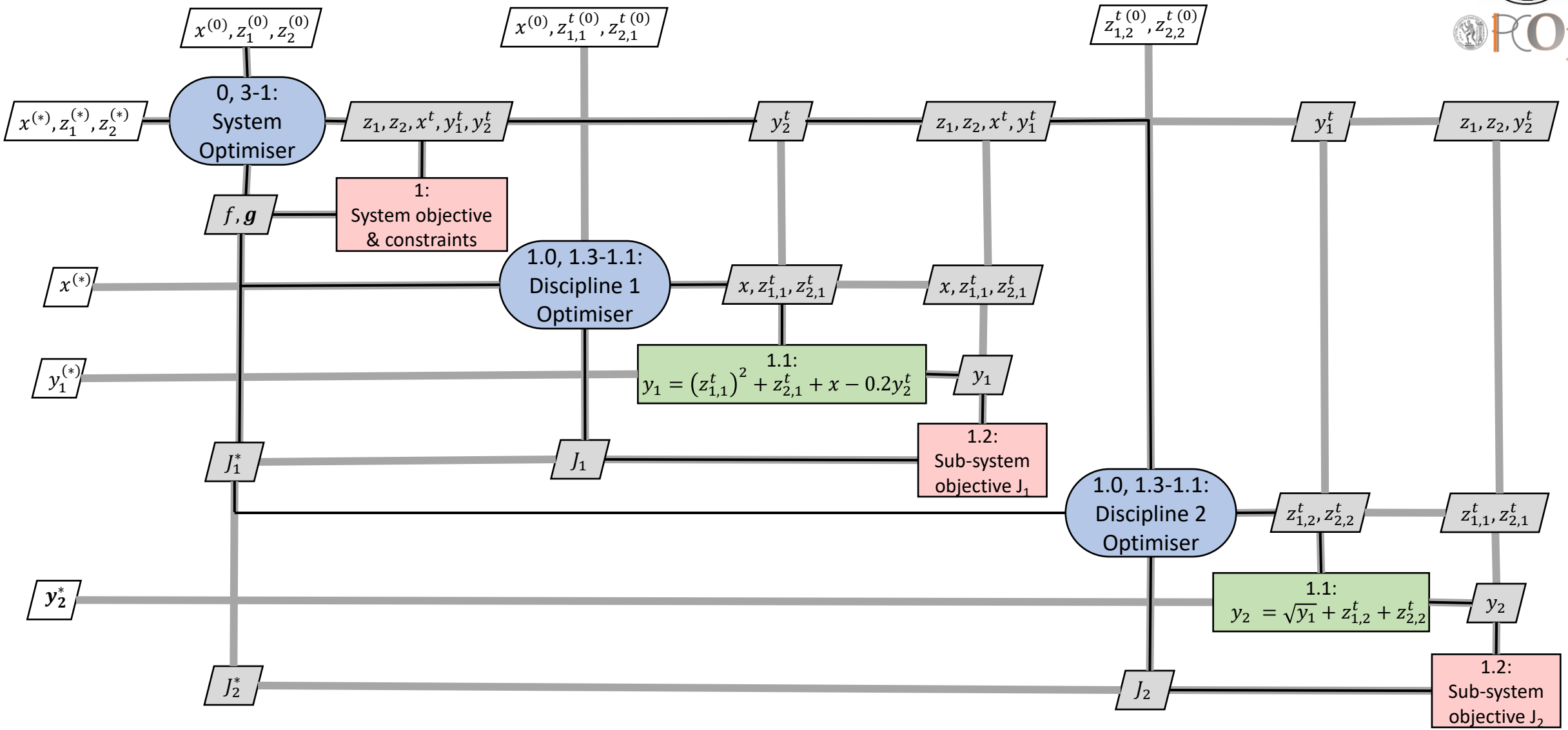

Distributed or Bi-Level MDO Architectures (4/5)

Concurrent Subspace Optimisation (CSSO): Decompose the MDO problem into independent subproblems with disjoint sets of variables, i.e. without shared variables.

- Sensitive to parameter selection. May require extensive tuning to run efficiently on large problems.

Bi-level Integrated System Synthesis (BLISS): Local design variables are assigned to discipline subproblems and shared ones to the system-level problem. At system-level, all disciplines using a series of linear approximations of the original design problem.

- MDA is required to restore the feasibility of the solution → BLISS-2000.

System-level problem

Min. $(f_0^*)_0 = \left(\frac{\partial f_0^*}{\partial z_1}\right)\Delta z_1 + \left(\frac{\partial f_0^*}{\partial z_1}\right)\Delta z_2$

w.r.t. $\Delta z_1, \Delta z_2$

subject to $(g_k^*)_0 = \left(\frac{\partial g_k^*}{\partial z_1}\right)\Delta z_1 + \left(\frac{\partial g_k^*}{\partial z_1}\right)\Delta z_2$

⇨

Discipline subproblem

Min. $(f_0)_0 = \left(\frac{\partial f_0}{\partial x}\right)\Delta x$

w.r.t. Δx

subject to $(g_k)_0 = \left(\frac{\partial g_k}{\partial x}\right)\Delta x$

Discipline subproblems are equal to the number of local design variables.

F. Torrigiani, P.D. Ciampa. MDO Architectures Comparison on Analytical Test Case and Aerostructural Aircraft System Design Problem. 6th CEAS Conference 2017.

Distributed or Bi-Level MDO Architectures – BLISS by Example (5/5)

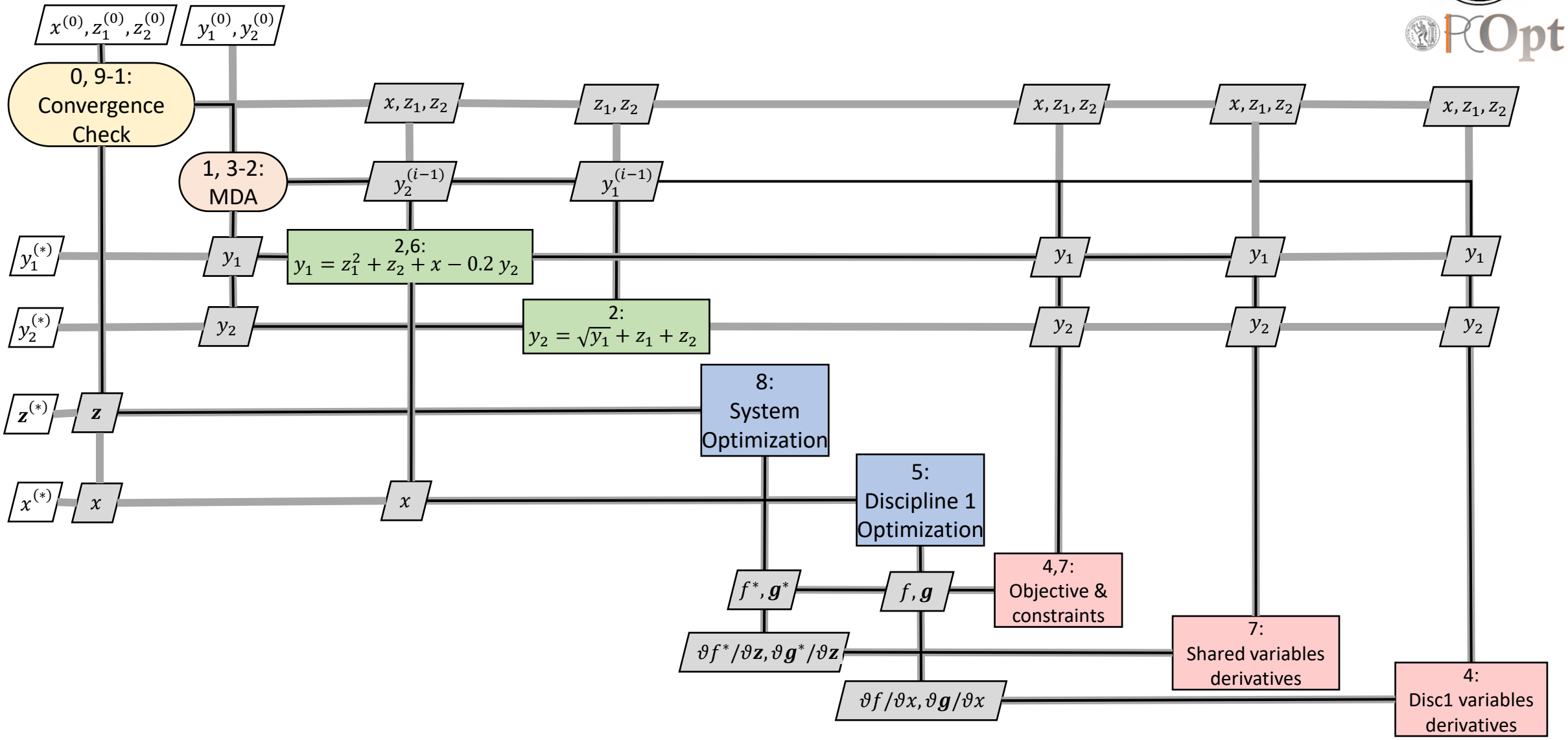

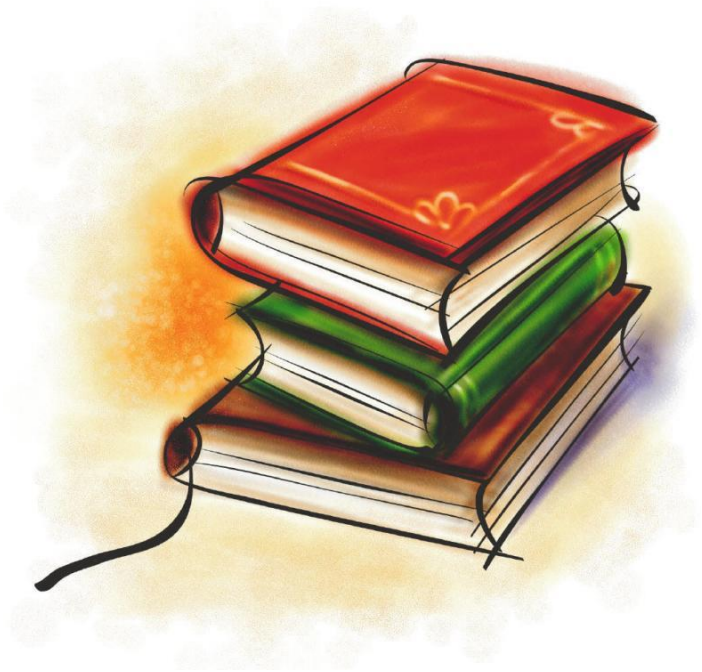

Simple MDO Examples

Sellar's Problem: MDO Architectures Performance Comparison

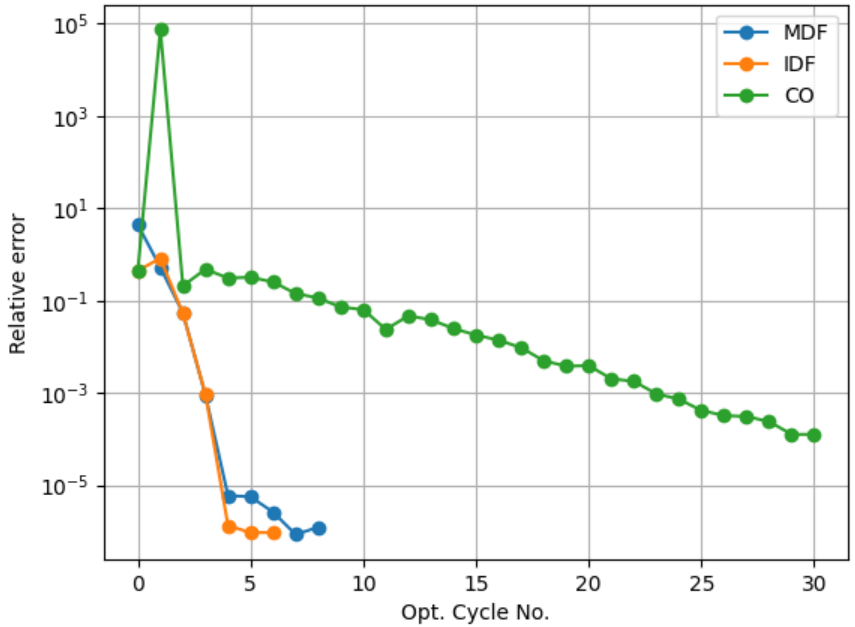

	MDF	IDF	CO
Discipline 1 evaluations	61	30	1210
Discipline 2 evaluations	53	24	601
Objective function calls	61	30	168
# Optimisation cycles	9	7	30
Objective value	3.1834	3.1834	3.233

- Both MDF and IDF are able to reach the optimal solution. MDF requires more function calls due to MDA during each optimization cycle.
- IDF is less computationally expensive compared to MDF.
- Despite a significantly larger number of function calls and optimization cycles, CO is unable to precisely reach the optimum.
- Trends are in agreement with similar comparisons in the literature.

Airfoil-Spring System (1/3)

- **Aerostructural system:**
  - **NACA-0012 airfoil at inviscid flow conditions**
  - **Torsional spring attached at quarter-chord**
- **Two discipline problem:**
  - **Aerodynamics (PUMA CFD primal & adjoint solver)**
  - **Spring (analytic equation)**
- **Airfoil parametrisation:**
  - **Volumetric NURBS**
  - **16 shape parameters**

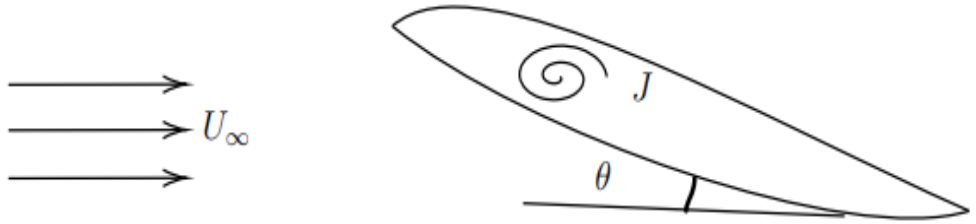

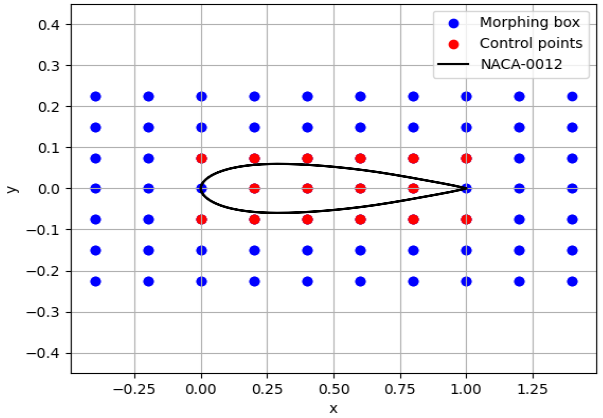

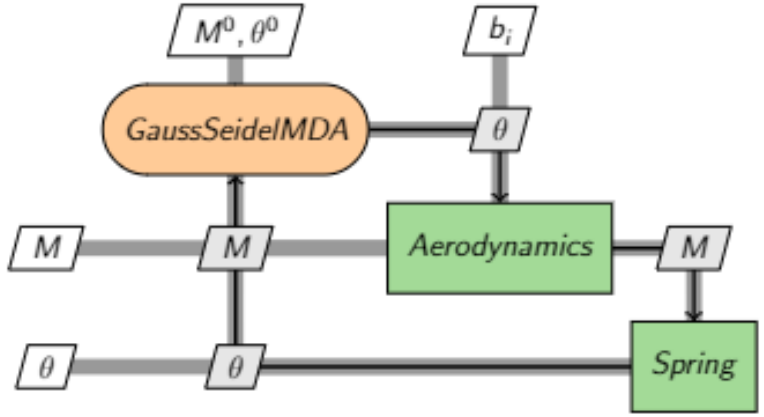

Airfoil-Spring System (2/3)

Multidisciplinary Feasible (MDF)

- **Design variables: 16 shape parameters (b_i)**
- **Solution of 2×2 linear system per cycle (coupled adjoint)**

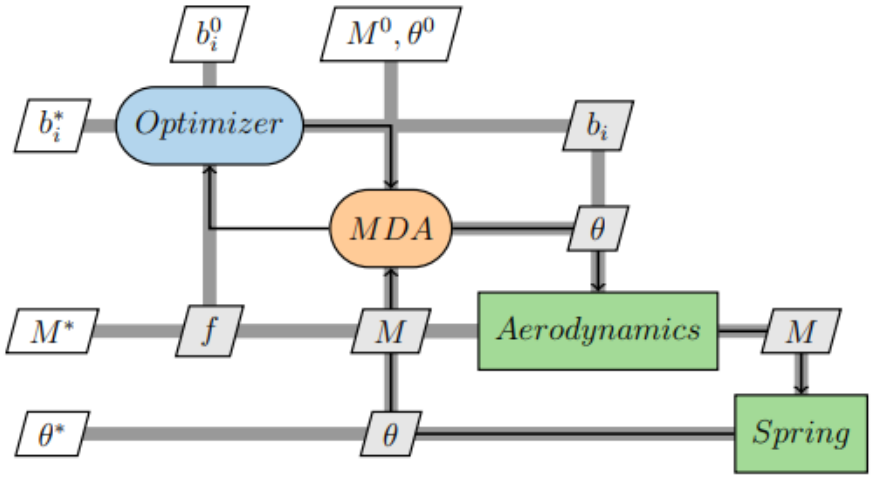

Individual Discipline Feasible (IDF)

- **Design variables: 16 shape parameters (b_i) and 2 target variables (M^t, θ^t)**
- **Consistency constraints:**

$$h_\theta^t = \theta^t - \theta = 0$$
$$M_\theta^t = M^t - M = 0$$

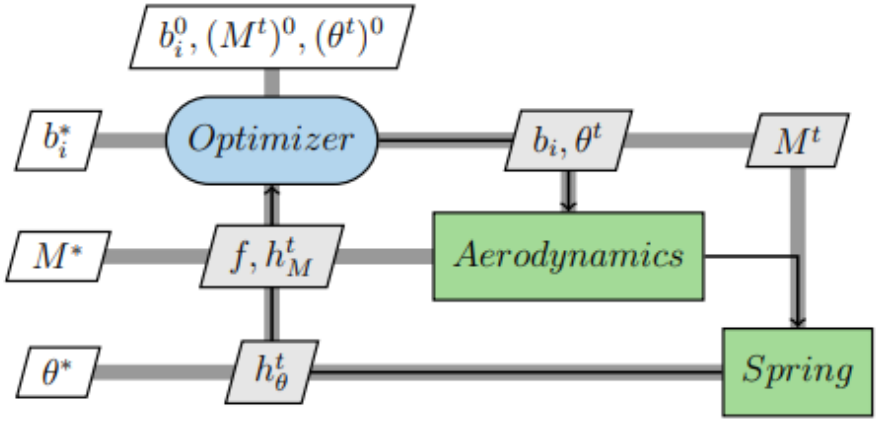

Airfoil-Spring System (3/3)

Objective: $\min f = \frac{1}{2}(L^{target} - L)^2$

with $L^{target} = 1.2\, L^{baseline}$

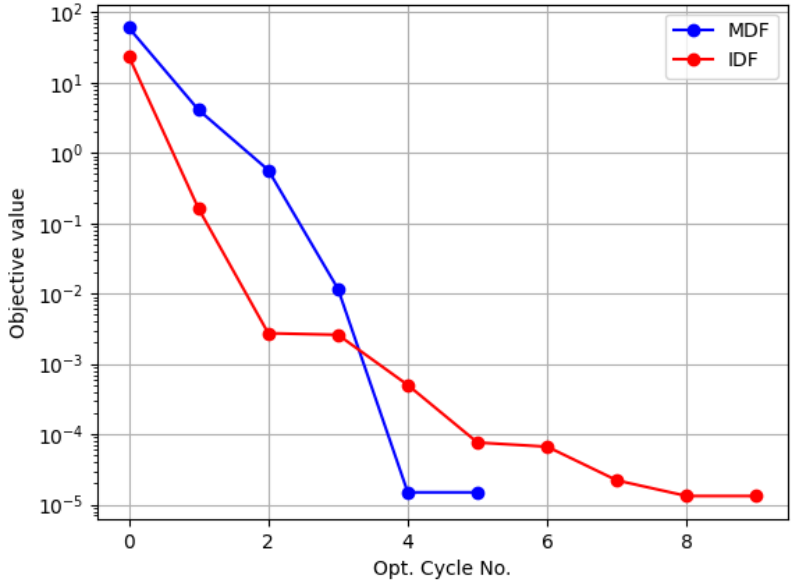

Architecture	MDF	IDF
Primal calls	30	27
Adjoint calls	5	9

Both architectures converge to the optimal solution.
MDF performs better than IDF (less TUs, less calls to the adjoint solver)

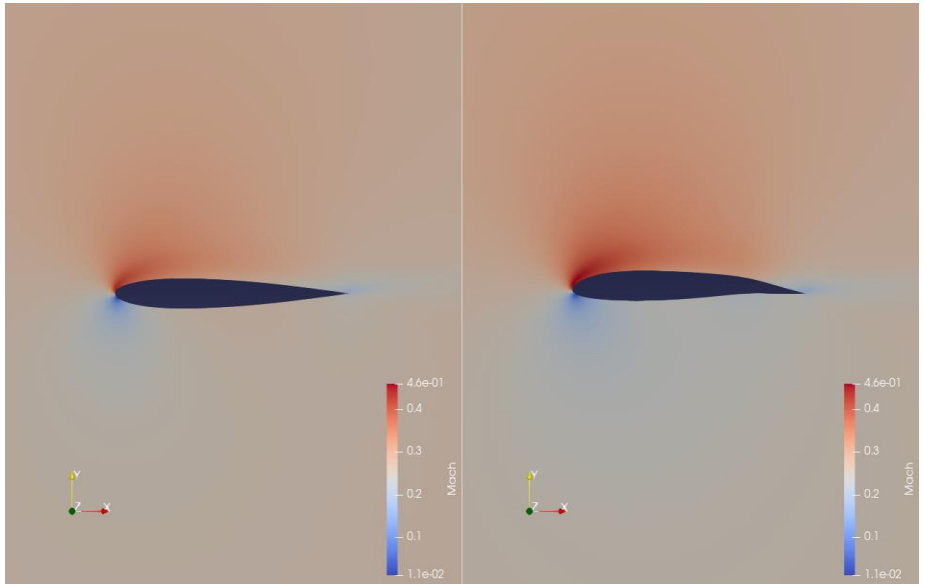

Baseline **Optimised**

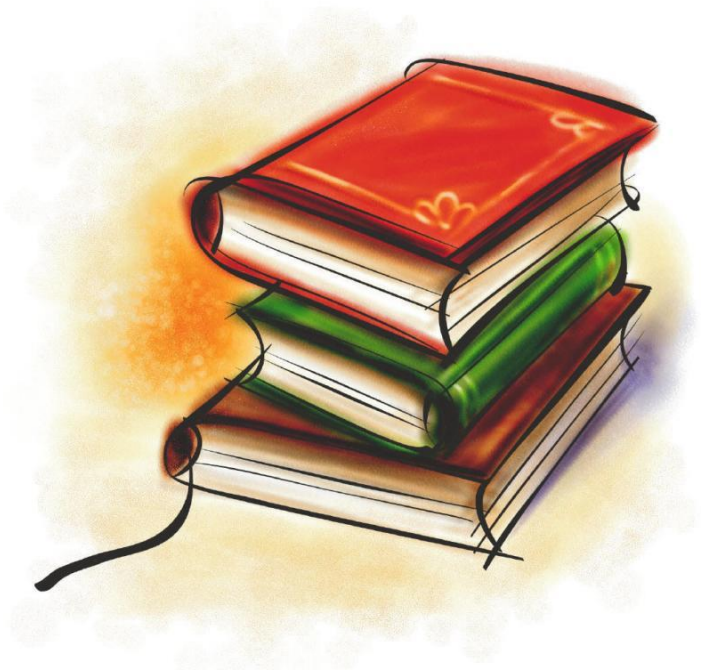

Aeroacoustic Optimisation

Prof. K.C. Giannakoglou, kgianna@mail.ntua.gr, Dr. V.G. Asouti, vasouti@mail.ntua.gr

ShpO of the Side Mirror of a Car for Noise Reduction – Is this an MDO?

$$J_N = \int_{\Omega'} \nu_t^2 d\Omega$$

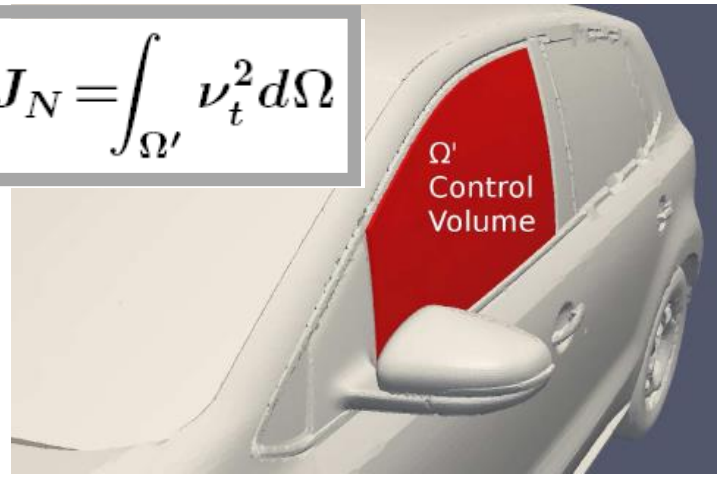

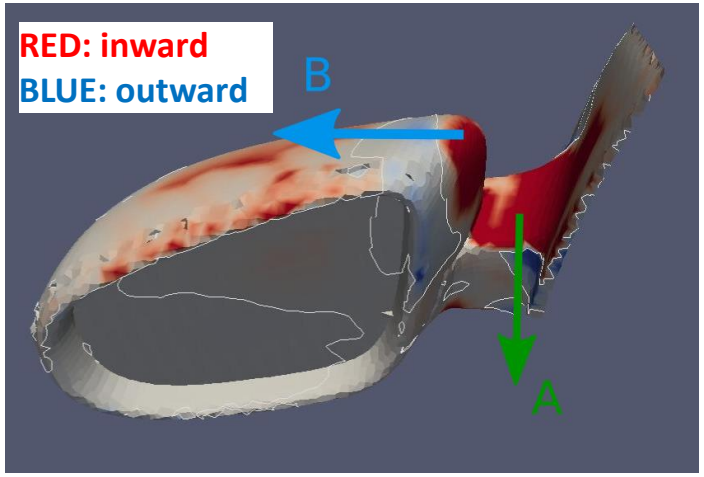

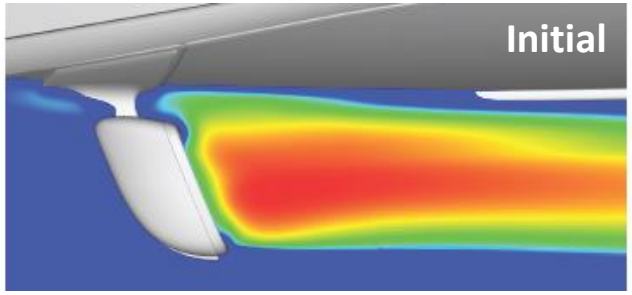

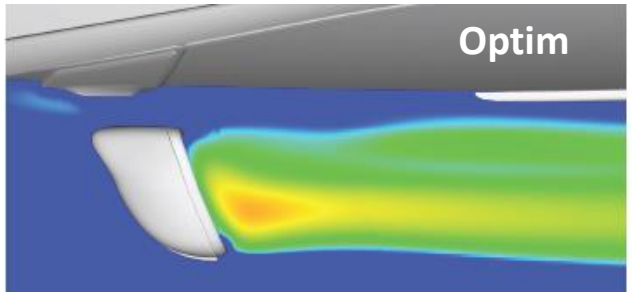

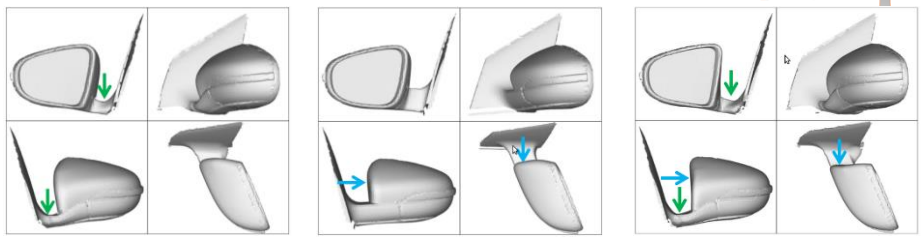

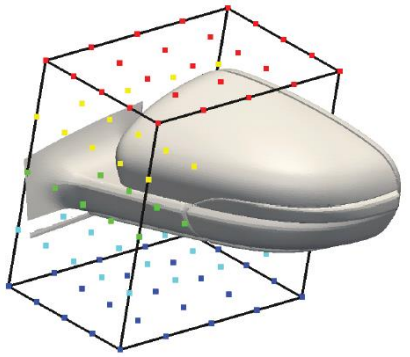

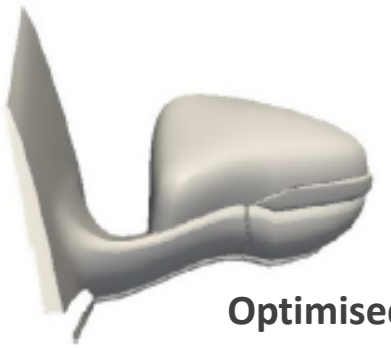

Optimised

Minimisation of the noise perceived by the driver. A turbulence-based objective function is used. This problem cannot be solved without the adjoint to the turbulence model equations. A relatively coarse grid (2.4 Mi cells) & the Volumetric B-Splines morpher (81 DoFs) were used in the adjoint optimisation. A re-evaluation of the optimal solution on a fine grid (31 Mi cells, flow 9h on 128CPUs) confirmed a reduction in J_N by 25%.

Computers & Fluids, 122:223-232, 2015.

Research funded by

Prof. K.C. Giannakoglou, kgianna@mail.ntua.gr, Dr. V.G. Asouti, vasouti@mail.ntua.gr

Aeroacoustic Analysis Solver

Objective function: **Total energy contained in the spectrum of sound pressure at the receiver's location:**

$$J = \int_{\omega} |\hat{p}'(\vec{x}_r, \omega)| \, \mathrm{d}\omega$$

$$|\hat{p}'| = \sqrt{\hat{p}'^2_{\mathrm{Re}} + \hat{p}'^2_{\mathrm{Im}}}$$

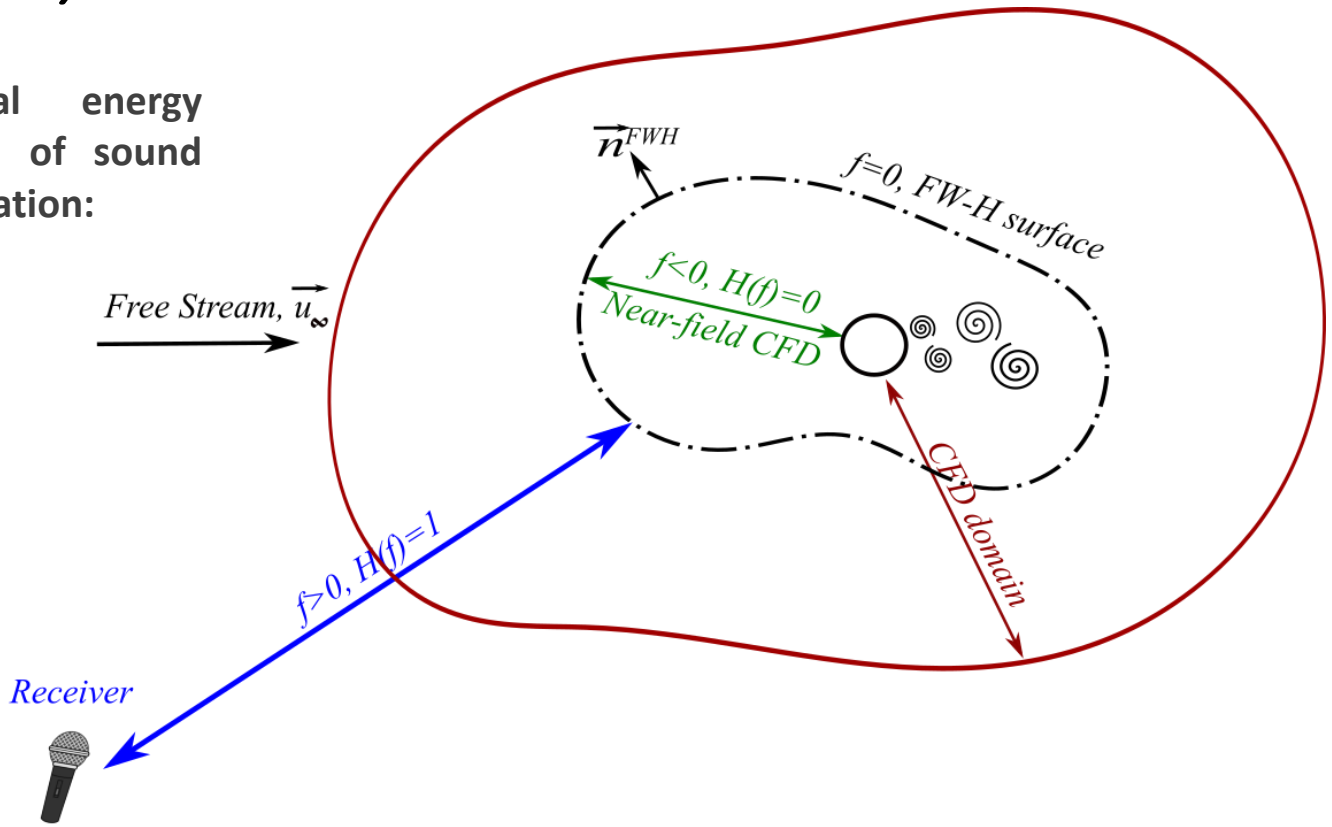

Ffowcs Williams-Hawkings (FW-H) acoustic analogy

$$H(f)\hat{p}'(\vec{x}_r, \omega) = -\int_{f=0} \hat{F}_k(\vec{x}_s, \omega) \frac{\partial \hat{G}(\vec{x}_r, \vec{x}_s, \omega)}{\partial x_{s_k}} \mathrm{d}S - \int_{f=0} i\omega \hat{Q}(\vec{x}_s, \omega) \hat{G}(\vec{x}_r, \vec{x}_s, \omega) \mathrm{d}S$$

Green function

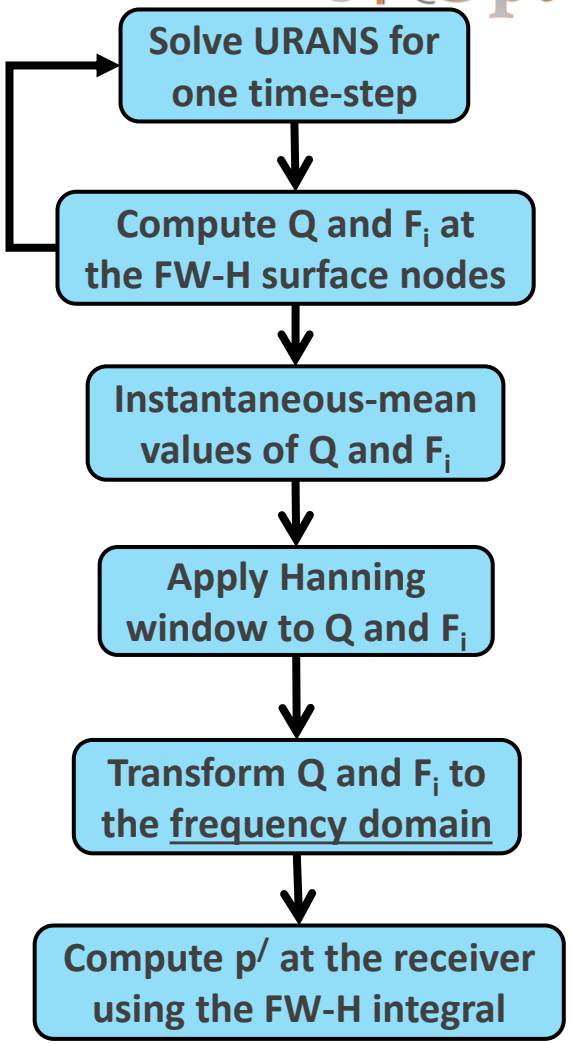

The Continuous Adjoint to the Aerocoustic Solver

Standard steps to develop the continuous adjoint method:

- **Define & differentiate (w.r.t. the design variables b_i) the Lagrangian or Augmented J:**

$$J_{aug} = J + \int_{T_s}\int_{\Omega} \Psi_n R_n \mathrm{d}\Omega \mathrm{d}t \quad \Rightarrow \quad \frac{\delta J_{aug}}{\delta b_i} = \frac{\delta J}{\delta b_i} + \int_{T_s}\int_{\Omega} \Psi_n \frac{\delta R_n}{\delta b_i} \mathrm{d}\Omega \mathrm{d}t$$

- **Re-arrange terms and bring it into the following form:**

$$\frac{\delta J}{\delta b_i} = \int_{T_s}\int_{\Omega} FAE_n \frac{\delta U_n}{\delta b_i} \mathrm{d}\Omega \mathrm{d}t + \int_{T_s}\int_{S_w} ABC_n \frac{\delta U_n}{\delta b_i} \mathrm{d}S \mathrm{d}t + \int_{T_s}\int_{\Omega} SD^{\Omega}_{ml} \frac{\partial}{\partial x_m}\left(\frac{\delta x_l}{\delta b_i}\right) \mathrm{d}\Omega \mathrm{d}t + \int_{T_s}\int_{\Omega} SD^{S}_{l} \frac{\delta x_l}{\delta b_i} \mathrm{d}S \mathrm{d}t + \int_{T_s}\int_{f=0} \left(S_{FW-H_n} + S^{Q}_{FW-H_n}\right) \frac{\delta U_n}{\delta b_i} ds dt$$

Field Adjoint Eqs. (FAE) & Adjoint Boundary Conditions (ABC)

Sensitivity Derivatives

Sources to the Field Adjoint Equations, on the FW-H surface nodes

Computers & Fluids, 230:105136, 2021.

Aeroacoustic ShpO Flowchart

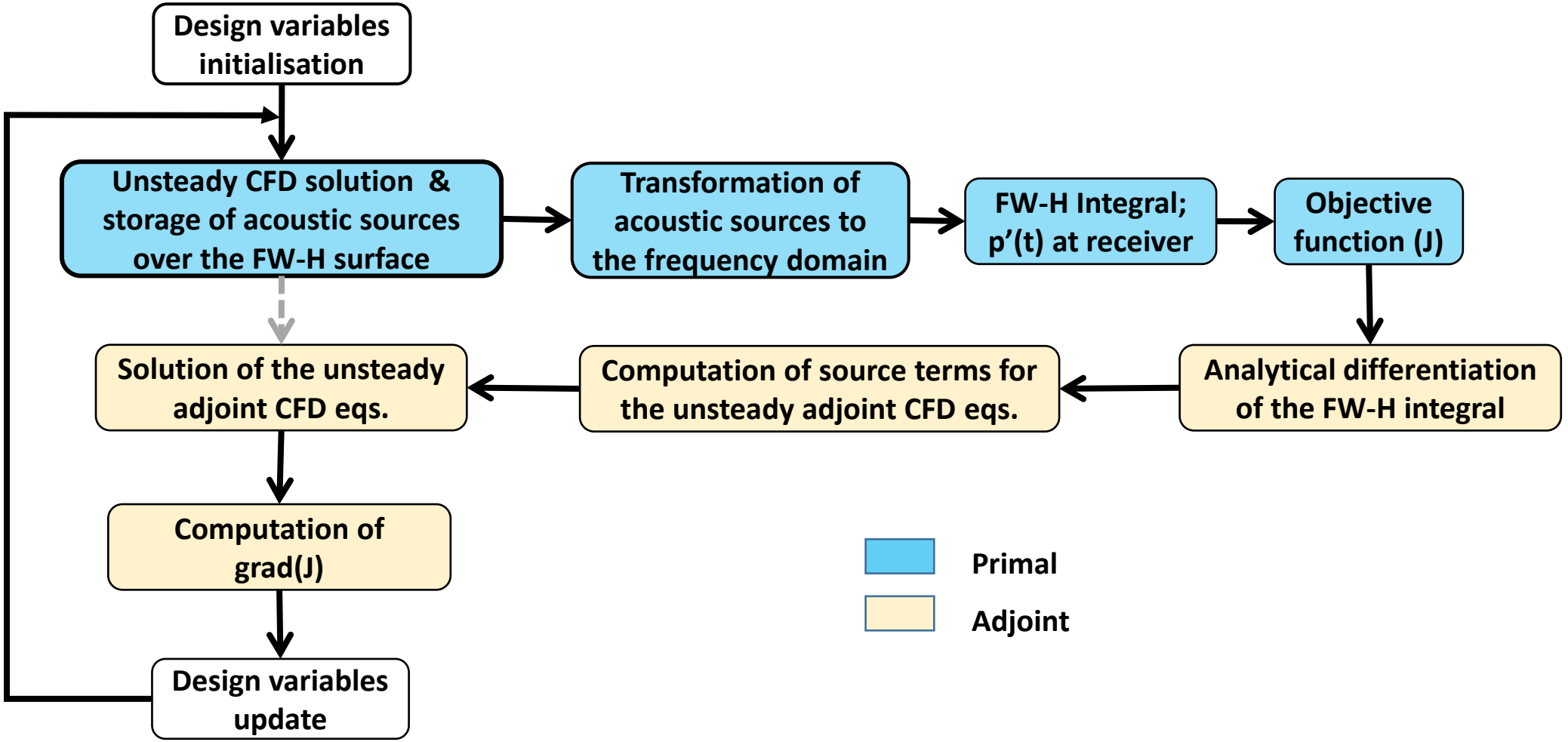

Computers & Fluids, 230:105136, 2021.

ShpO of a Plunging Airfoil (1/4)

- NACA64A010 airfoil at turbulent flow conditions: M_∞ = 0.8, Re = 4.9x10^6, AoA = 0°
- Plunging amplitude= 0.05 C, Period=0.2 sec., 50 Δt/period
- Parametrisation: FFD box with 5x8 CPs, 24 DoFs (in y)
- Noise objective, receiver @ (1C, 30C)
- FWH surface @ R=3C
- Computation for 5 periods (primal), 4 periods (adjoint)

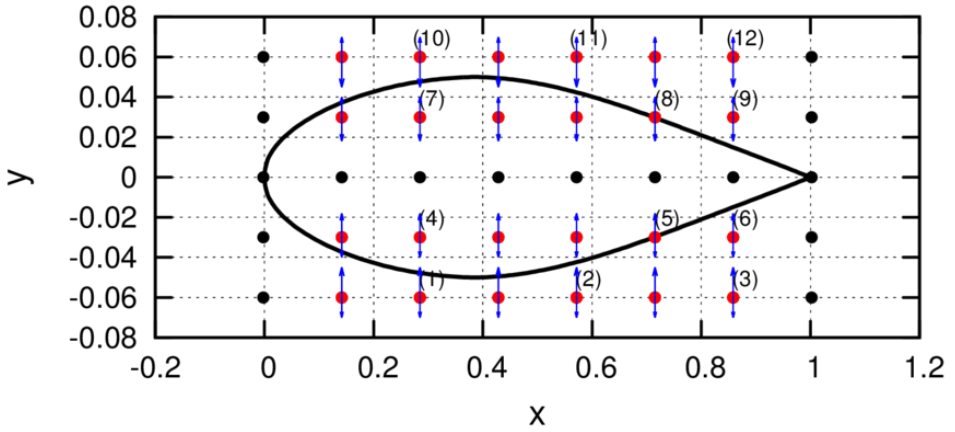

Noise

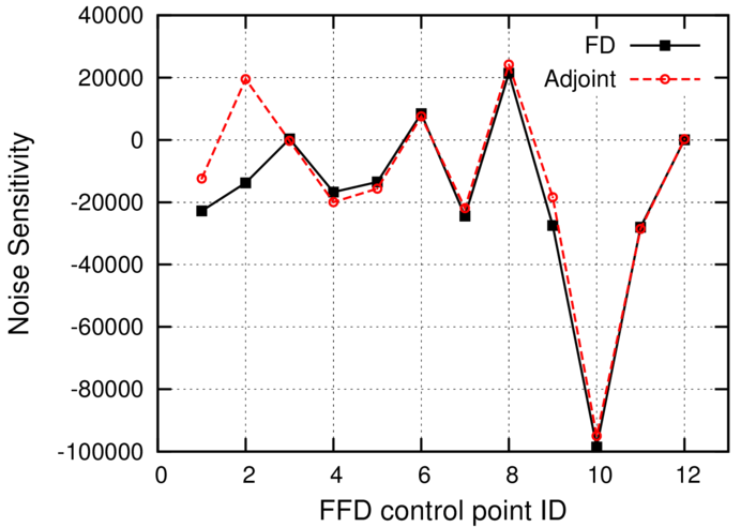

Time-averaged lift

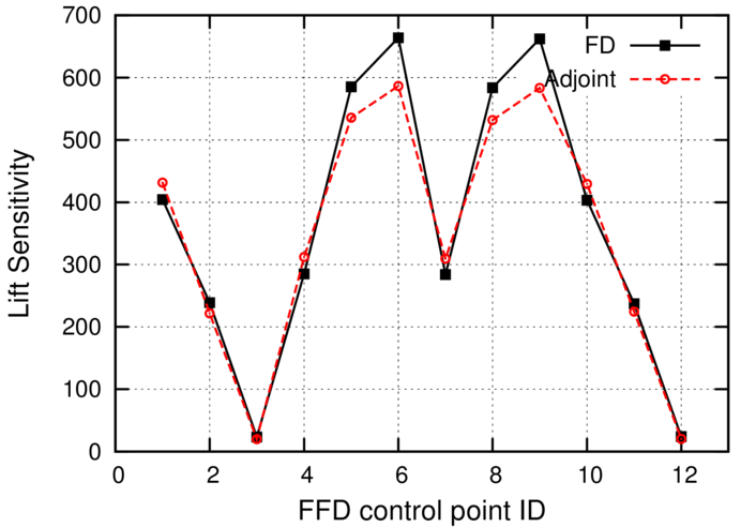

Time-averaged drag

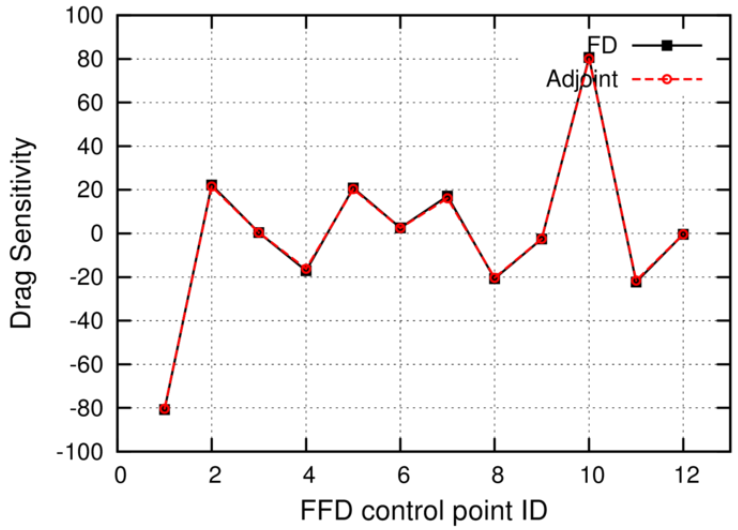

ShpO of a Plunging Airfoil (2/4)

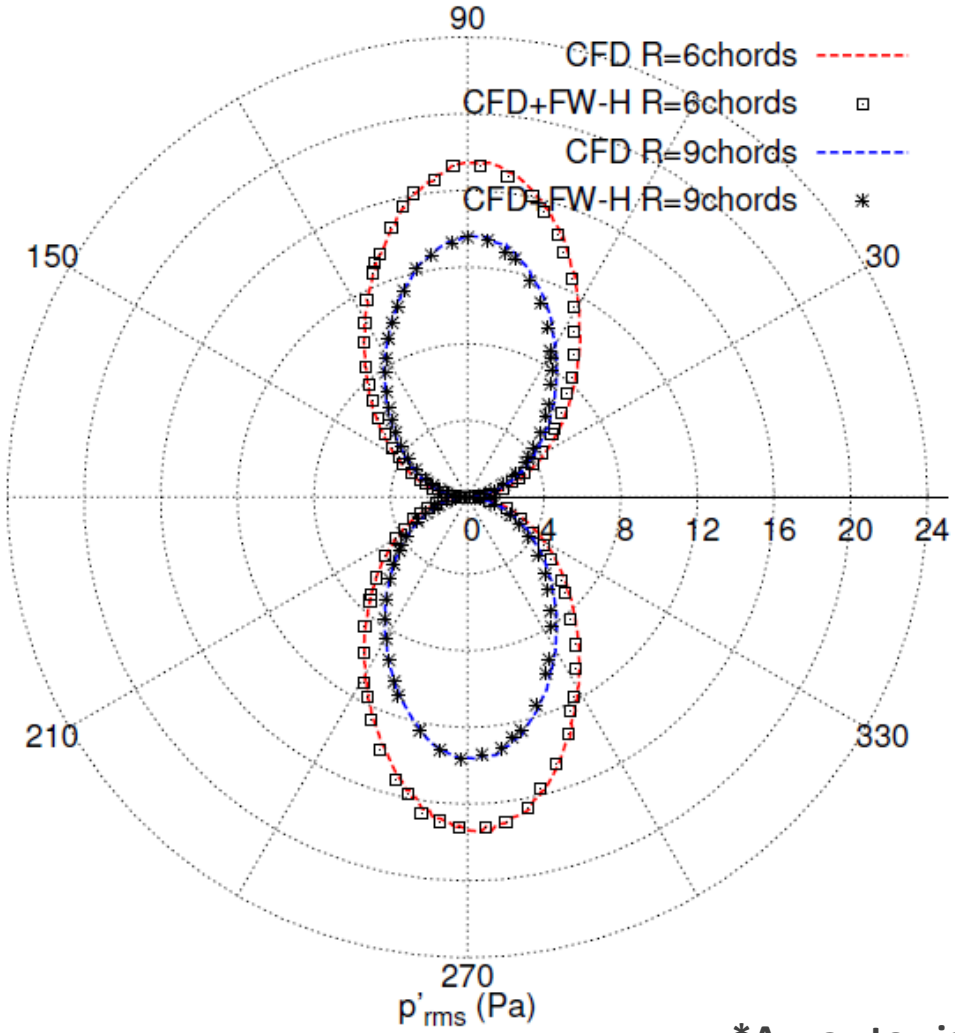

Comparison of directivity plots* computed by the hybrid method and pure CFD simulations (URANS only!), at two radii: R=6C & R=9C.

***A way to visualise how an acoustic source distributes energy in all directions**

ShpO of a Plunging Airfoil (3/4)

Comparison with a Metamodel-Assisted EA (S/W EASY)

Adjoint cost = 5 (front point) x 20 (cycle/front point) x 3 (eval/cycle) = 300 evaluations

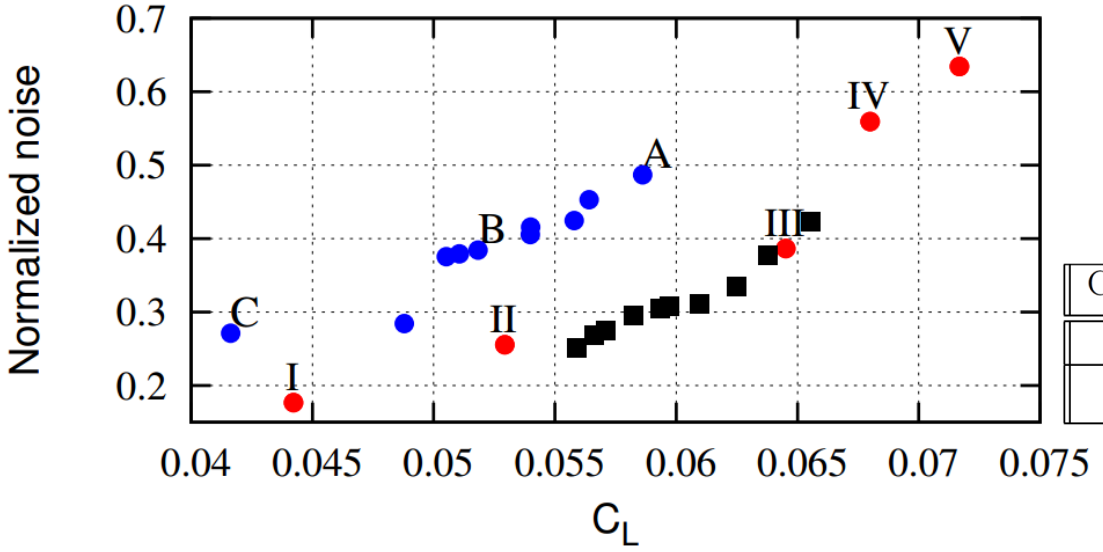

Adjoint
EA, 200 evaluations
EA, 450 evaluations

$\mathcal{W}_{\text{noise}}\, noise - \mathcal{W}_{\text{lift}}\, lift$

Case name	*I*	*II*	*III*	*IV*	*V*
$\mathcal{W}_{noise}$	1	0.75	0.5	0.25	0
$\mathcal{W}_{lift}$	0	0.25	0.5	0.75	1

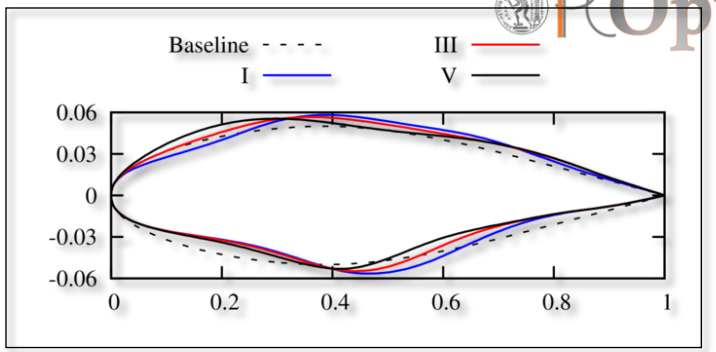

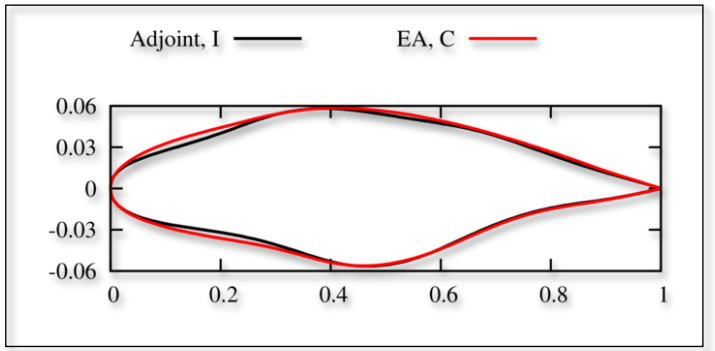

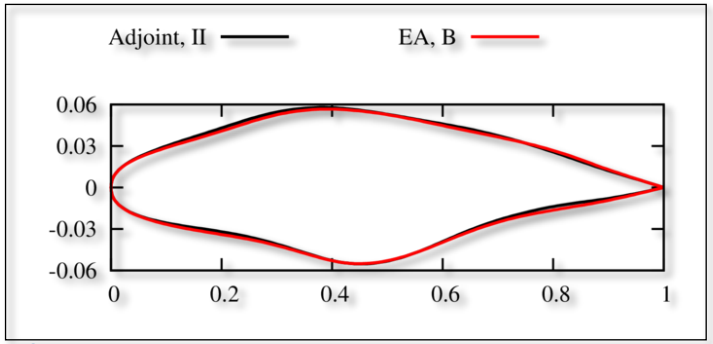

ShpO for min. noise and max. average lift (two-objectives, Pareto-seeking MAEA) or their weighted sum (one-objective, adjoint). Drag in optimised airfoils is x2.5 compared to the baseline one:

Airfoil	Baseline	A	B	C
C_d	3.5×10^{-3}	9.7×10^{-3}	10.3×10^{-3}	10.1×10^{-3}

ShpO of a Plunging Airfoil (4/4)

Comparison of the sound pressure at receiver location and directivity plot at R=9C

MAEA

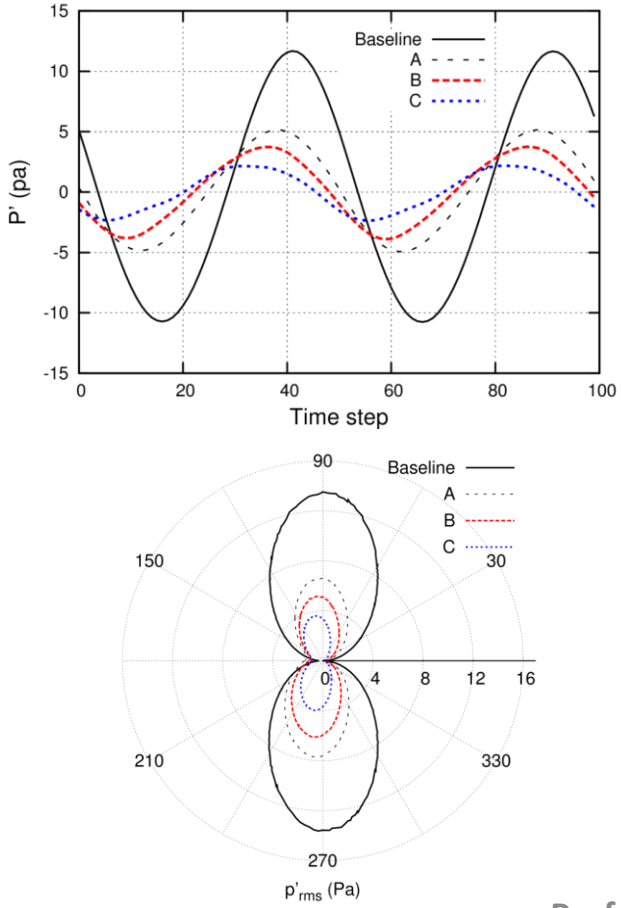

Adjoint

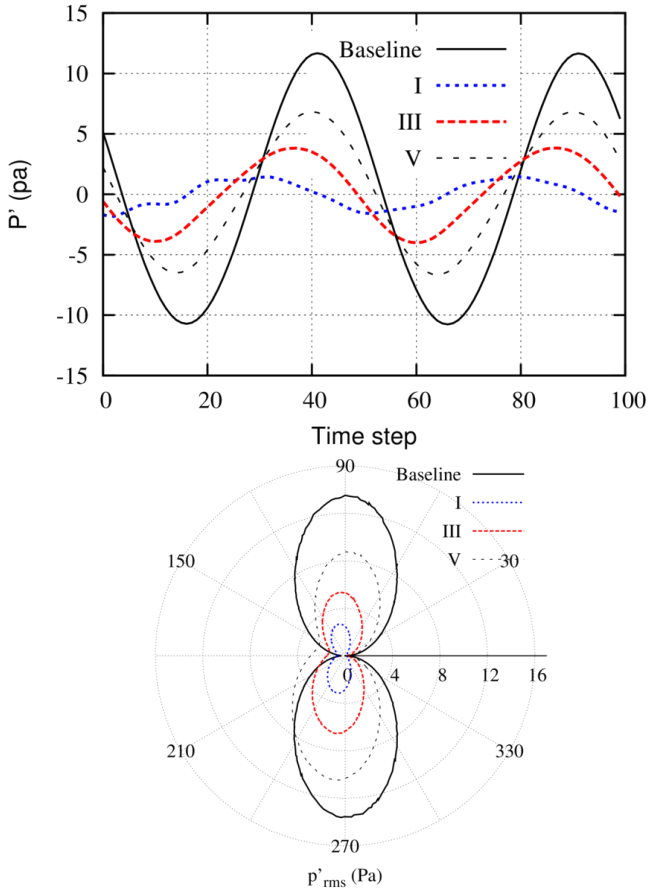

Pressure fluctuation fields
(Initial vs. Adjoint-based noise optimised)

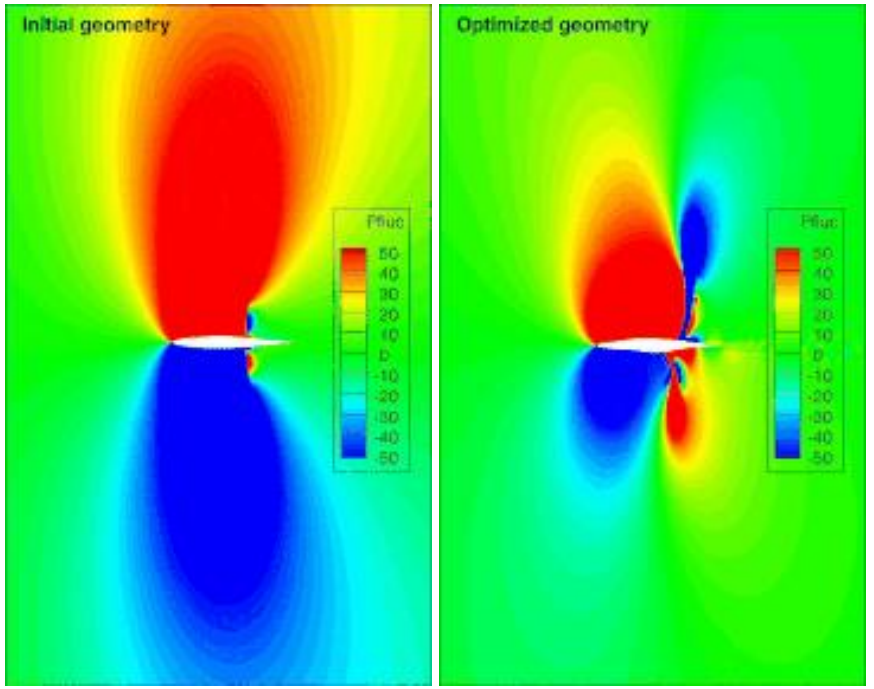

Prof. K.C. Giannakoglou, kgianna@mail.ntua.gr, Dr. V.G. Asouti, vasouti@mail.ntua.gr

ShpO of a Laminar Vortex Shedding Cylinder (1/3)

- Cylinder (D=0.019m) at laminar flow: M_∞=0.2, Re=1000.
- Δt=0.00122sec., 50 Δt/period, Str=0.24
- Parametrisation: Two Bezier curves, 5 design variables each (only y coordinate) → 10 DoFs
- Noise sensitivity for a receiver @ (-4D, -20D)
- FW-H surface at R=3.5D, with 308 nodes.

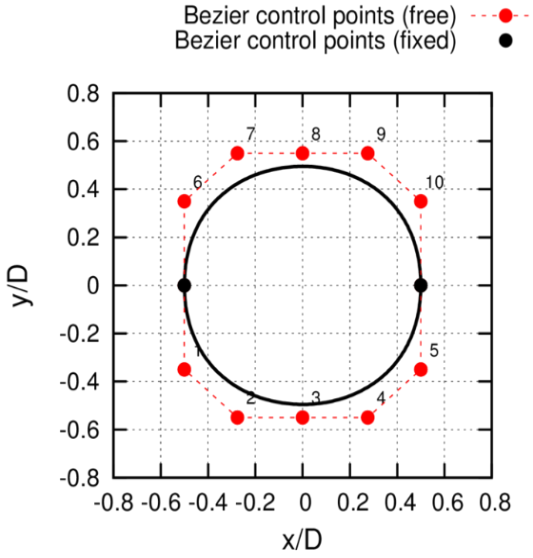

Noise

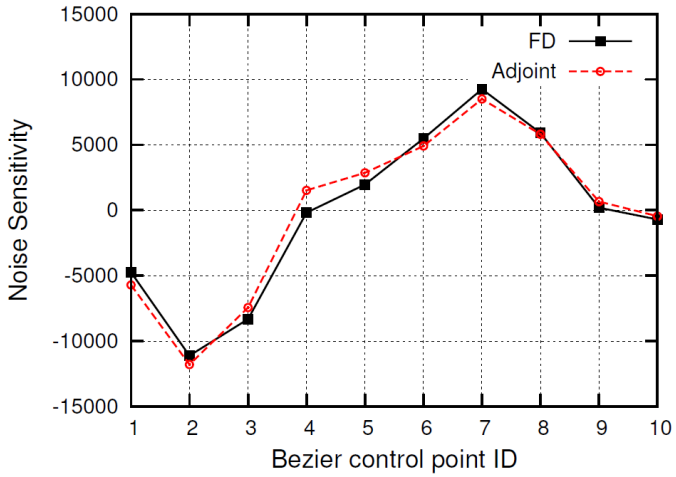

Time averaged lift

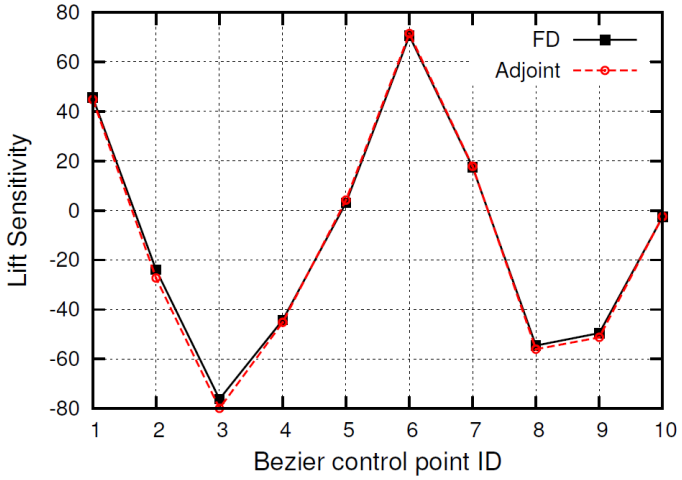

Time averaged drag

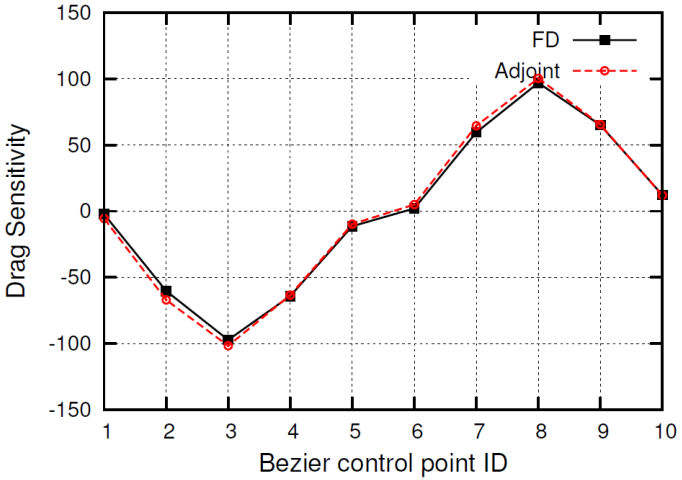

ShpO of a Laminar Vortex Shedding Cylinder (2/3)

min. noise at 4 receivers $J = \frac{1}{N_r} \sum_{a=1}^{N_r} \int_{\omega} |\hat{p}'(\vec{x}_{r_a}, \omega)| \mathrm{d}\omega$

Constraint imposed on the min. body volume.

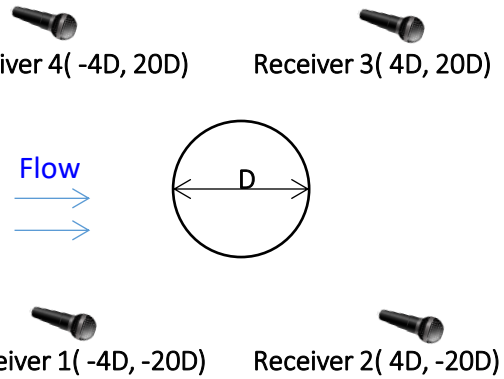

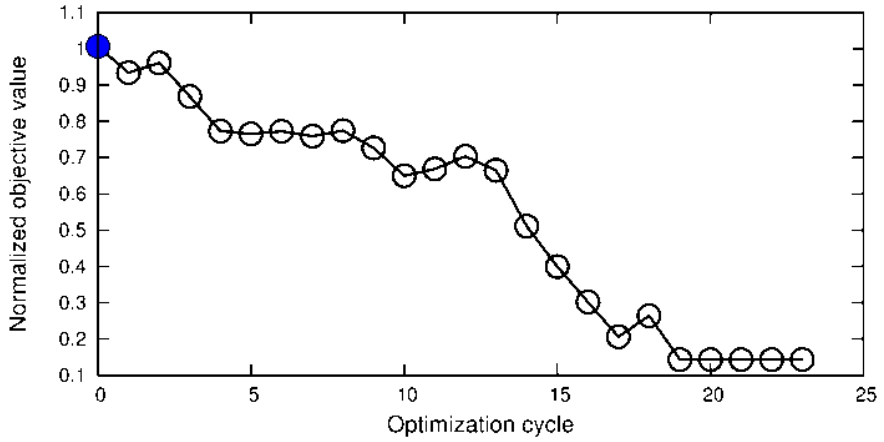

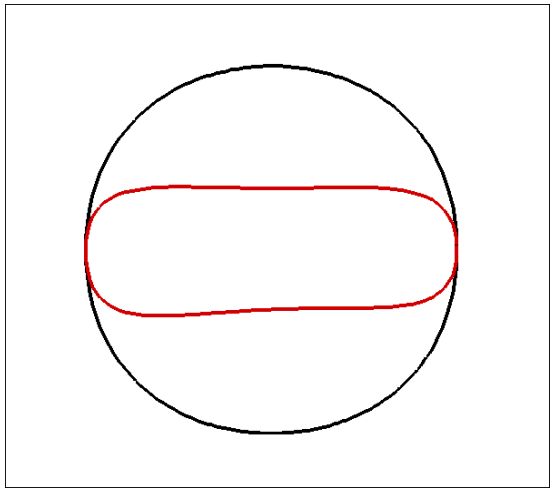

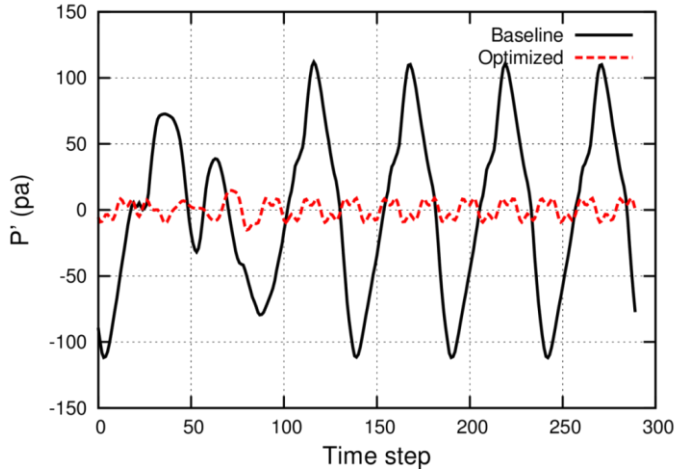

ShpO of a Laminar Vortex Shedding Cylinder (3/3)

Pressure fluctuation field

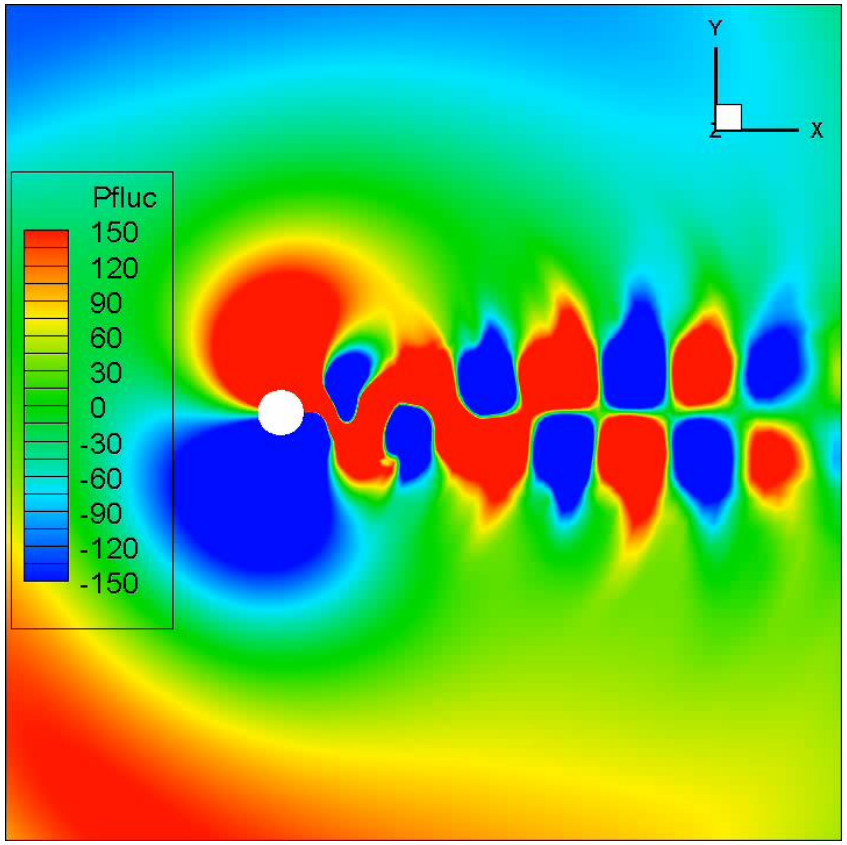

Baseline

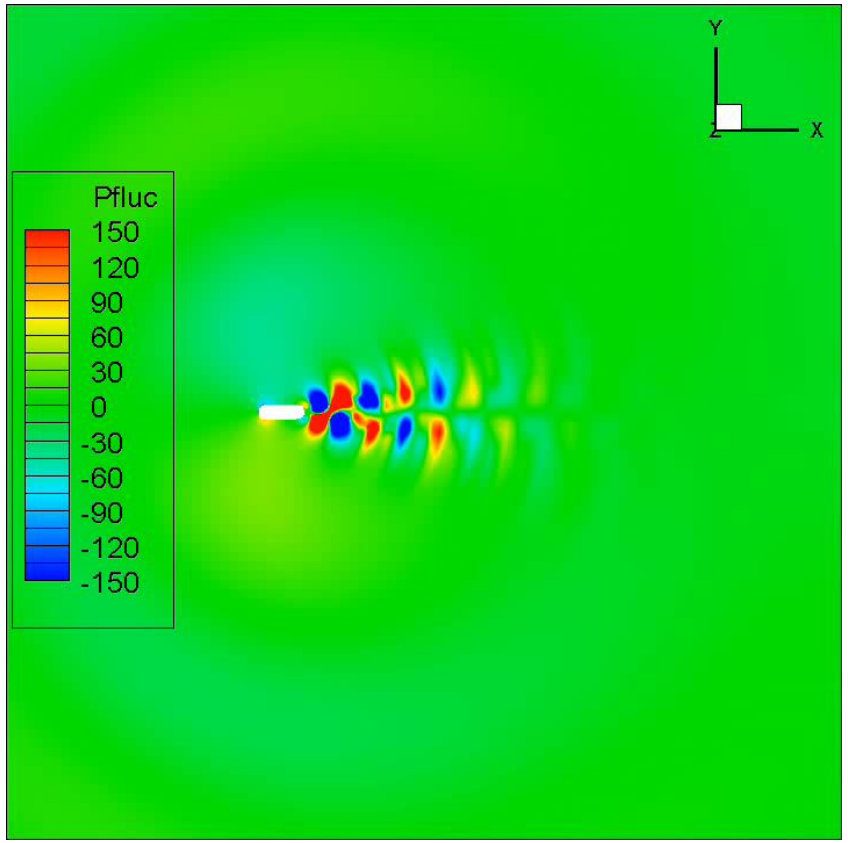

Optimised

Airfoil ShpO in the Rod-Airfoil Configuration (1/5)

- NACA0012 at turbulent flow conditions: AoA=0° , M_∞ = 0.2, $Re_c=4.8x10^5$
- C = 0.1m & D=0.1C
- ~300 Δt/T, Computed Str = 0.24
- Computation for 20000 Δt
- The FW-H integral computed in the last 2030 Δt (~7T)

Benchmark to study noise generated by aircraft components, such as the landing gear

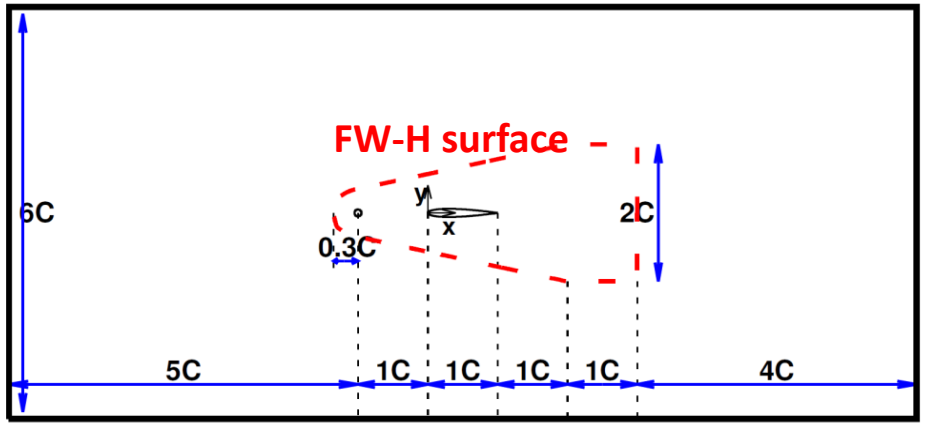

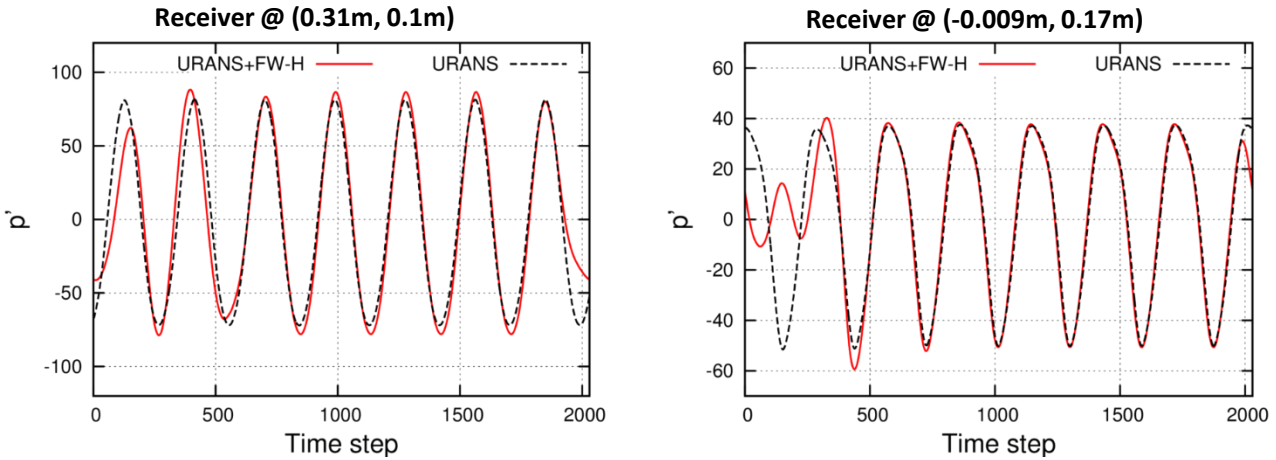

Comparison of pressure fluctuations at different receiver locations

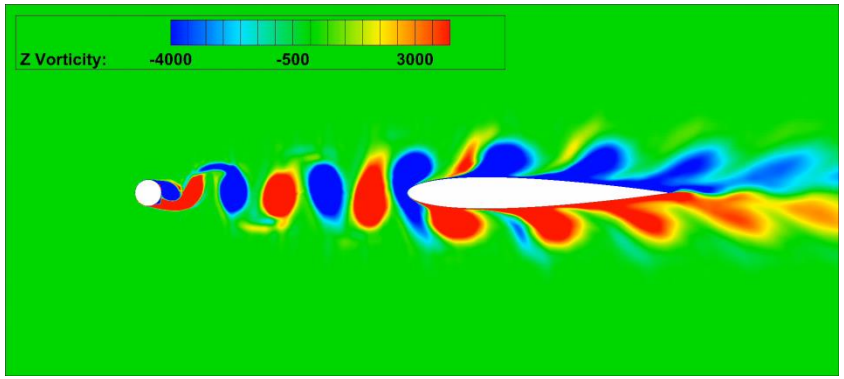

Computers & Fluids, 230:105136, 2021.

Airfoil ShpO in the Rod-Airfoil Configuration (2/5)

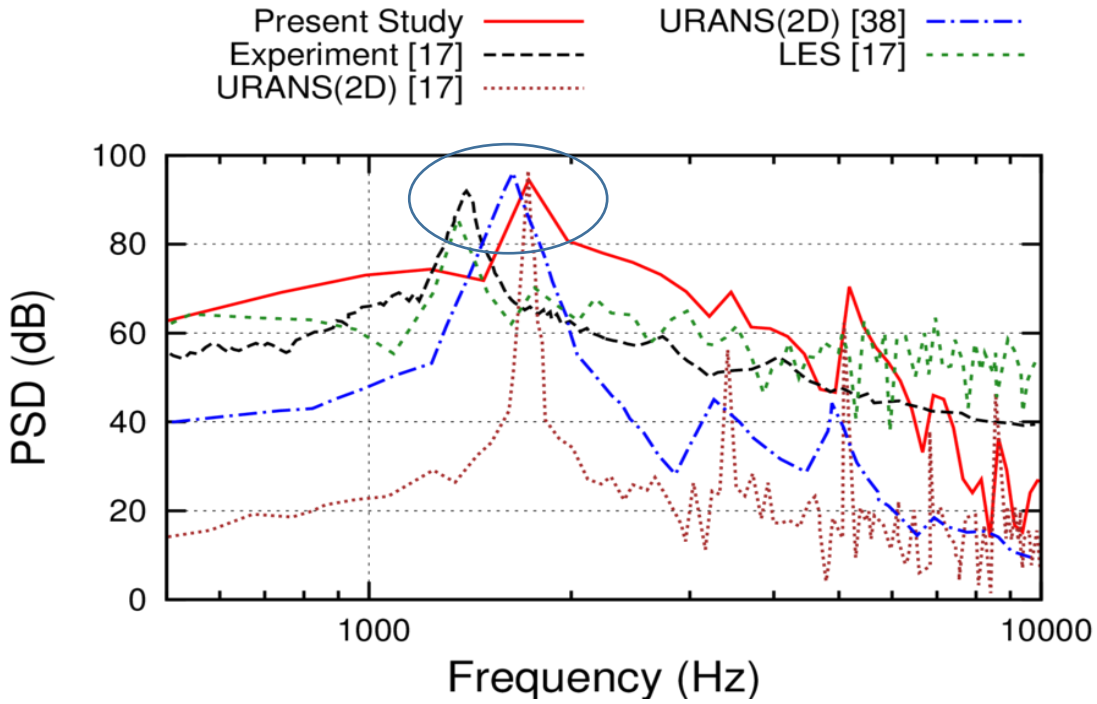

Comparison of Power Spectral Density (PSD) at a receiver located 1.85m above the airfoil center with other URANS & LES results as well as experimental measurements.

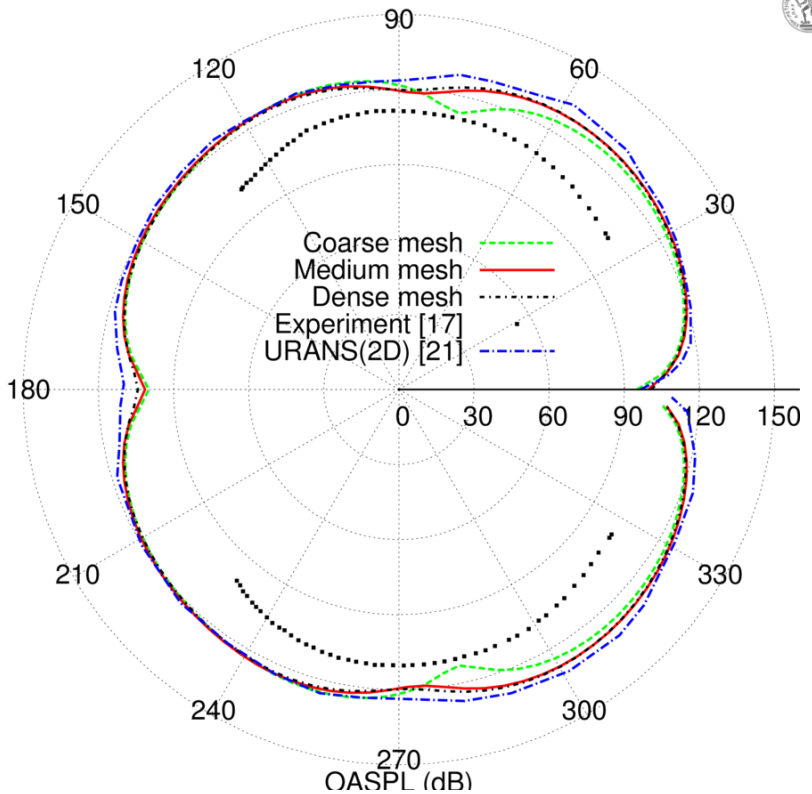

Directivity of overall SPL (OASPL) at R = 1.85m, computed on a coarse (124K nodes), a medium (161K) and a fine (240K) grid. Comparison with other URANS & experimental measurements.

Airfoil ShpO in the Rod-Airfoil Configuration (3/5)

- **Objective: min. Noise @ (0.05,1.85), one receiver.** $J = \int_{\omega} |\hat{p}'(\vec{x}_r, \omega)| \, \mathrm{d}\omega$
- **Parametrisation: FFD box with 5x10CPs (only y) → 50 DoFs.**
- **Terminate the adjoint solution earlier 30% less comp. time compared to full time horizon & 60% less storage (240 Gb > 80 Gb)**

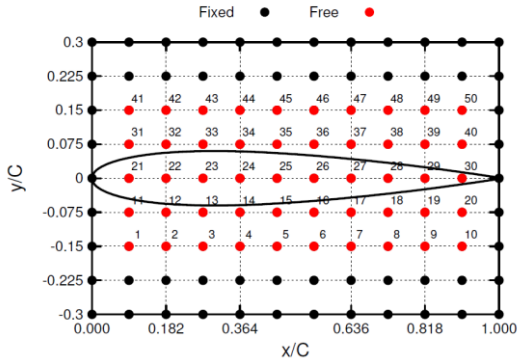

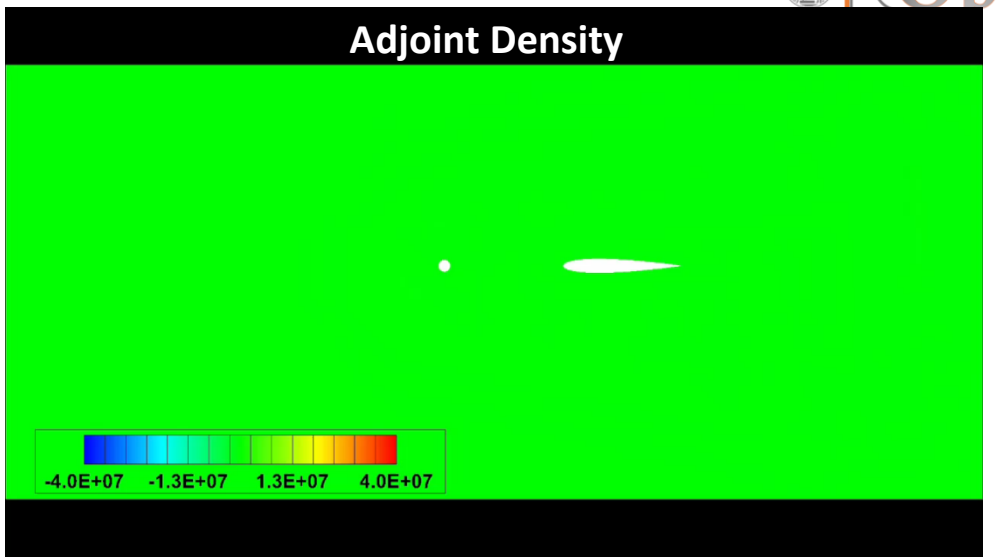

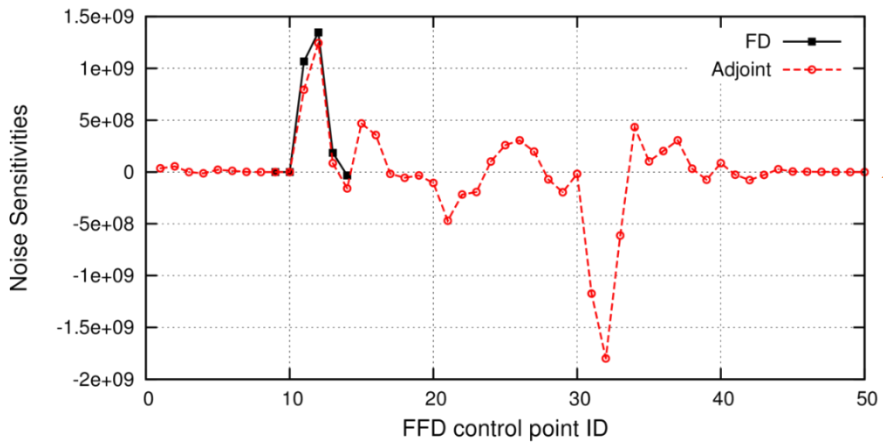

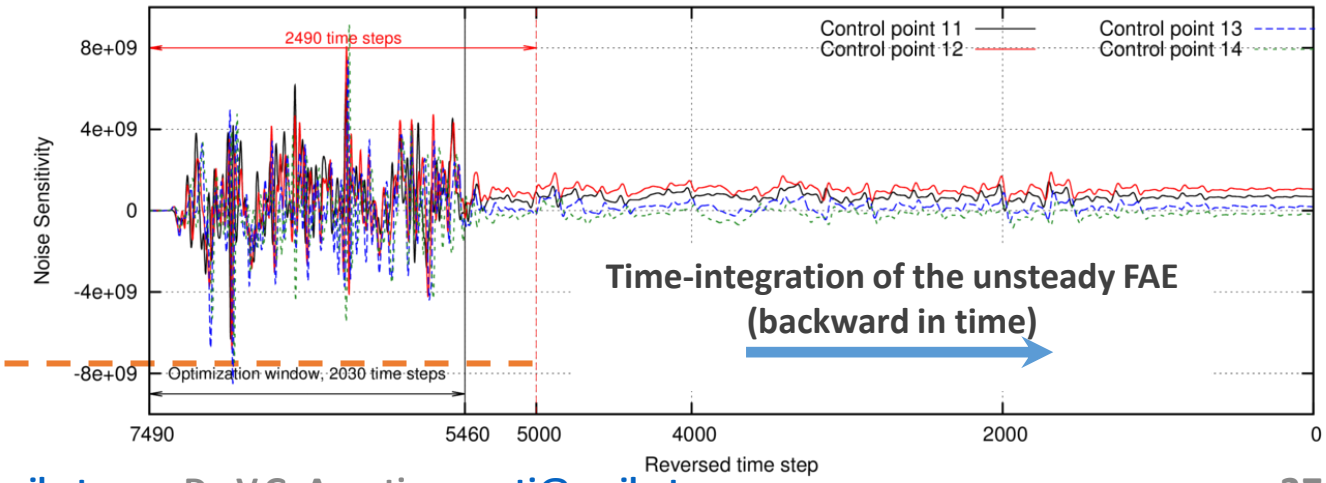

Airfoil ShpO in the Rod-Airfoil Configuration (4/5)

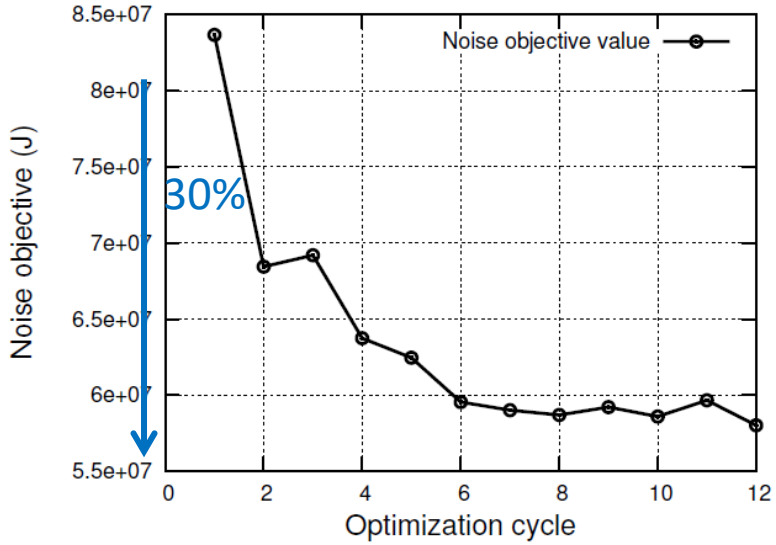

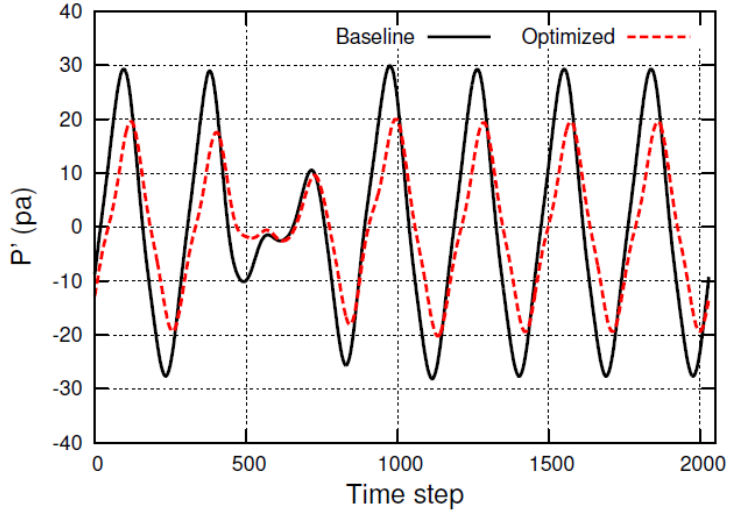

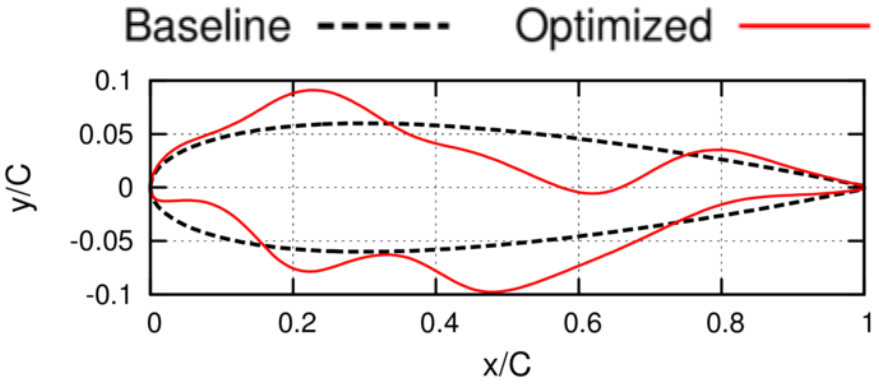

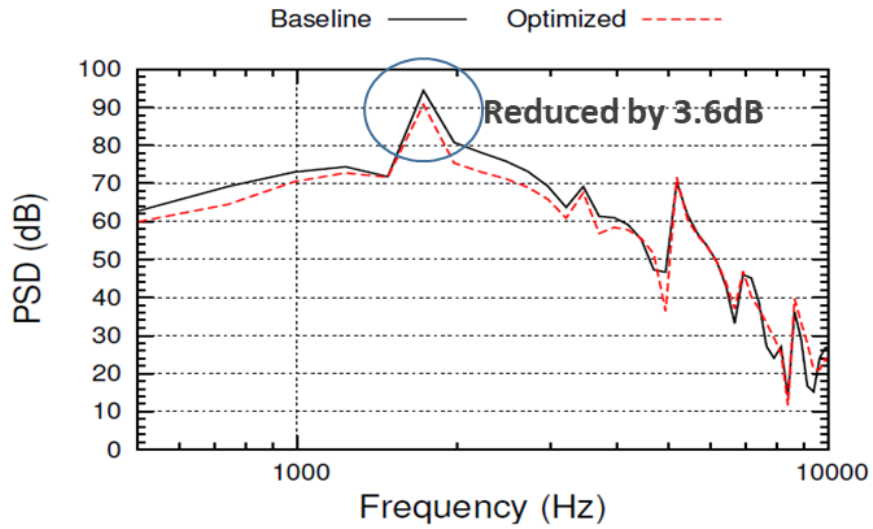

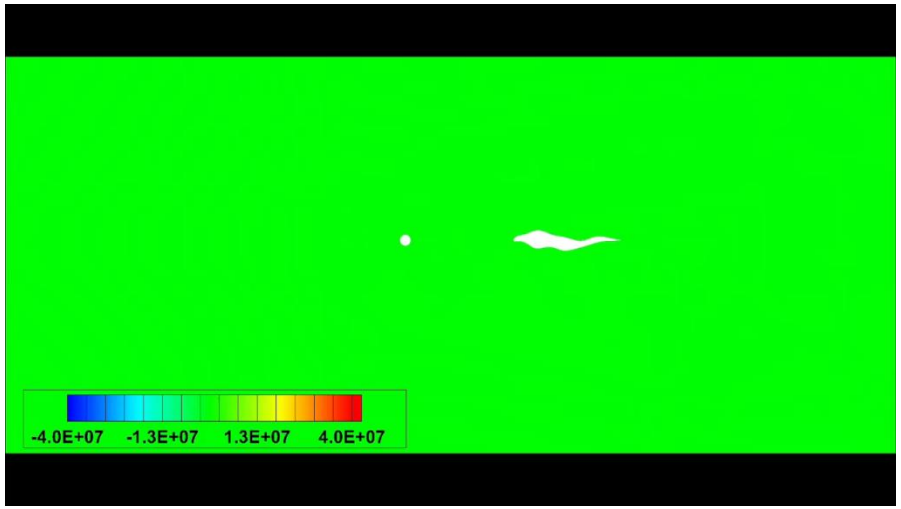

Airfoil ShpO in the Rod-Airfoil Configuration (5/5)

Quality of the optimised solution vs. the baseline one.

OASPL contour outside the FWH surface

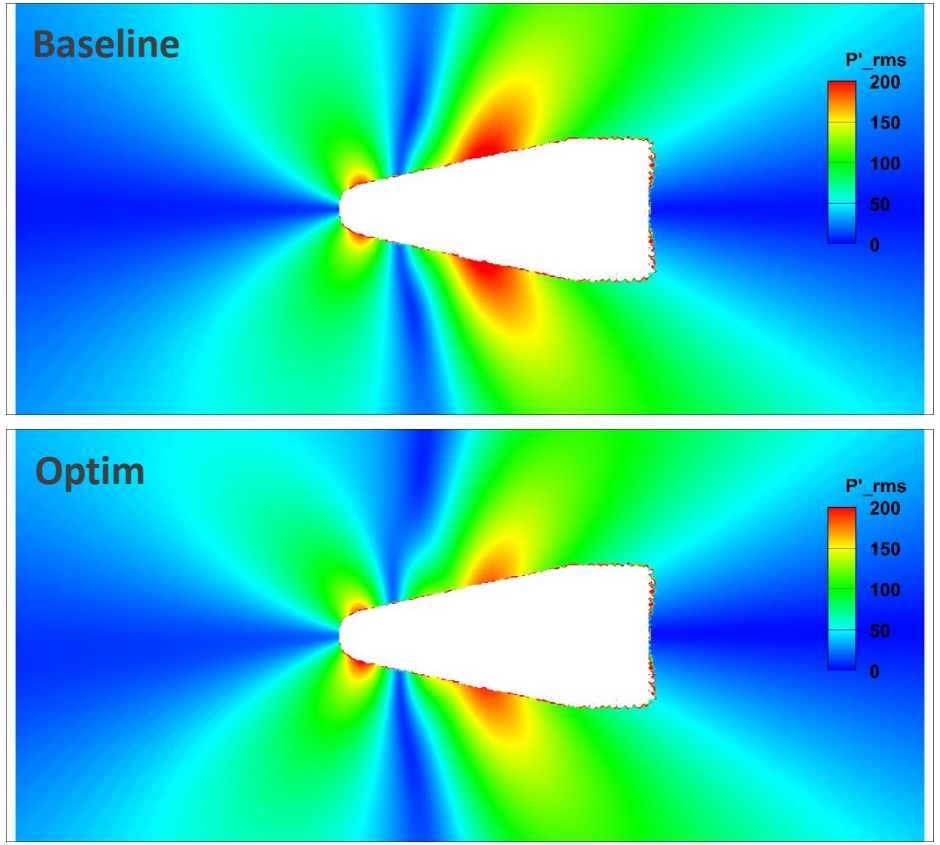

OASPL directivity at R = 1.85m
Optimization performed for a receiver @ (0.05,1.85),
i.e. almost 90º up.

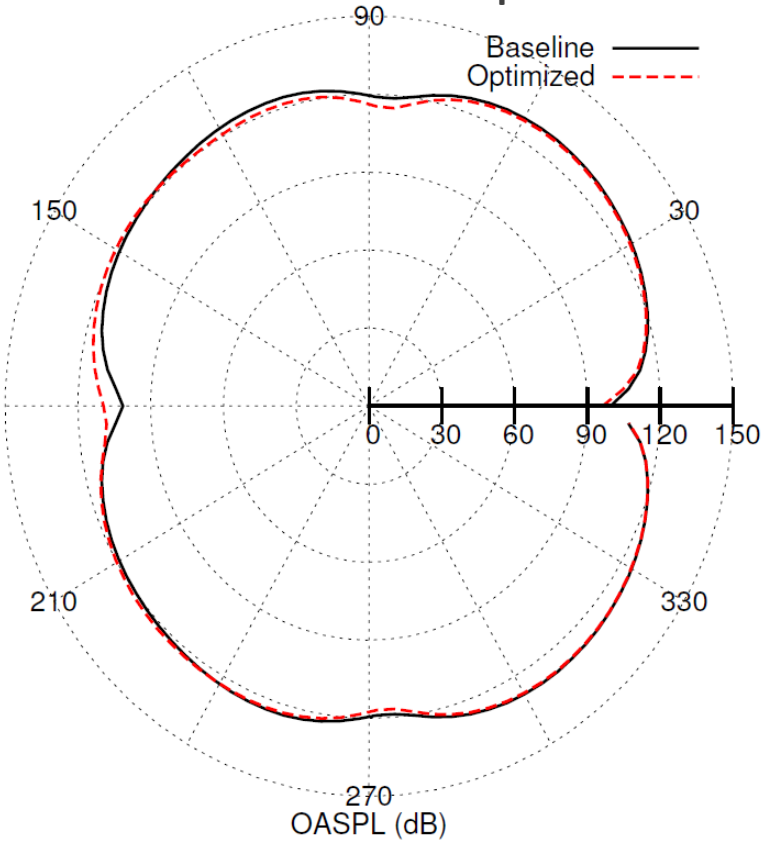

Aeroacoustic ShpO of a Turbofan Intake (1/5)

- Generic intake geometry (scaled to match the Vital fan) by Rolls Royce.
- Pressure distribution at the fan inlet provided by the Univ. of Southampton.
- CFD mesh in a single blade passage, ~ 3.7M nodes, (~16K on the FWH surface).
- Flow and adjoint solved in a rotating frame of reference (steady solver).
- Unsteady data on the FW-H surface created by rotating the steady solution.
- Generatrix parametrised using 15 control points; 26 DoFs.
- Noise objective defined at the BPF (2318Hz).
- Cost per optimisation cycle = 1day.

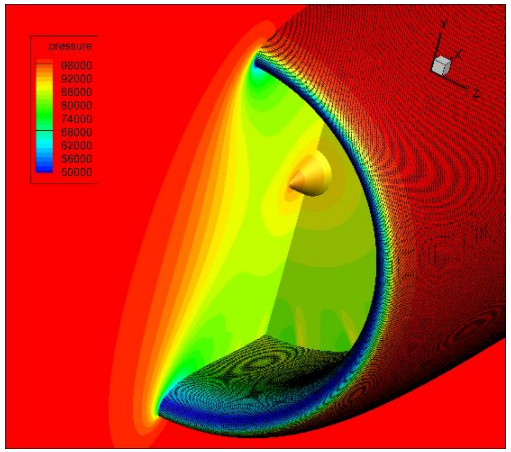

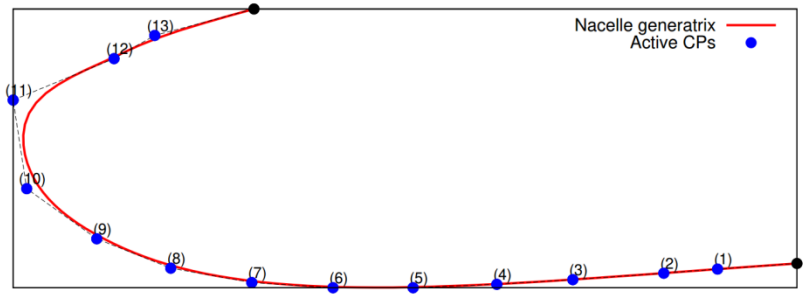

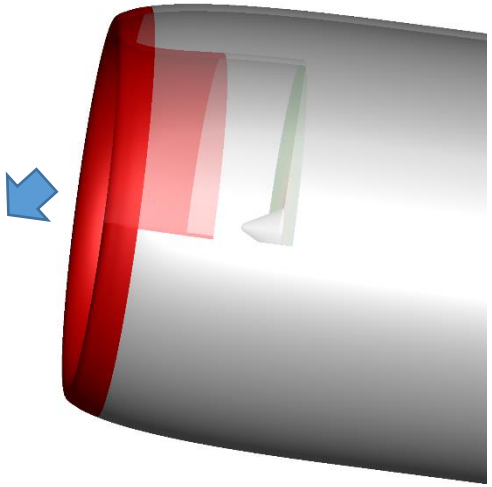

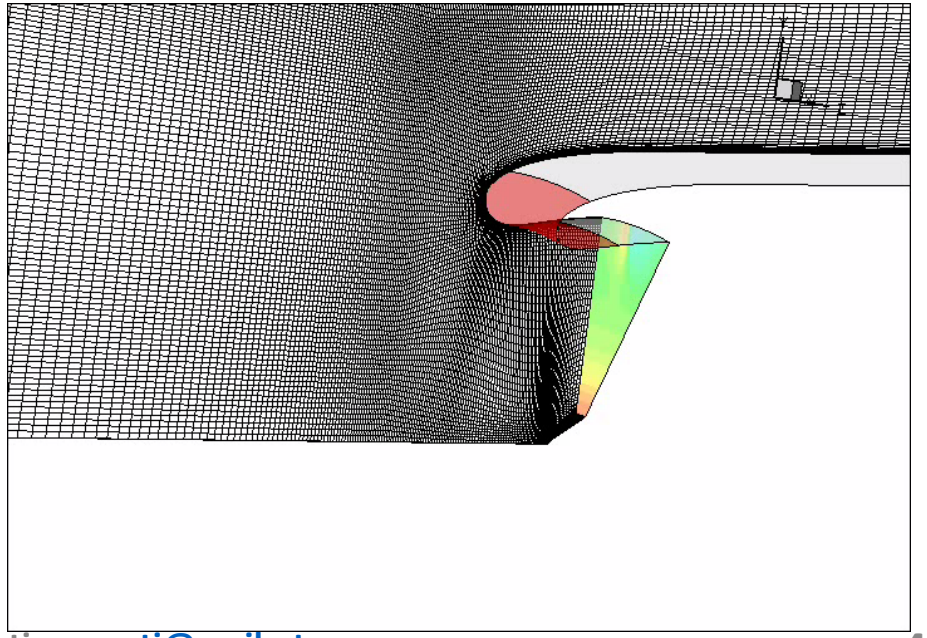

Aeroacoustic ShpO of a Turbofan Intake (2/5)

The "usual" verification of the Primal Hybrid Solver vs. an expensive URANS solution, separately at three receivers.

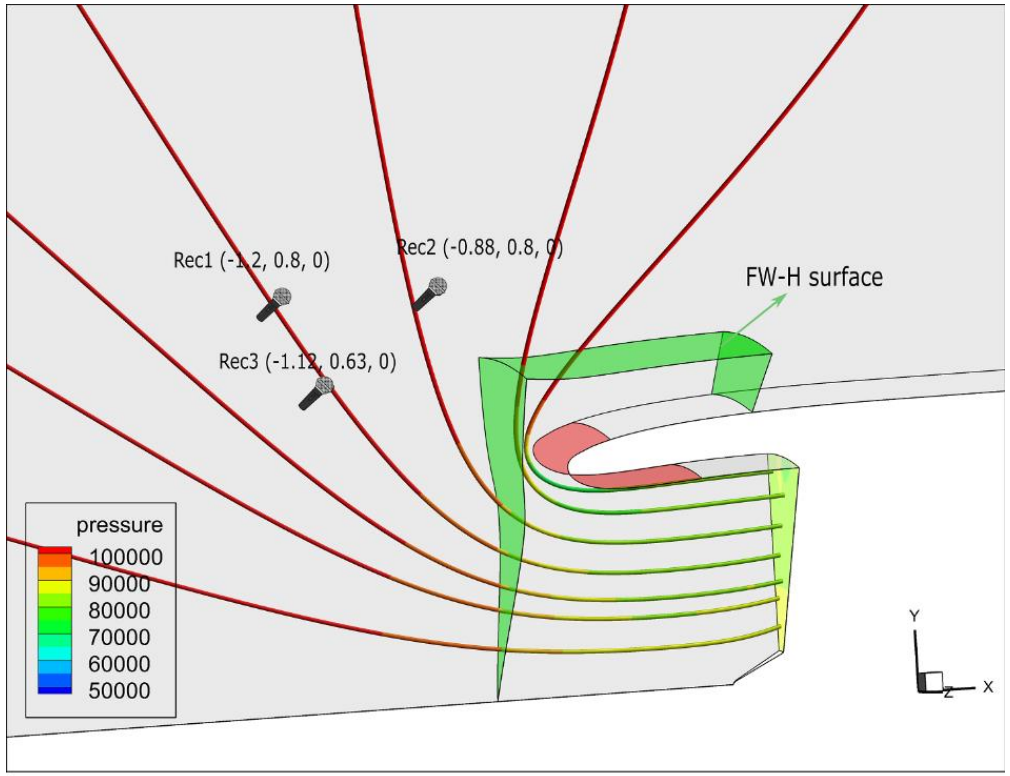

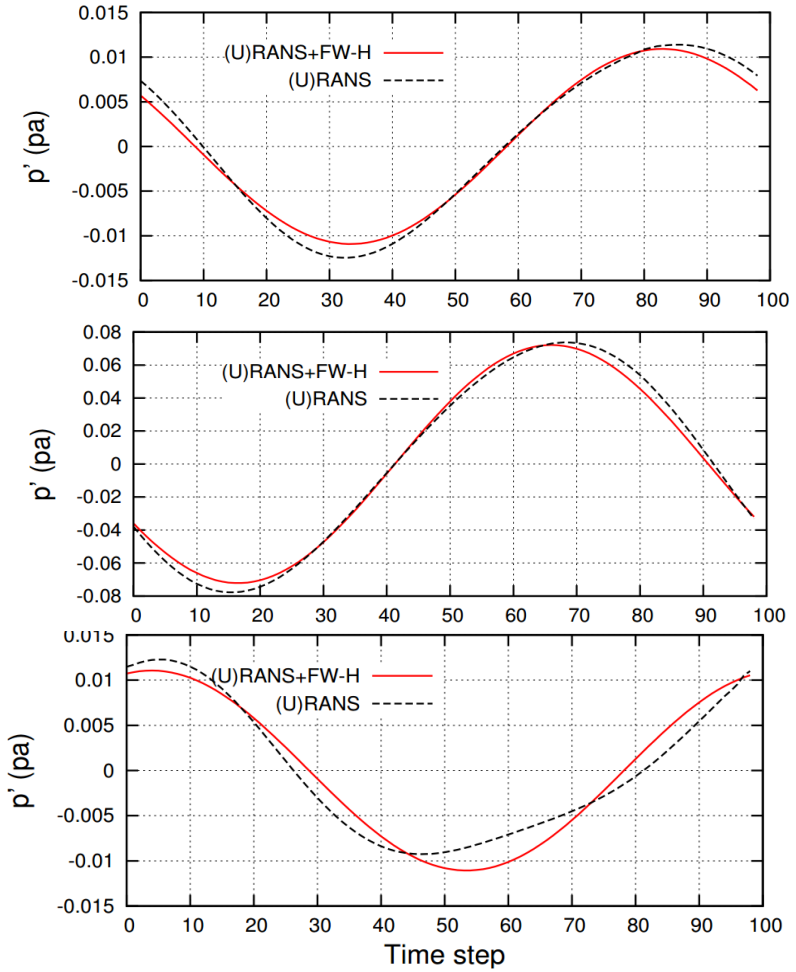

Prof. K.C. Giannakoglou, kgianna@mail.ntua.gr, Dr. V.G. Asouti, vasouti@mail.ntua.gr

Aeroacoustic ShpO of a Turbofan Intake(3/5)

- **Single circumferential row of receivers.**
- **~70% reduction in the noise objective**
- **Reduced amplitude of sound pressure**
- **Max. reduction in directional noise by ~10 dB**
- **Slightly worse aerodynamic performance. Higher Pt losses by ~0.6%.**

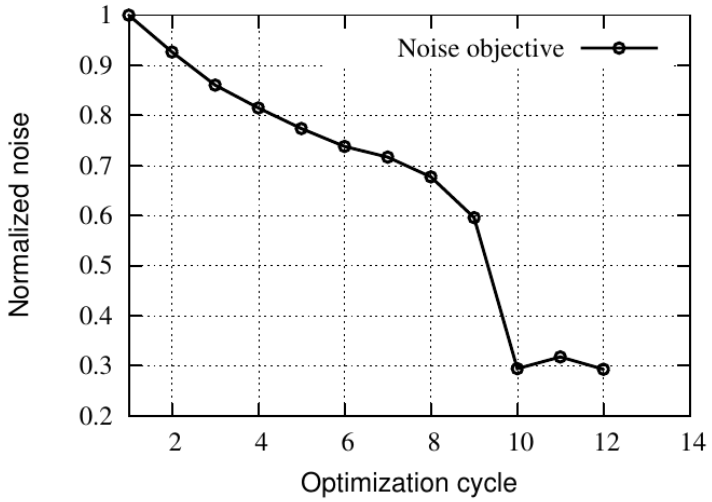

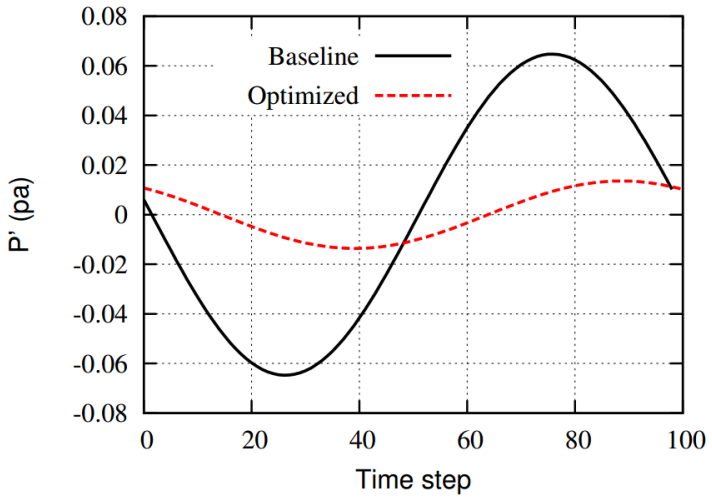

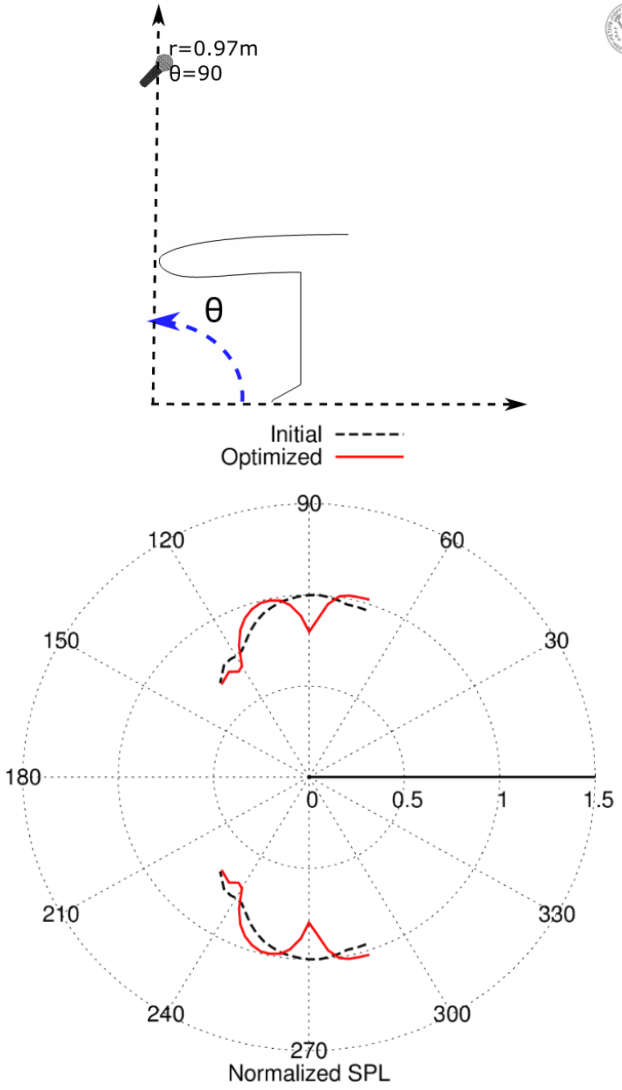

Aeroacoustic ShpO of a Turbofan Intake (4/5)

- **Three circumferential rows of receivers.**
- **~20% reduction in the noise objective.**
- **Reduced amplitude of sound pressure for all rows.**
- **Directional noise reduction with max. reduction ~2.5 dB.**
- **Slightly better aerodynamic performance. ~0.12% reduced Pt losses.**

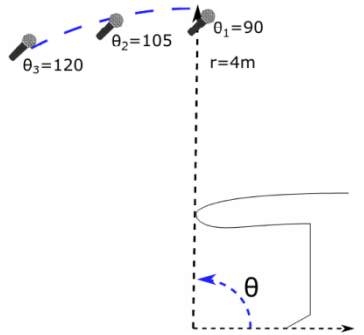

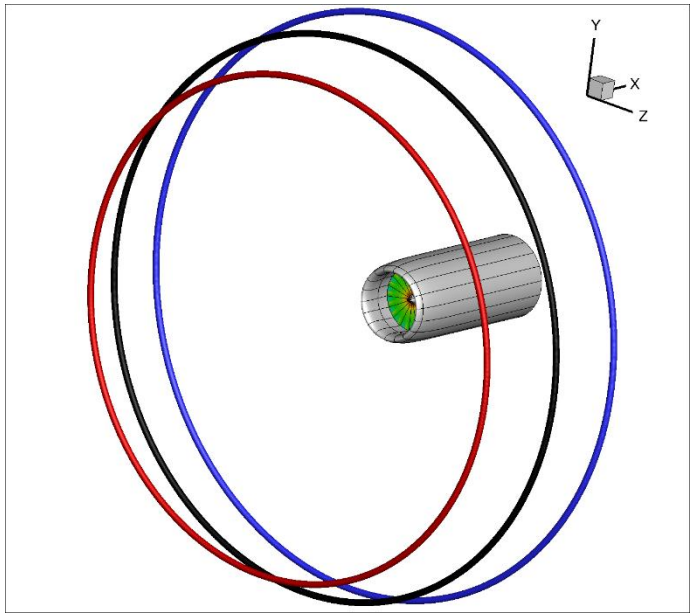

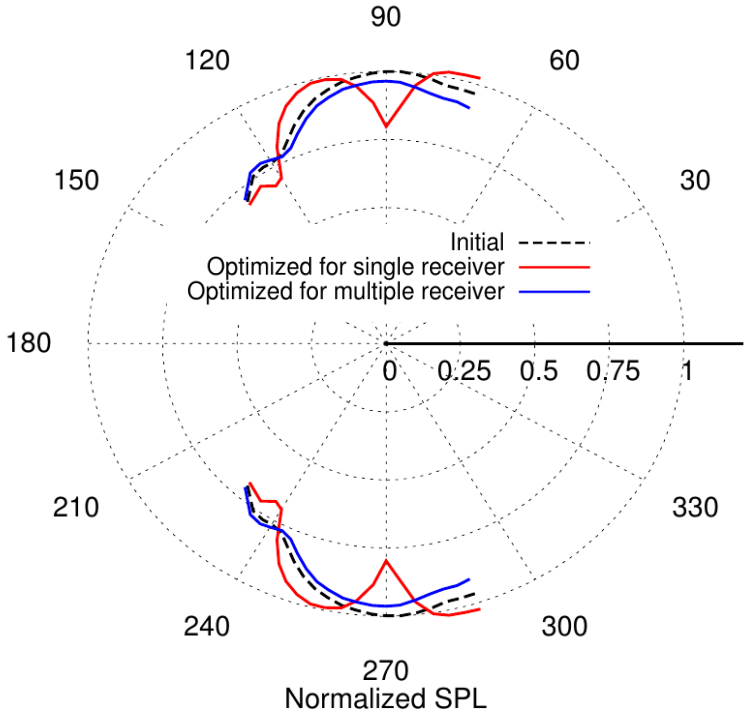

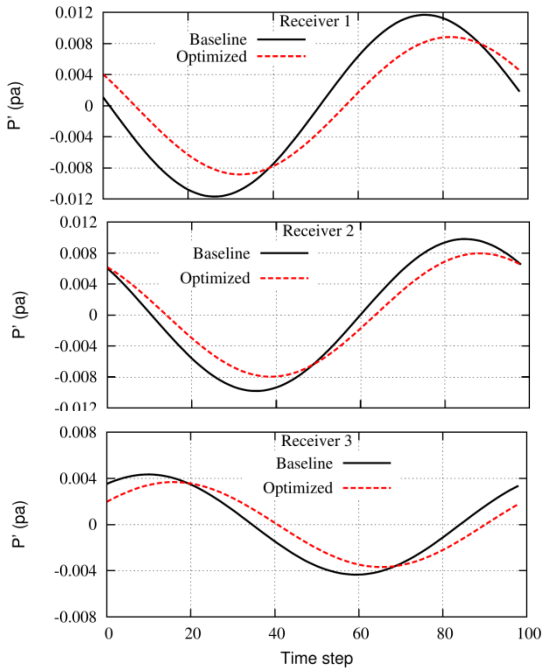

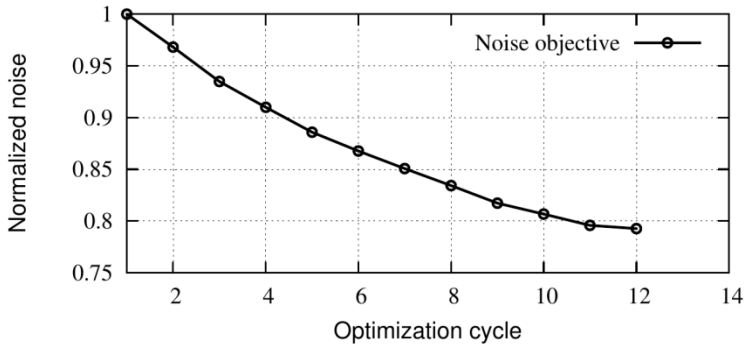

Aeroacoustic ShpO of a Turbofan Intake (5/5)

Aeroacoustic optimisation
1 Circumferential Row of Receivers

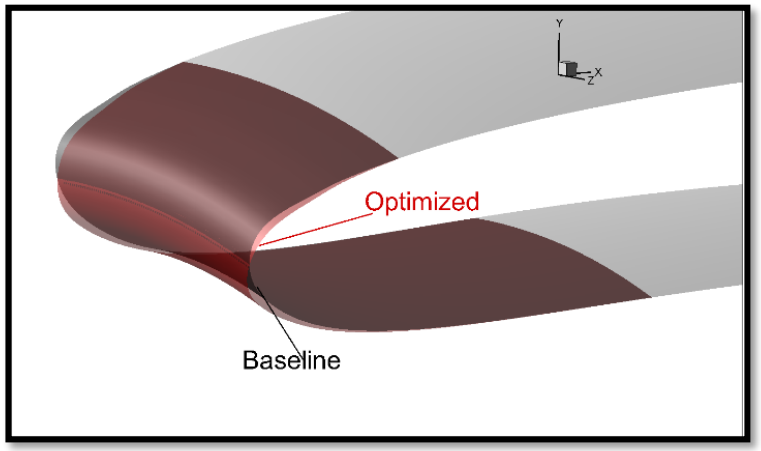

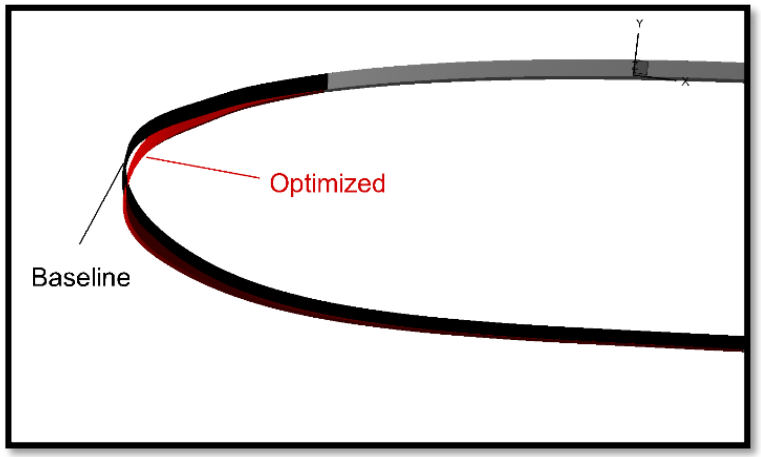

Aeroacoustic optimisation
3 Circumferential Rows of Receivers

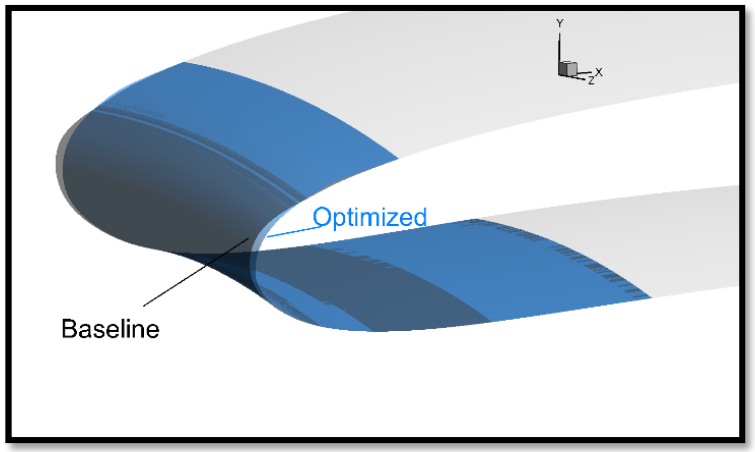

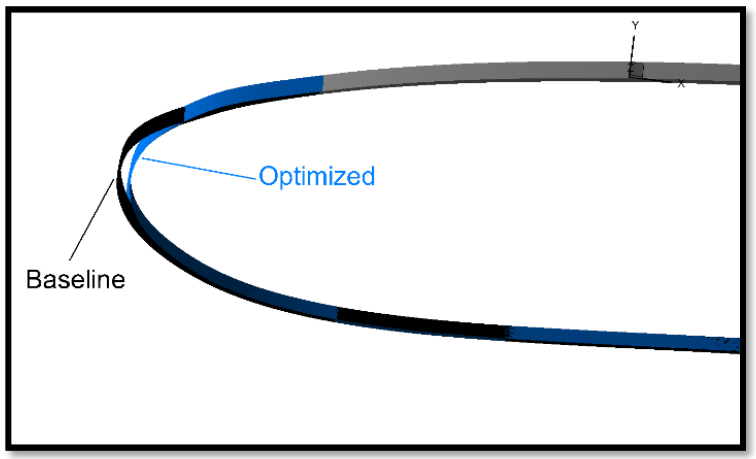

Aerodynamic optimisation

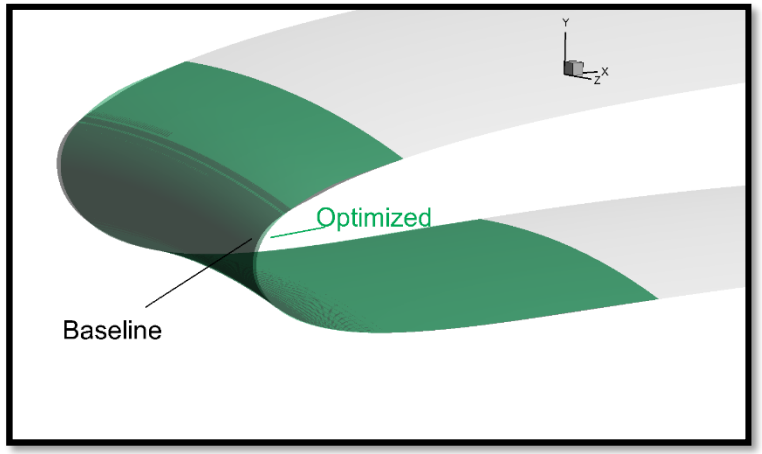

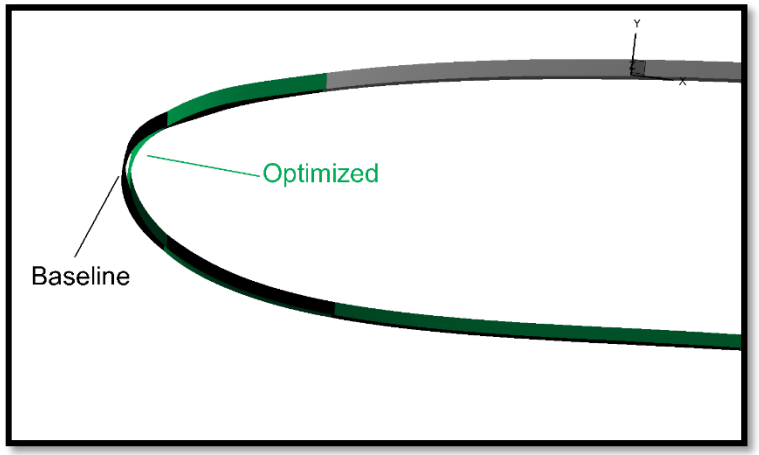

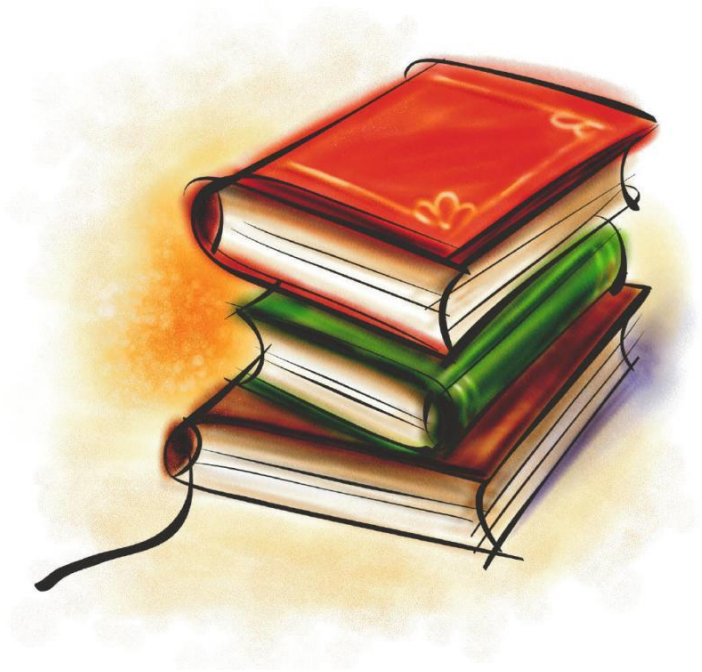

Aerostructural Optimisation

Prof. K.C. Giannakoglou, kgianna@mail.ntua.gr, Dr. V.G. Asouti, vasouti@mail.ntua.gr

Aerostructural ShpO Workflow

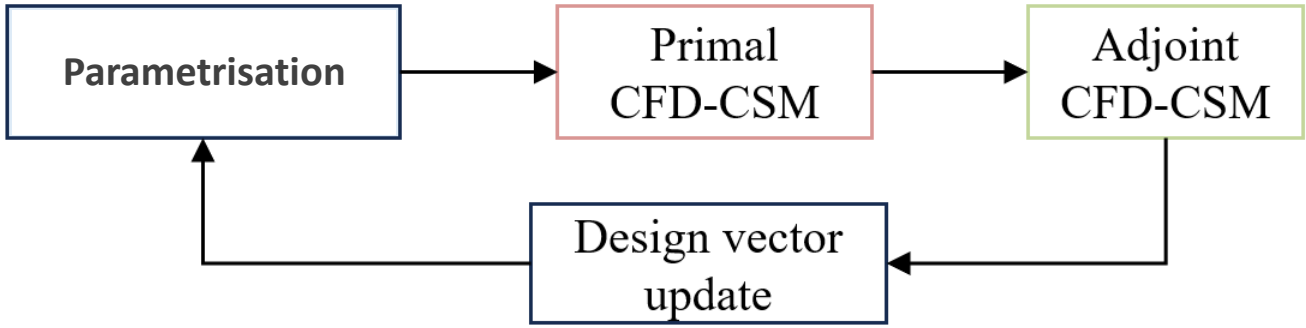

CFD-CSM primal loop

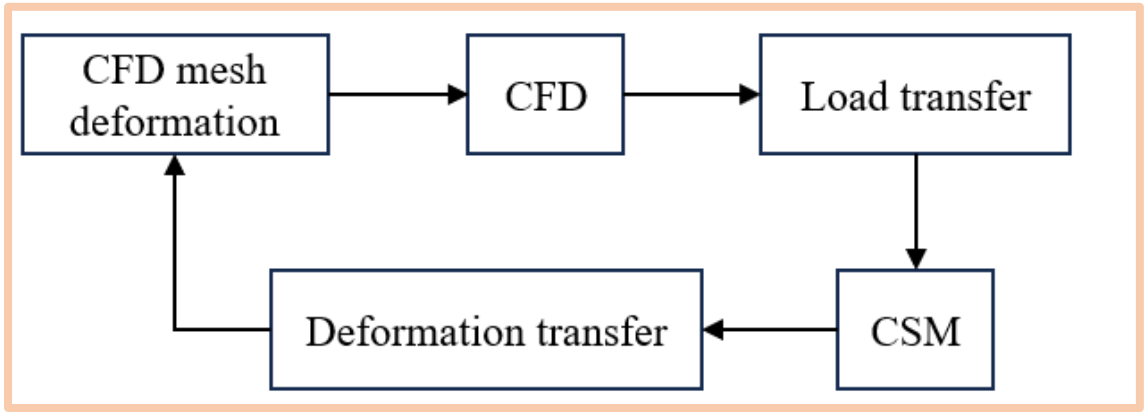

CFD-CSM adjoint loop

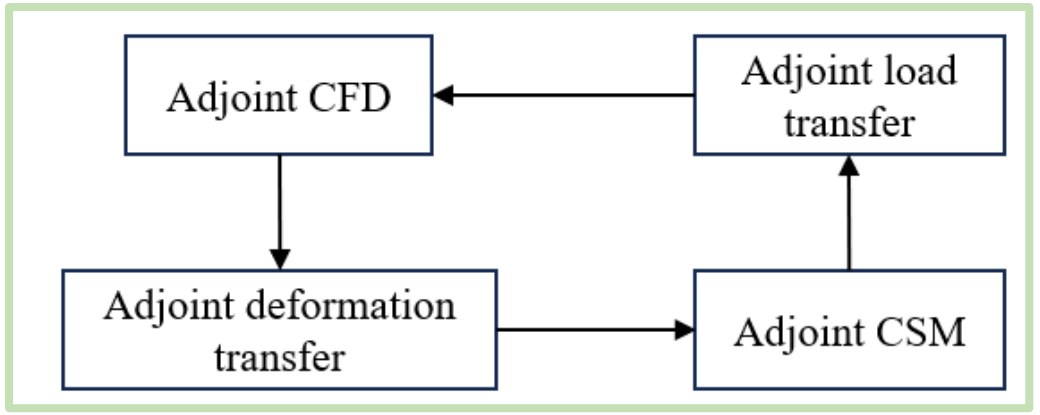

Aerostructural Optimisation of a Generic Business Jet (1/4)

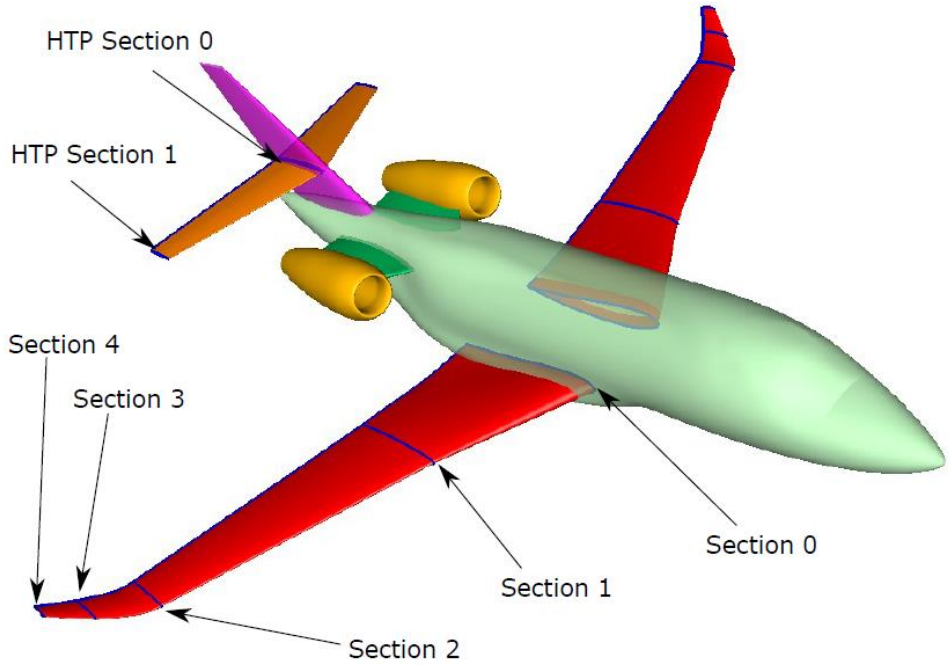

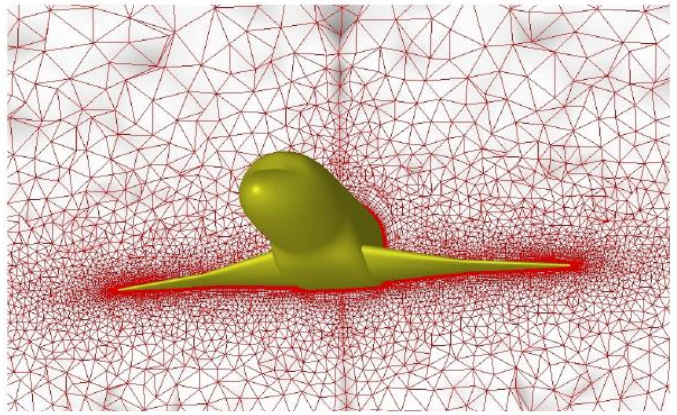

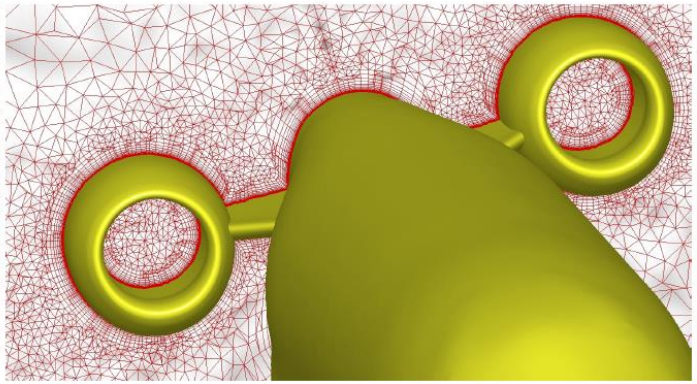

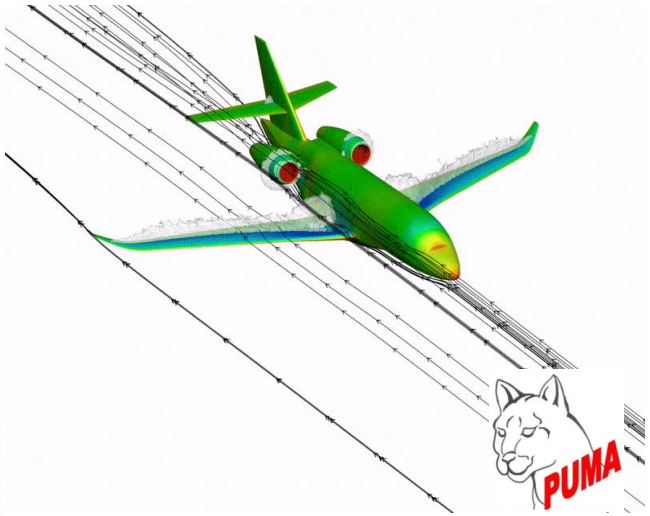

Sections of the wing and HTP directly controlled by the design variables. In specific: b1 (b5), b2 (b6) and b3 (b7) control the twist (trailing edge camber) of sections 0, 1 and 2. b4 (b8) controls the twist (trailing edge camber) of both sections 3 and 4. b9 controls the rotation of both (0 and 1) HTP sections.

Studies performed in collaboration with (& with data provided by)

DASSAULT AVIATION

Research funded by MADELEINE

On the Accuracy of the Computed Sensitivity Derivatives (2/4)

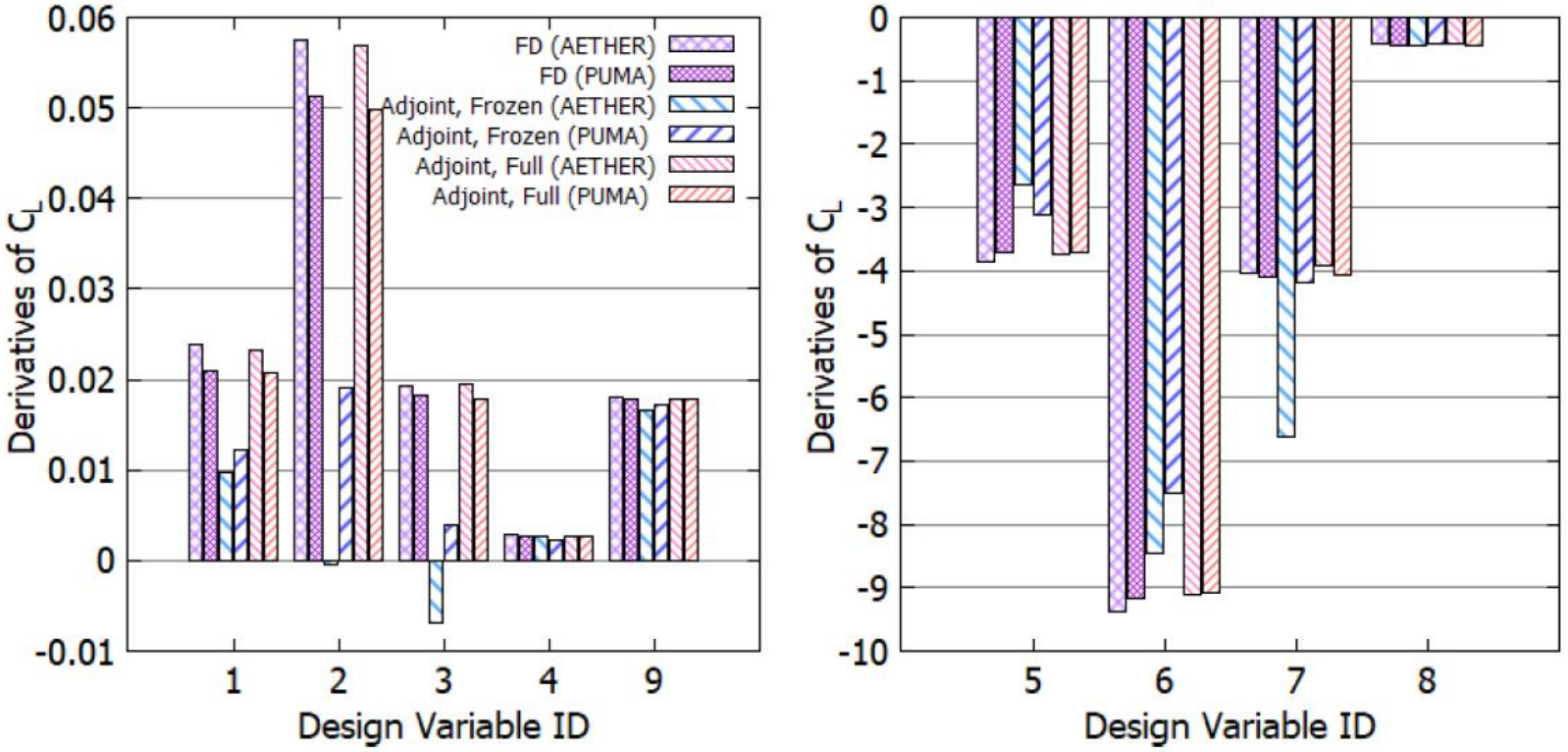

Studies performed in collaboration with (& with data provided by)

DASSAULT AVIATION

C_L SDs of w.r.t. the 5 design variables (b1 to b4 and b9) controlling the wing twist distribution and the HTP rotation (left) and the other 4 design variables (b5 to b8) controlling the wing's trailing edge camber distribution (right). The SDs computed by the adjoint of PUMA (continuous, finite volumes; by NTUA) and AETHER (discrete, finite elements; by DASSAULT AVIATION) are compared with FDs, at M=0.82, AoA=2.5deg.

Research funded by MADELEINE

Aerostructural Optimisation of a Generic Business Jet (3/4)

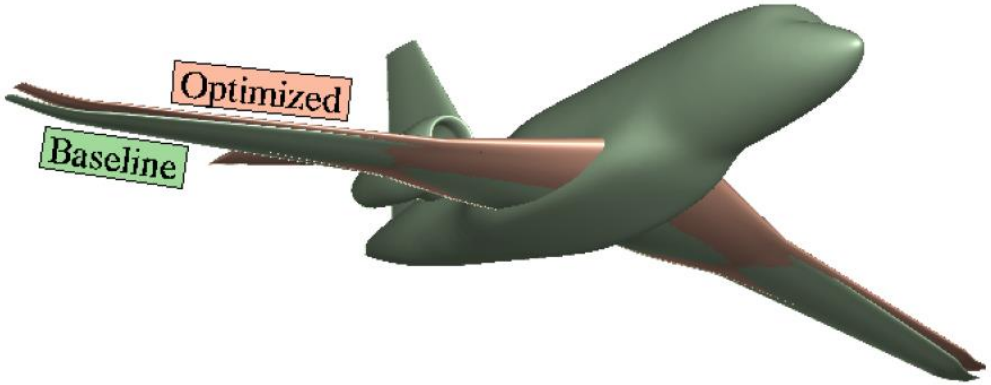

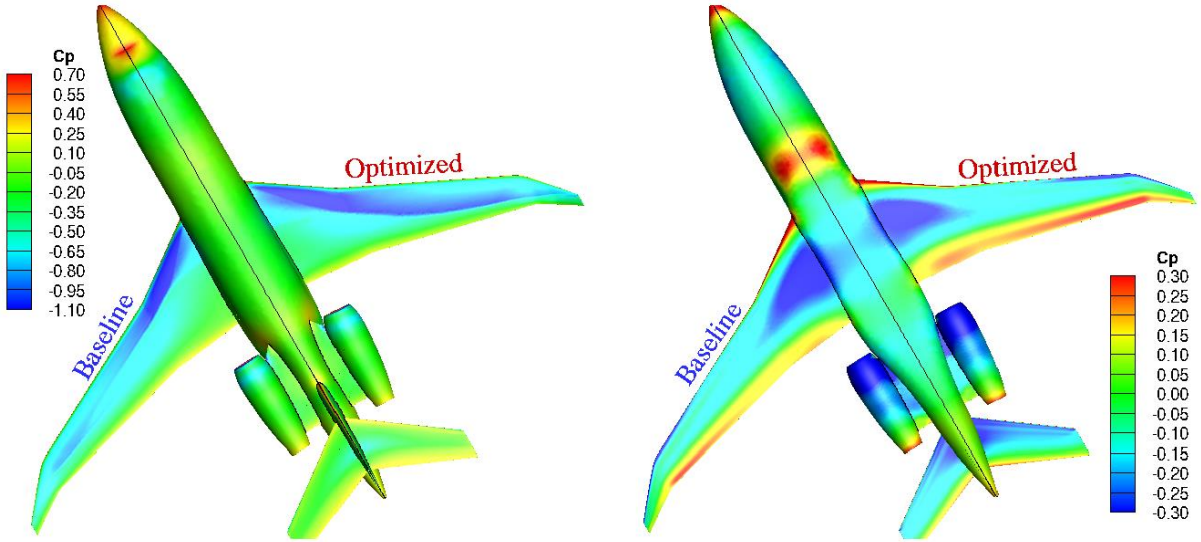

Aerostructural ShpO using the GPU-accelerated PUMA (CFD) code (continuous adjoint) and a commercial CSM S/W (discrete adjoint). Target: min. Fuel Burn, with constraints on C_L & C_M.

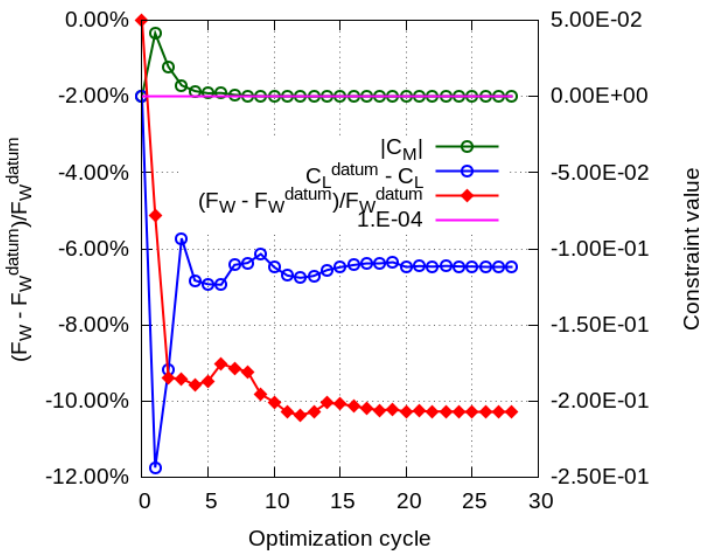

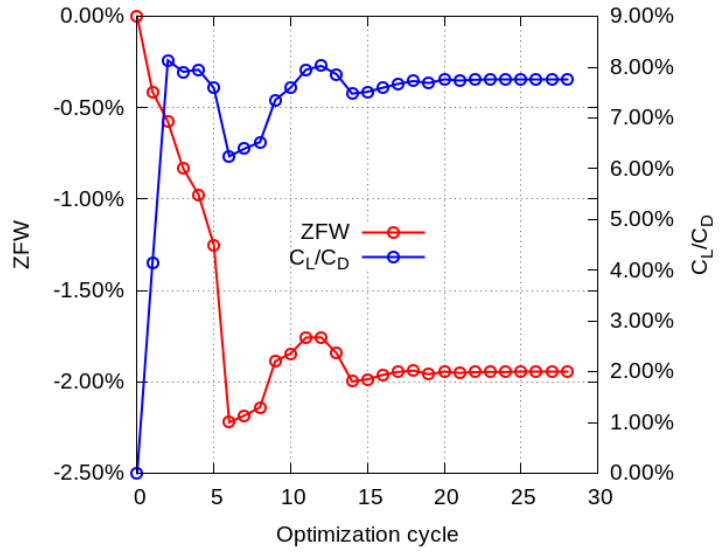

Pressure coefficient fields computed on the suction (left) and pressure (right) side for the baseline and the aerostructurally optimised aircrafts.

10% reduction in fuel burn
8% increase in C_L/C_D
2% reduction in ZFW

Research funded by MADELEINE

Aerostructural Optimisation of a Generic Business Jet (4/4)

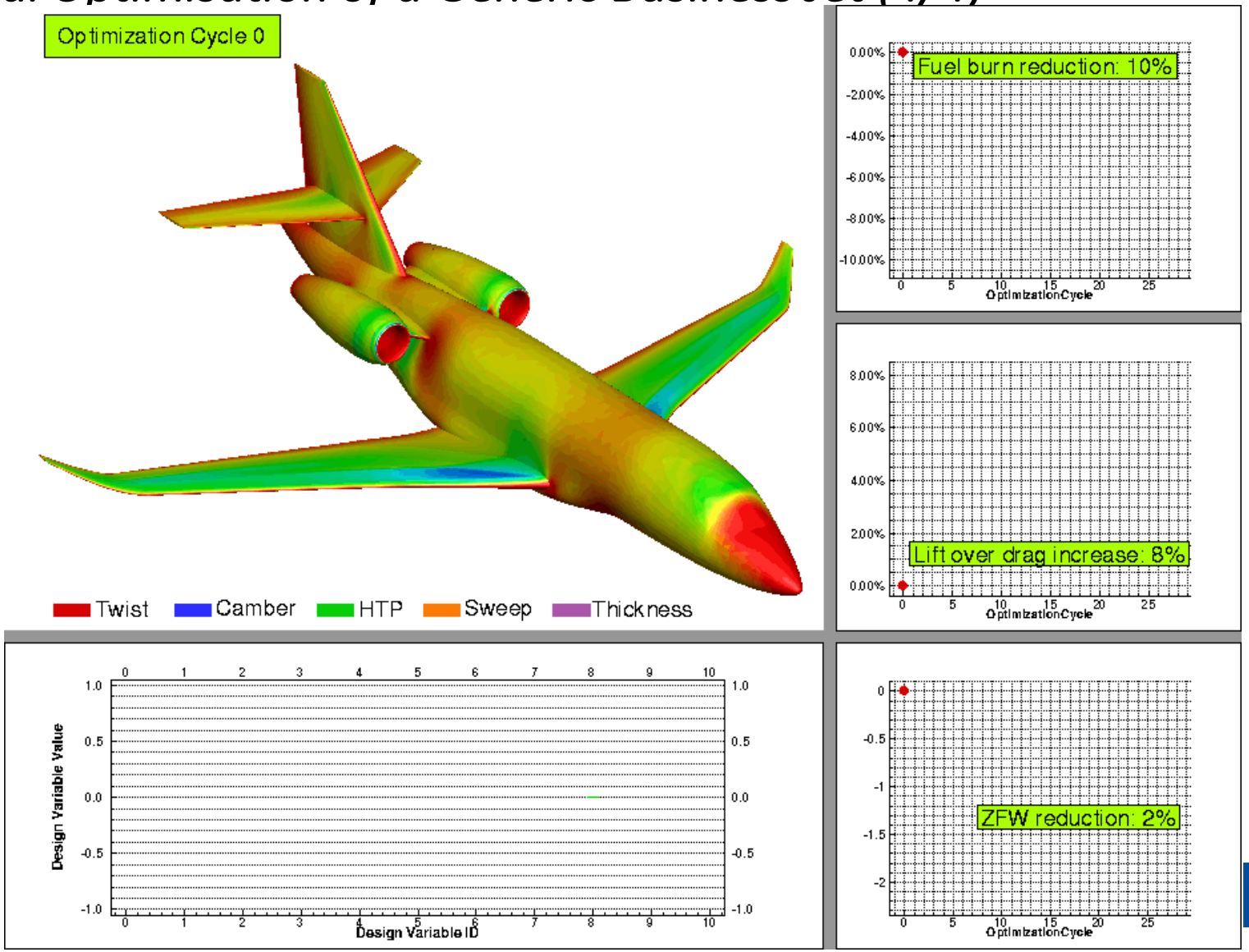

Studies performed in collaboration with (& with data provided by)

DASSAULT AVIATION

Prof. K.C. Giannakoglou, kgianna@mail.ntua.gr, Dr. V.G. Asouti, vasouti@mail.ntua.gr

Aerostructural ShpO Workflow

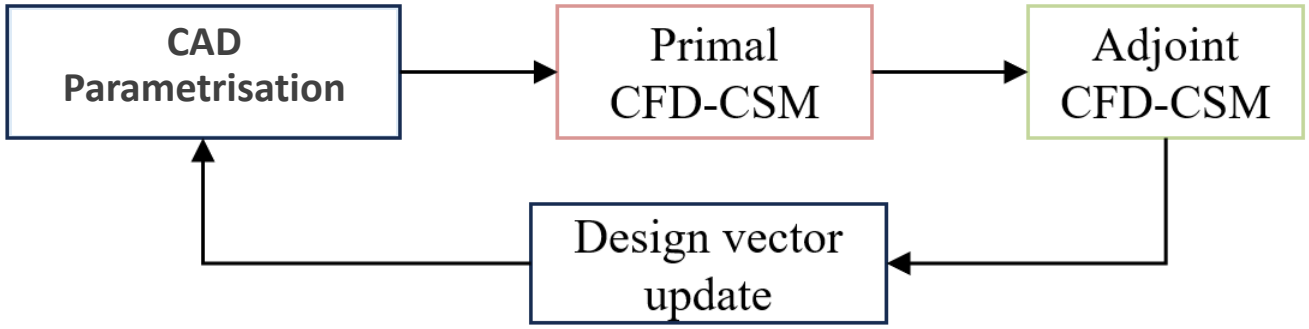

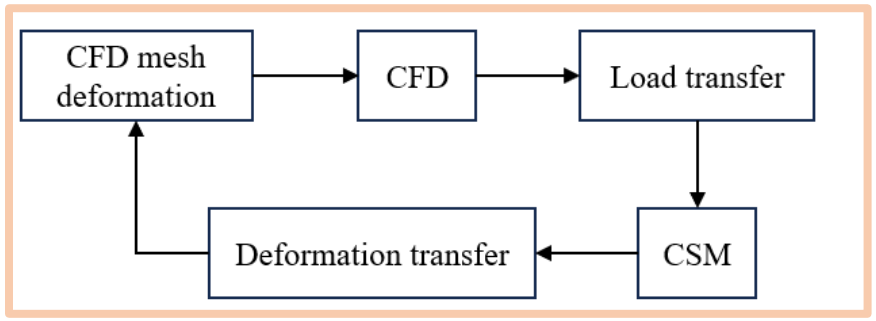

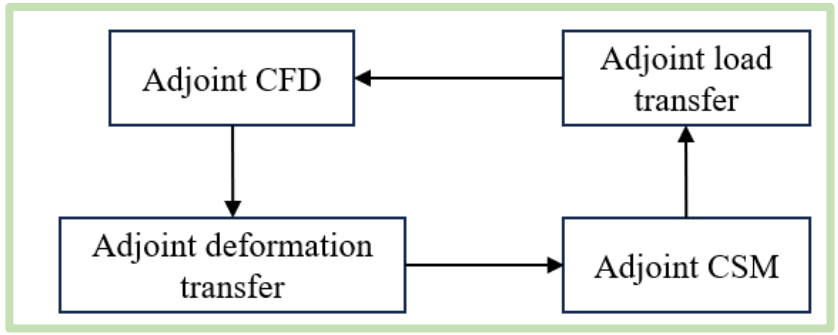

The λ-DNN and the ShpO Loop

Neural Comput Appl, 34:843-854, 2022.

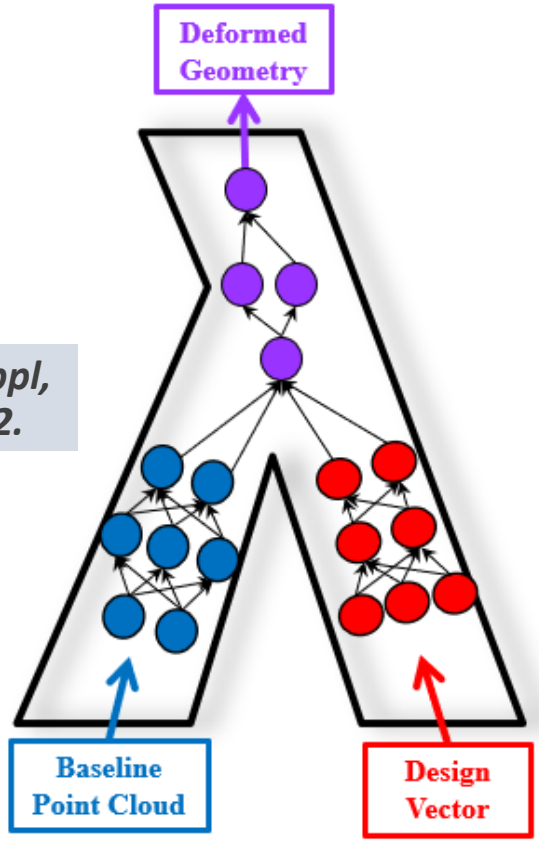

(surface nodes different from those of the CFD mesh)

(CAD variables b_n)

$$\frac{dx_i}{db_n^{CAD}}$$

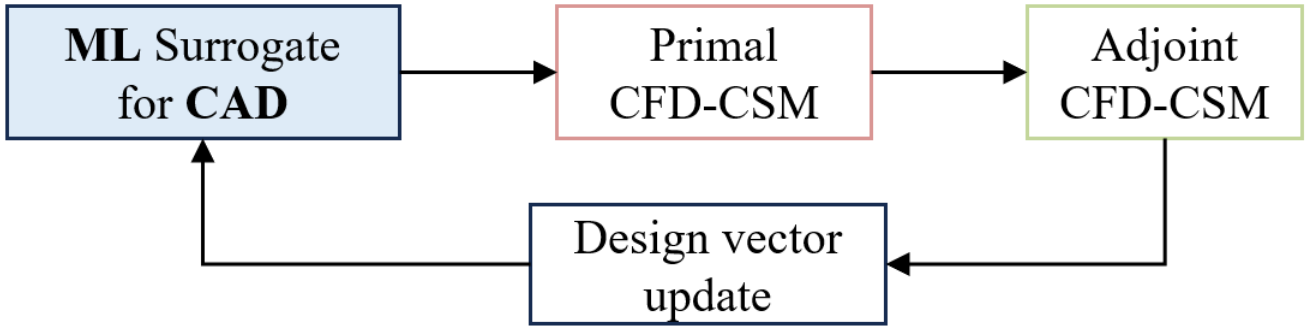

$$\frac{dF}{db_n^{CAD}} = \frac{dF}{dx_i} \cdot \frac{dx_i}{db_n^{CAD}}$$

From the Adjoint!

From the differentiated ML Surrogate

Training the λ-DNN (Surrogate CAD) – Optimal Configuration

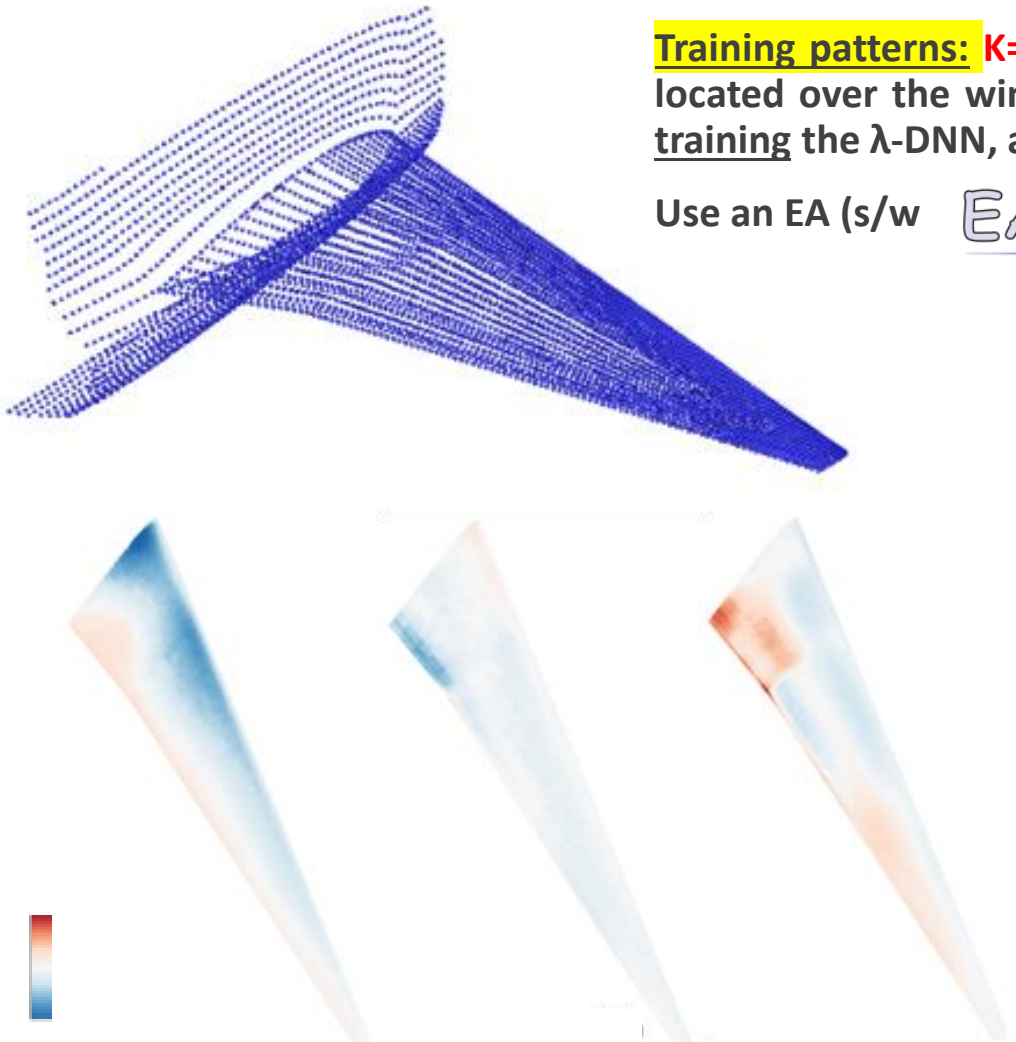

Prediction error of the λ-DNNs at the x, y and z directions.

Training patterns: **K=1992** aircraft shapes (**N=53** design variables → **P=7080** nodes), located over the wing and the wing-to-fuselage fairing. **1972** shapes were used for training the λ-DNN, and **20** (plus the baseline; **21**, in total) for testing.

Use an EA (s/w EASY) to optimise the ML hyperparameters.

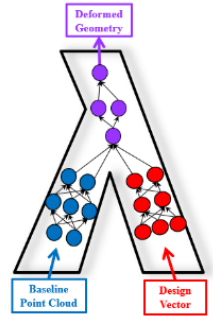

		Layers	Neurons/Layer	Act. Fun.
x	Left input branch	4	128/2048/1024/256	*tanh*
	Right input branch	4	128/1024/2048/256	*tanh*
	Output branch	3	64/128/256	sigmoid
y	Left input branch	5	1024/128/64/256/64	GELU
	Right input branch	4	128/2048/2048/64	GELU
	Output branch	1	256	sigmoid
z	Left input branch	5	32/128/64/64/2048	GELU
	Right input branch	3	256/4096/2048	sigmoid
	Output branch	2	256/1024	sigmoid

Why the λ-DNN? FCNN vs. λ-DNN

Error Bounds 0-4%

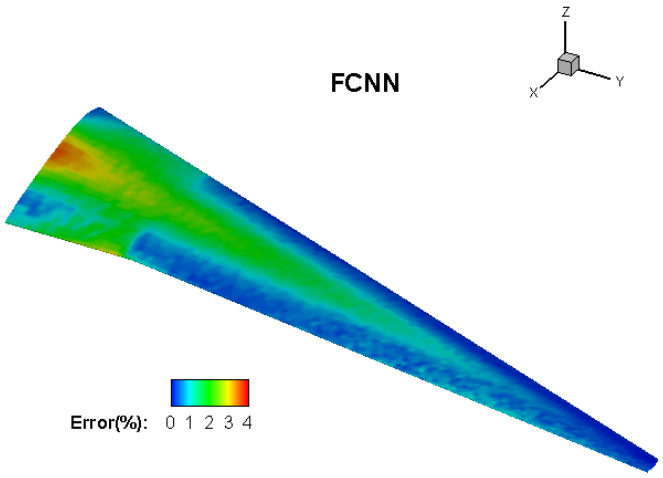

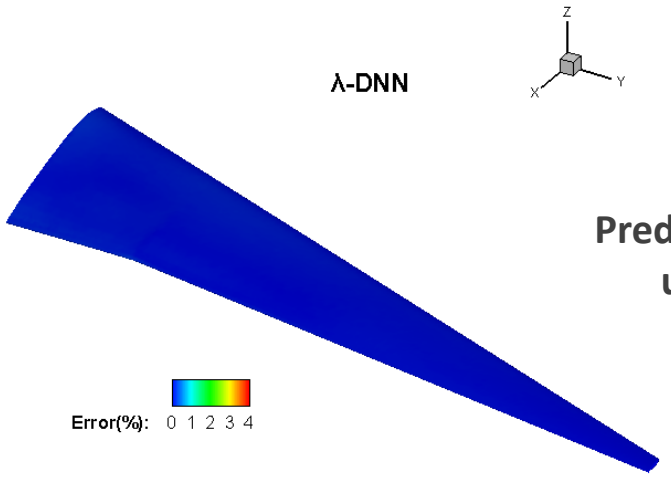

or

Error Bounds 0-0.3%

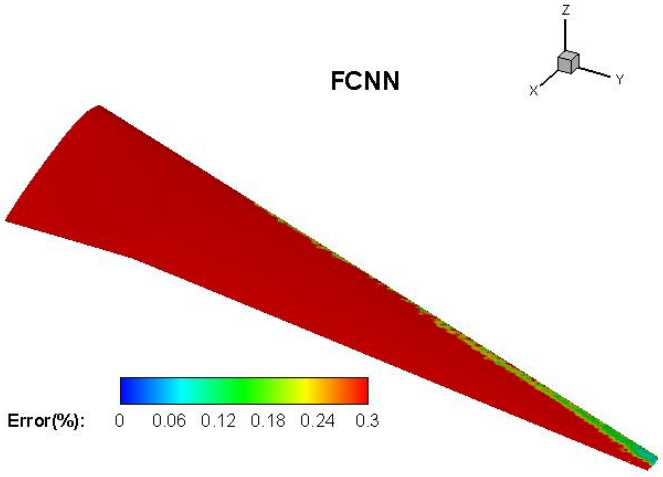

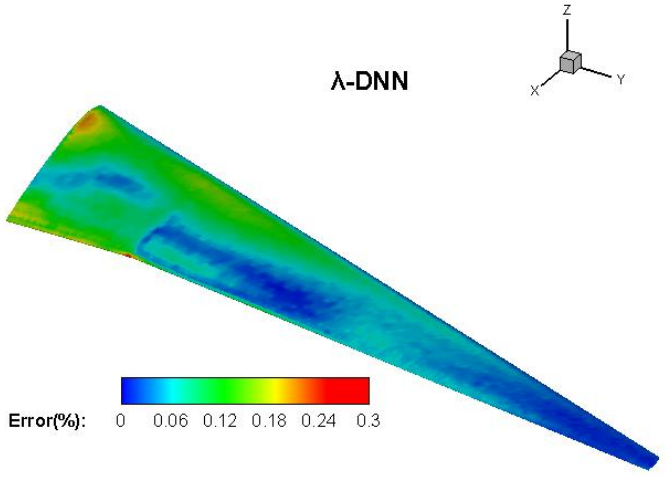

Prediction Error on the Wing Surface using a *FCNN* and the *λ-DNN*.

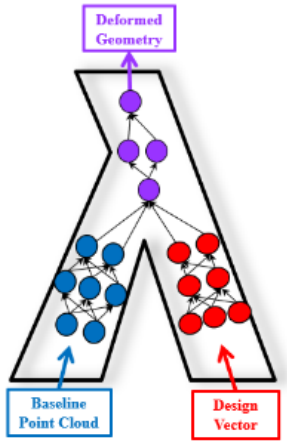

Why predicting δ(x,y,z), rather than (x,y,z) coordinates?

Predict Coordinates

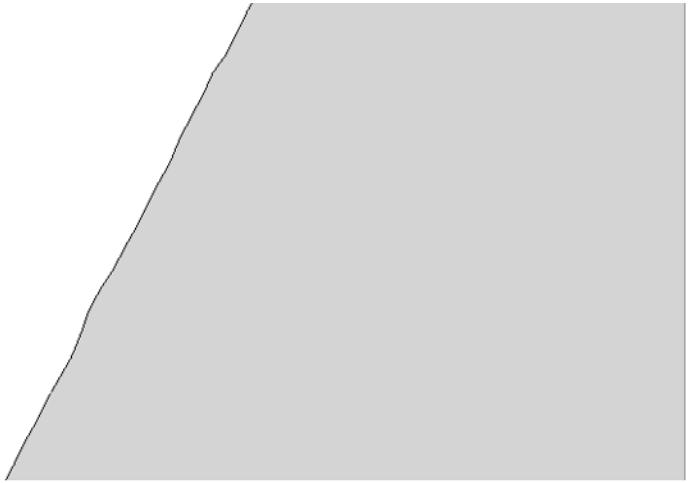

Predict Deviation from Baseline

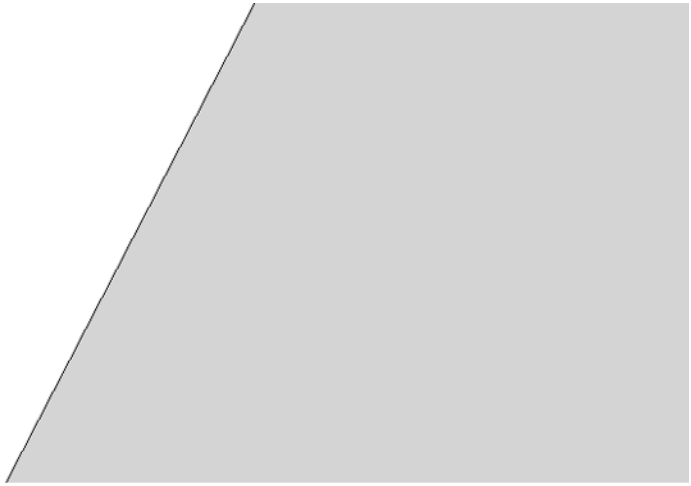

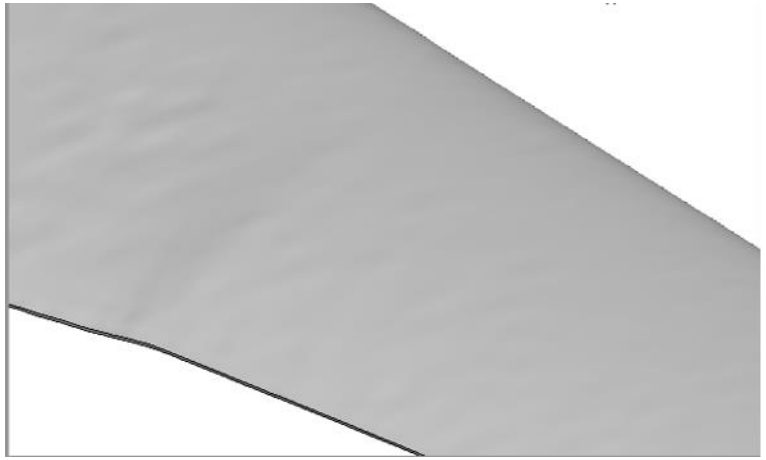

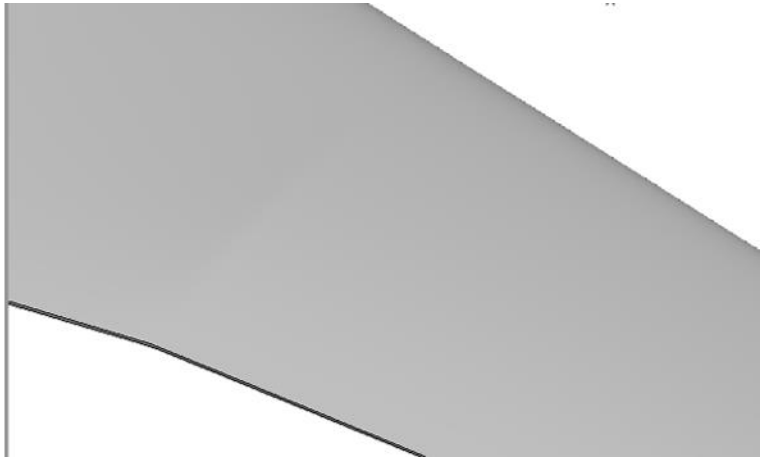

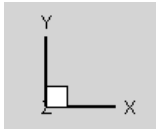

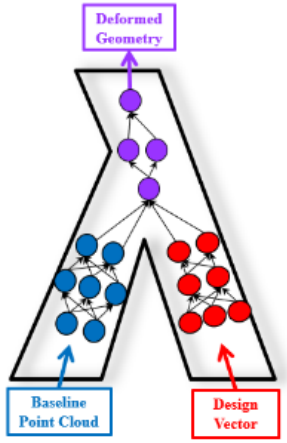

Aerodynamic & Aeroflexible Wing ShpO of the DLR-F25 Aircraft

- **Flight conditions: altitude 36000 ft and M_∞=0.78. Spalart-Allmaras turbulence model (& its adjoint).**
- **Min. C_D subject to C_M=0 or $|C_M|<10^{-4}$; $|C_L-0.59|<10^{-4}$**
- **Adapt the Horizontal Tail Plane (HTP) angle & AoA to meet the two constraints.**

Aeroflexible = fixed structural model; aerodynamic objective/constraints.

Aerorigid = no structural model; pure aerodynamic, i.e. SDO.

DLR-F25

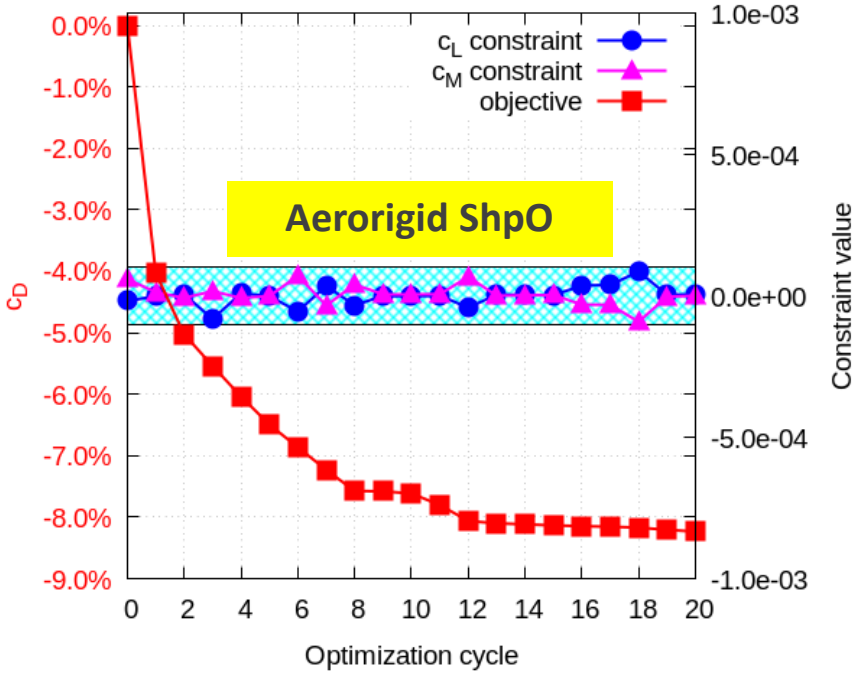

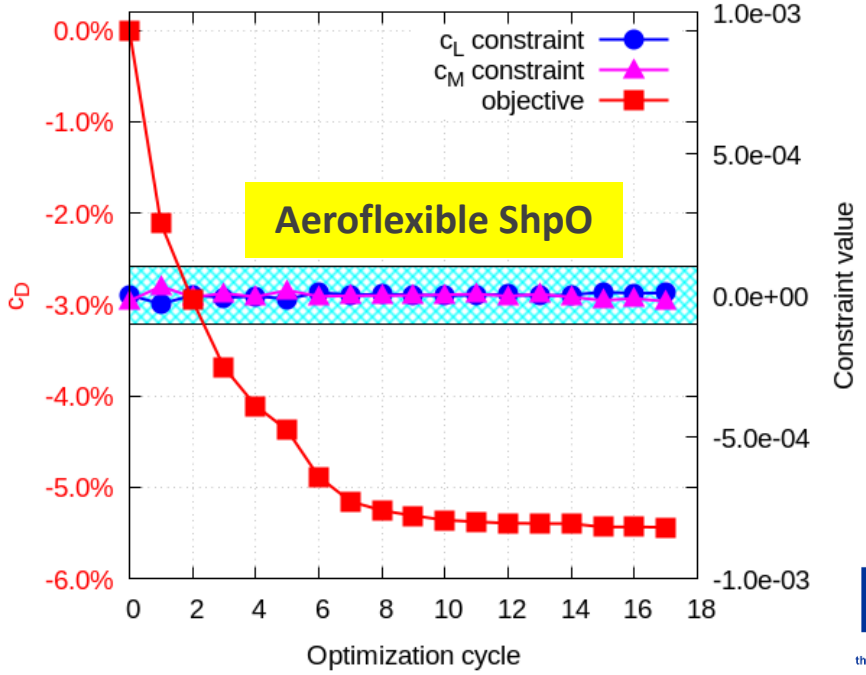

Funded by the European Union

The Aerorigid Optimised Wing

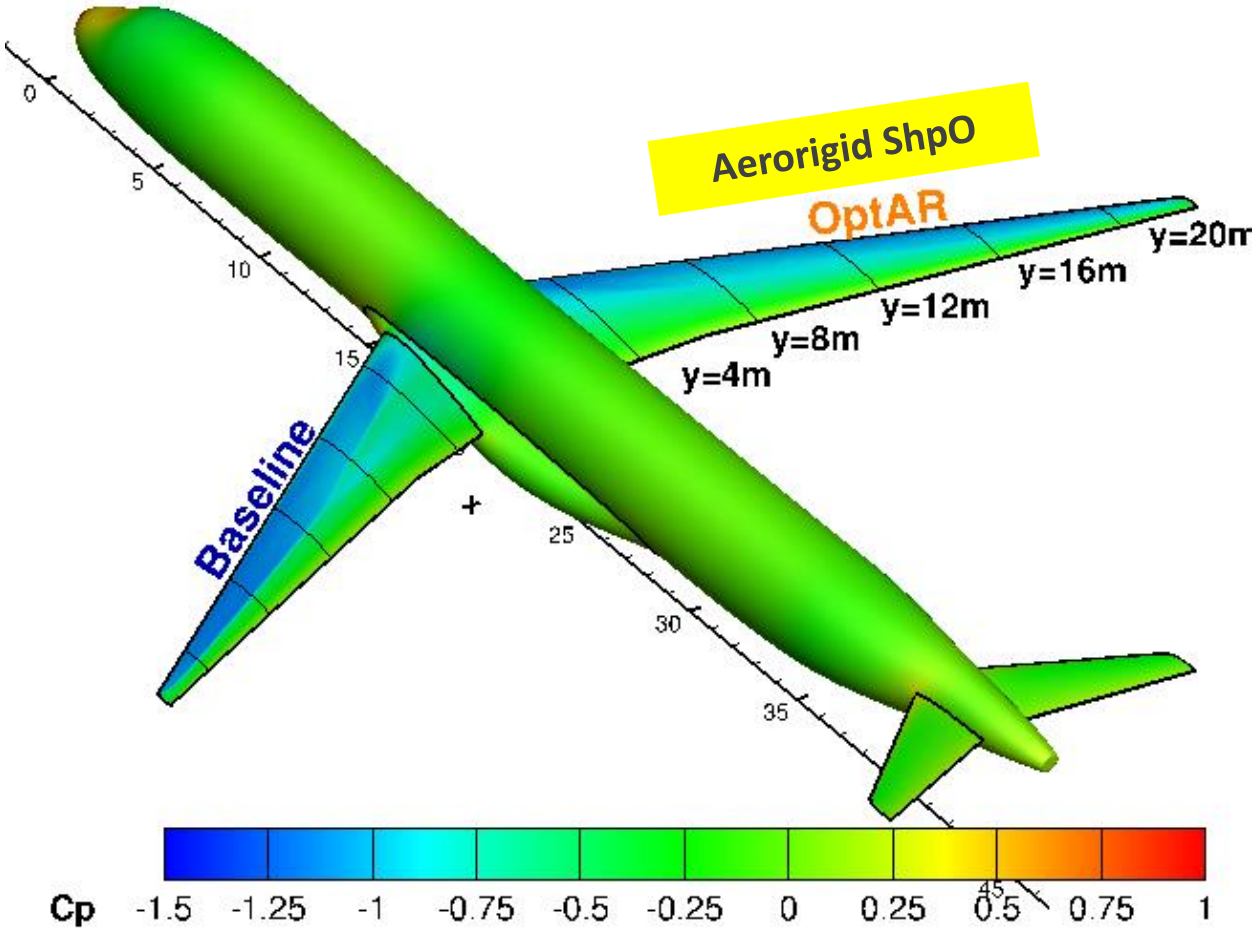

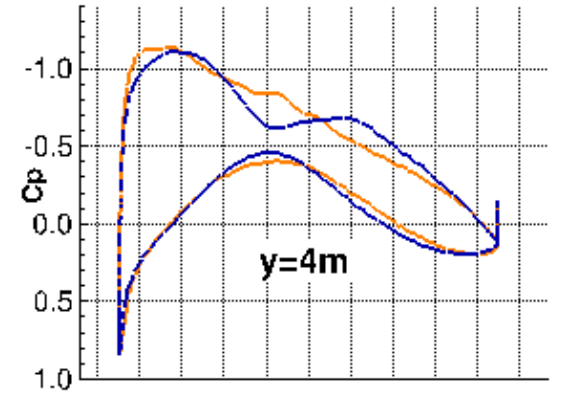

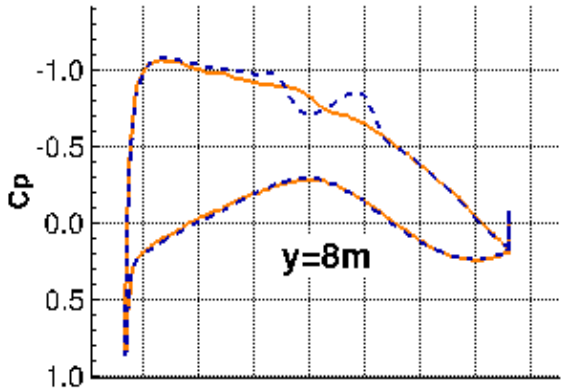

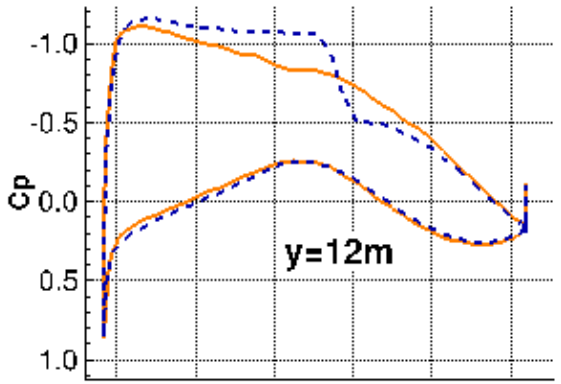

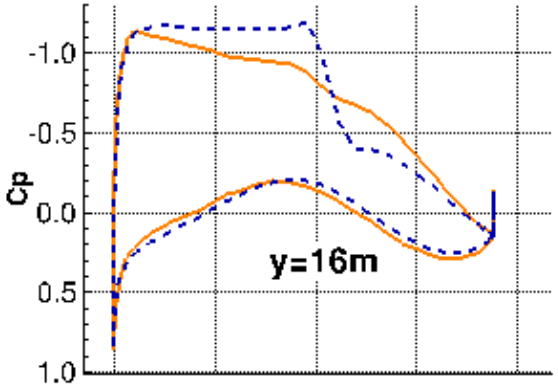

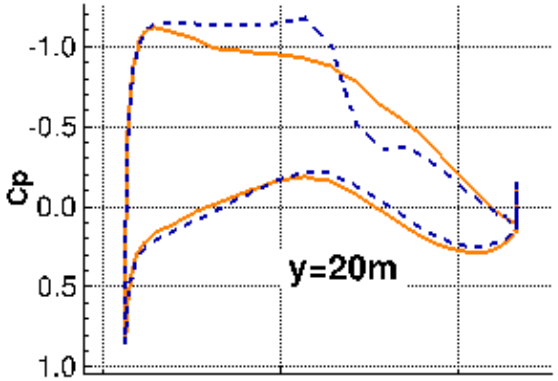

The Aeroflexible Optimised Wing

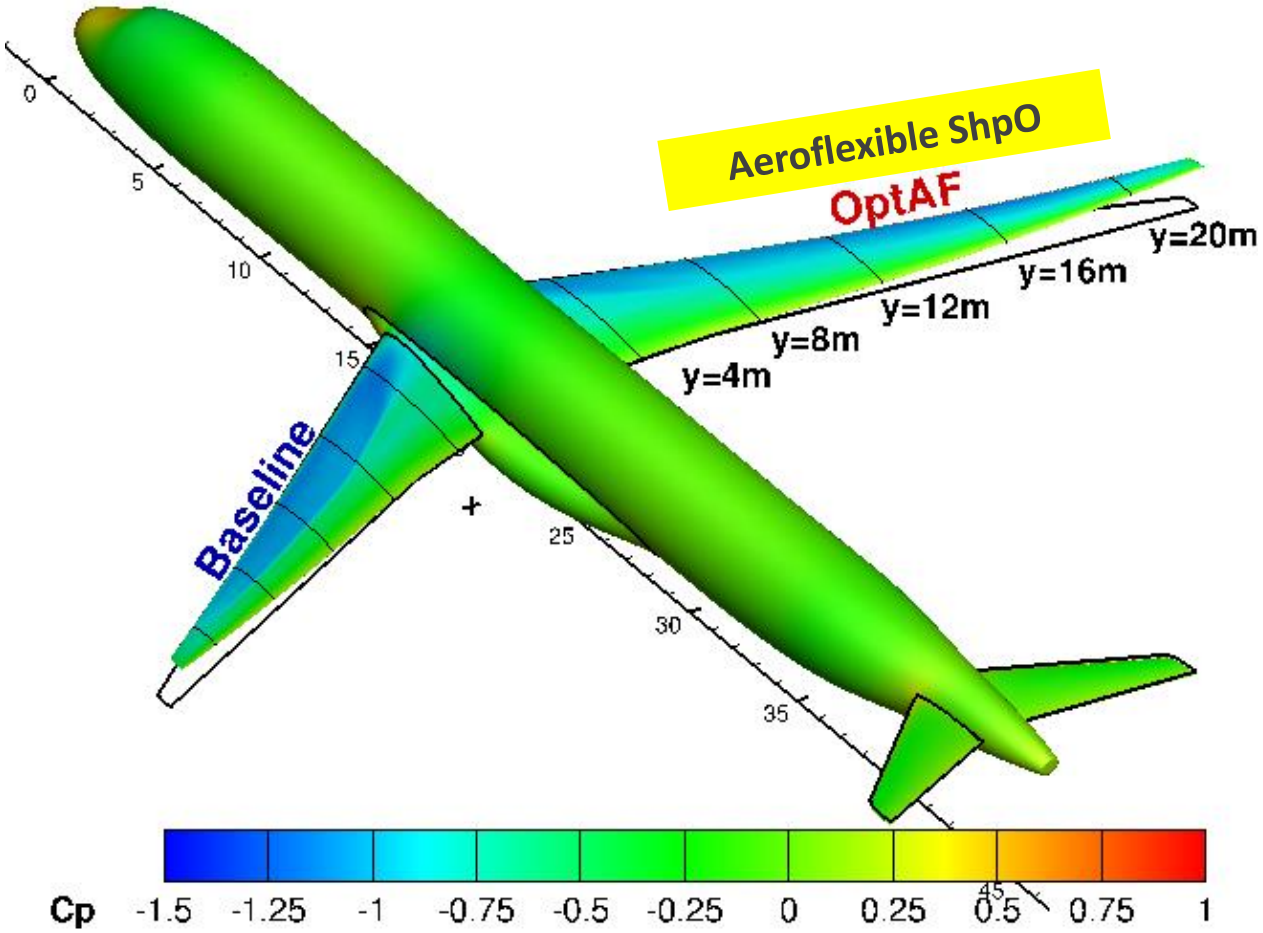

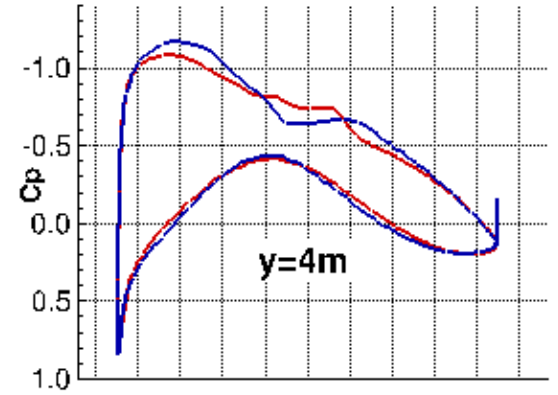

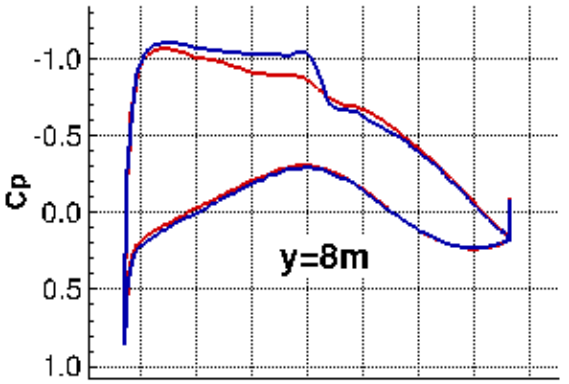

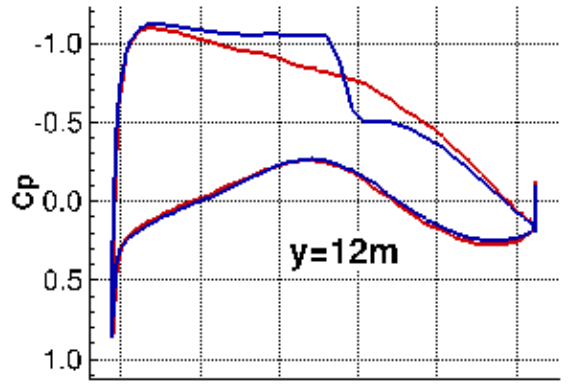

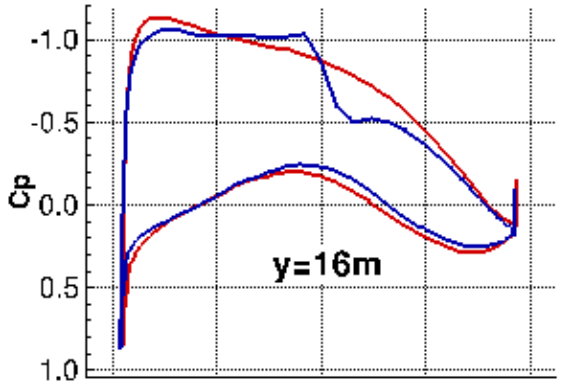

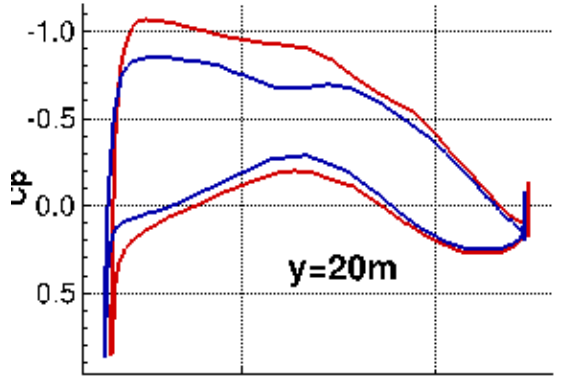

Aerorigid vs. Aeroflexible Wing ShpO

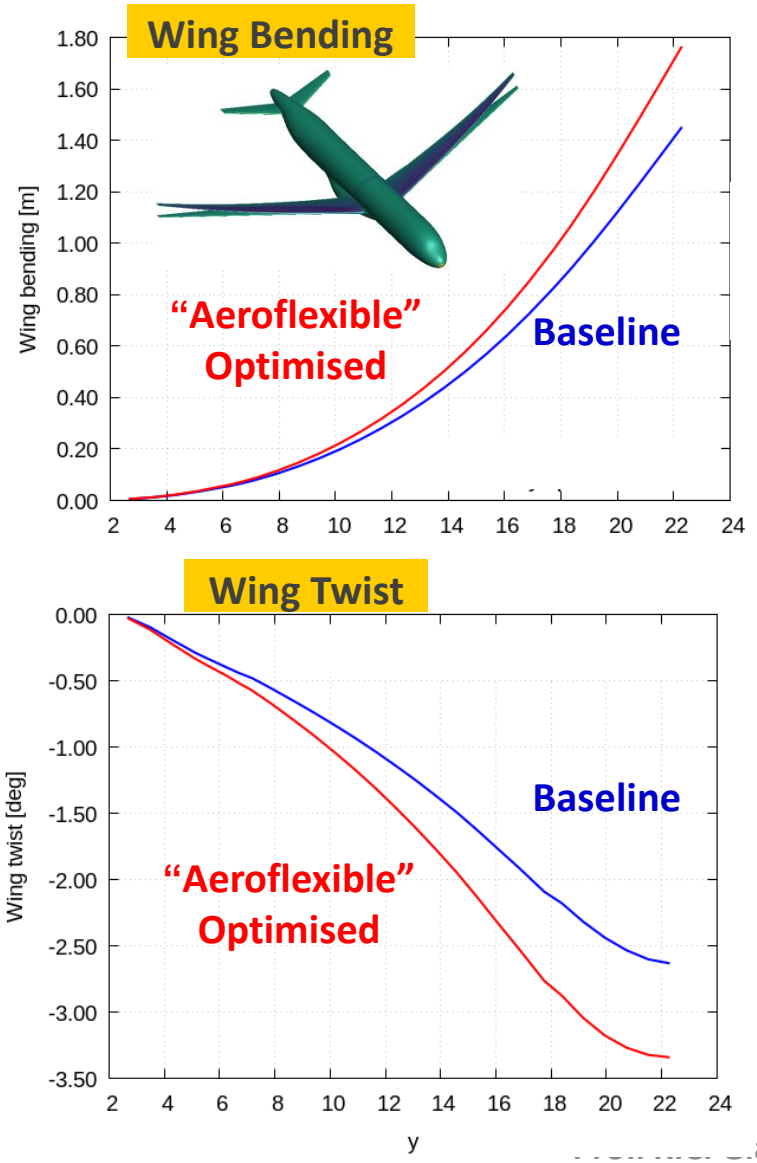

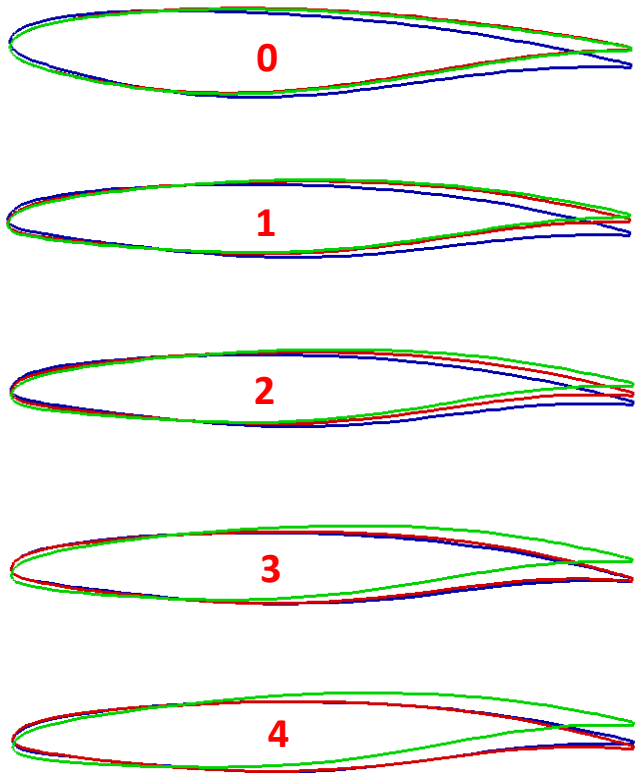

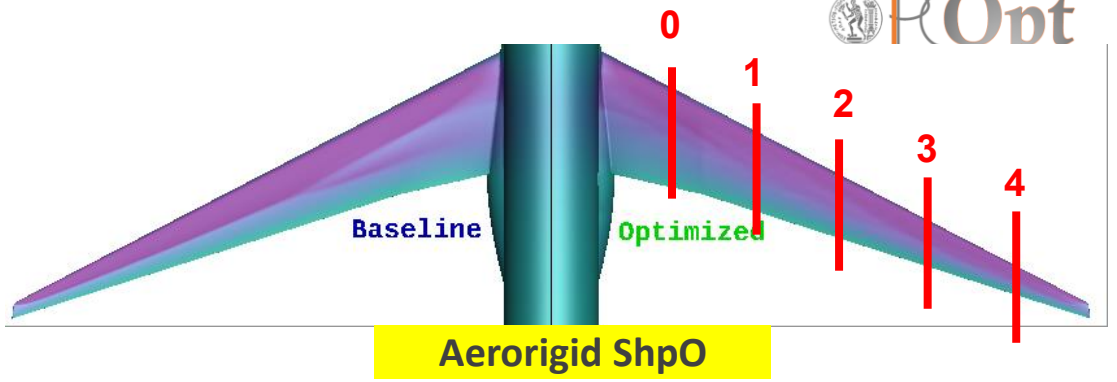

Aerorigid ShpO

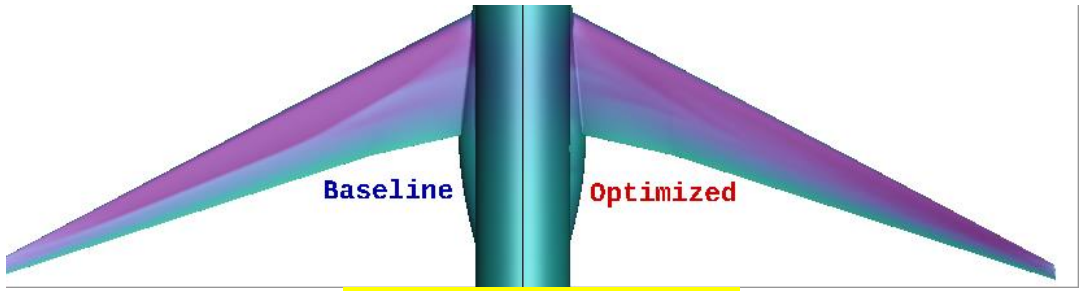

Aeroflexible ShpO

Wing airfoil profiles at different spanwise cross-sections (18%, 35%, 50%, 70%, 90%) for the baseline (blue), the "Aerorigid" (green) and the "Aeroflexible" optimised (red) wings.

annakoglou, kgianna@mail.ntua.gr, Dr. V.G. Asouti, vasouti@mail.ntua.gr

Aerostructural Wing ShpO of the DLR-F25 Aircraft

✓ **Minimize C_D at cruise conditions (same conditions, C_L=0.59), fixed HTP = 0º.**

(a) Empty markers: (new) Aeroflexible optimisation followed by a sizing of the structural model and re-evaluation of aerodynamic performance (OptAS1). Filled marks: Aerostructural optimisation (OptAS2).

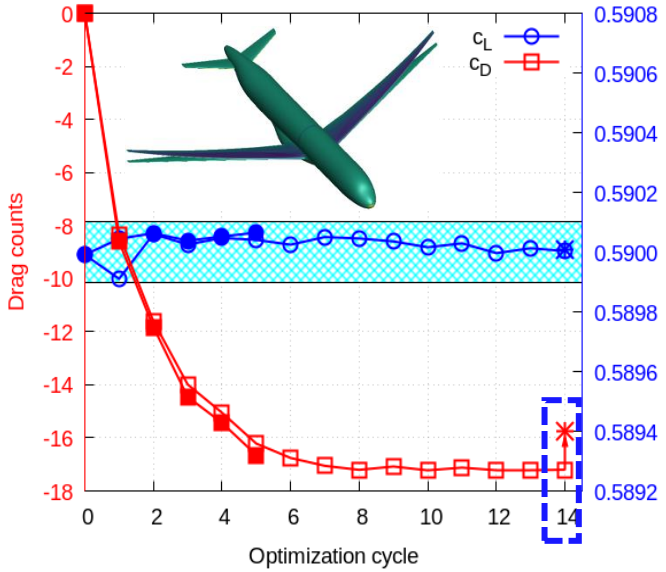

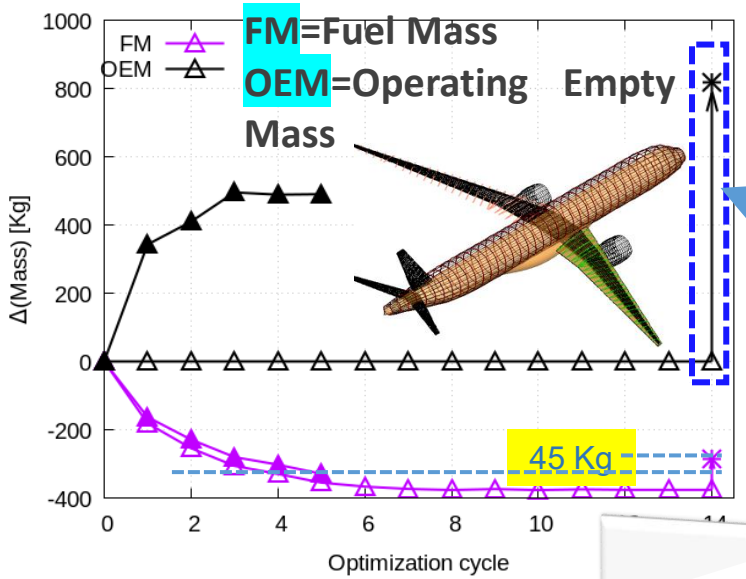

The Aeroflexible optimised wing (blue) is highly deflected, calling for a thicker structure to withstand the resulting structural loads. Thickening the wing structure reduces wingtip deflection, bringing the design closer to the aerostructurally optimised one (red).

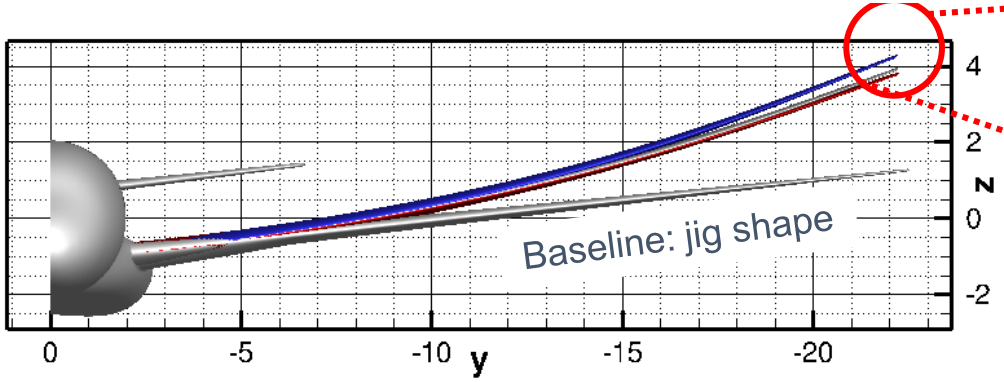

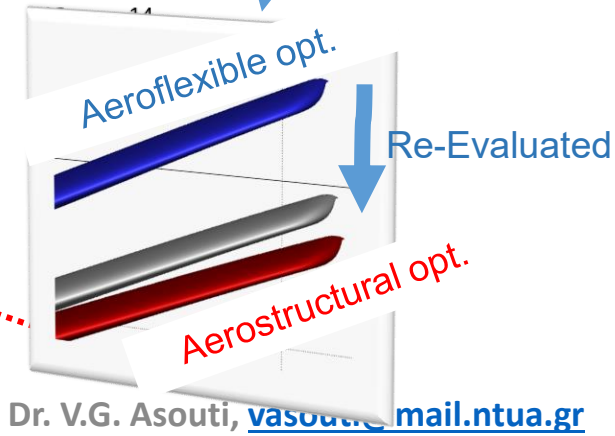

gianna@mail.ntua.gr, Dr. V.G. Asouti, vasouti@mail.ntua.gr

OptAS1 vs. OptAS2

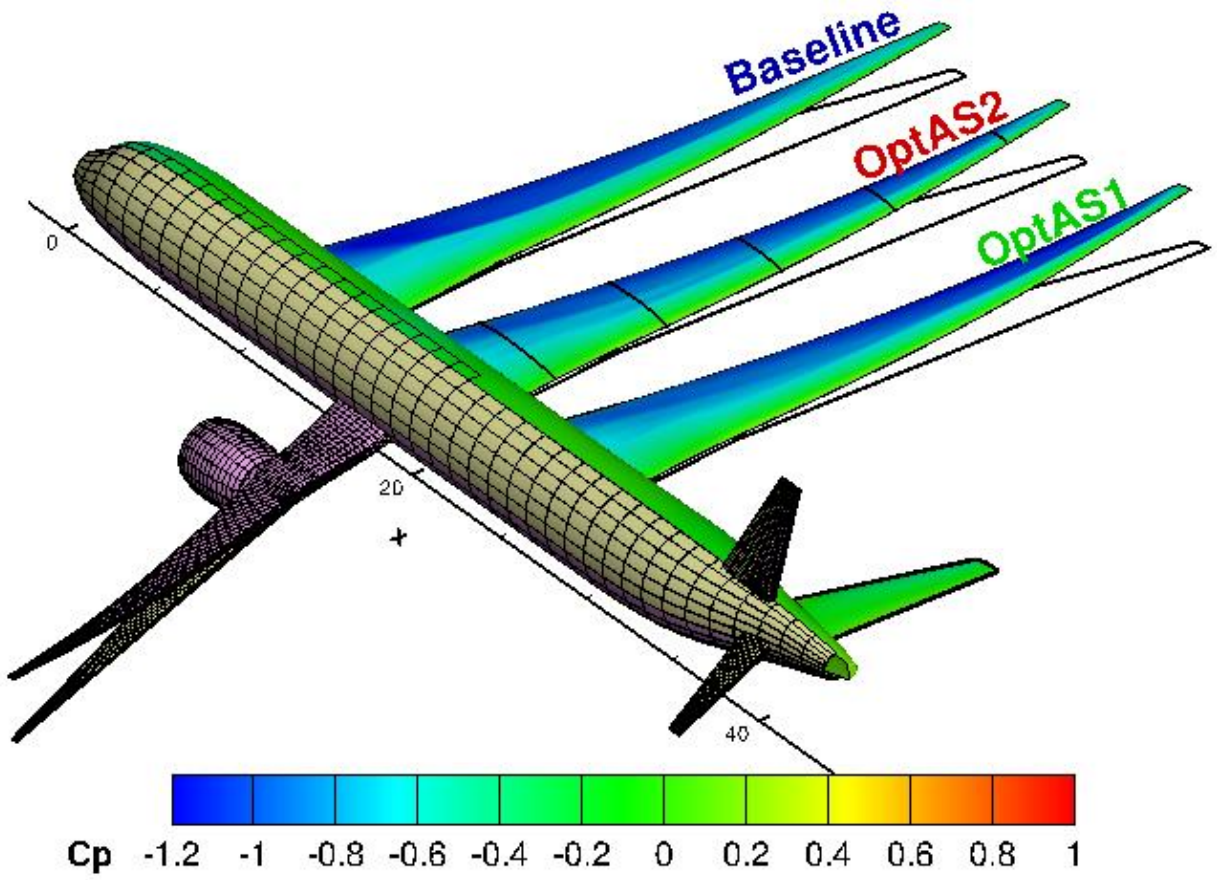

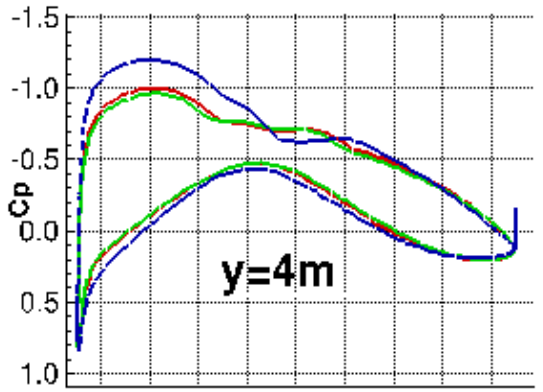

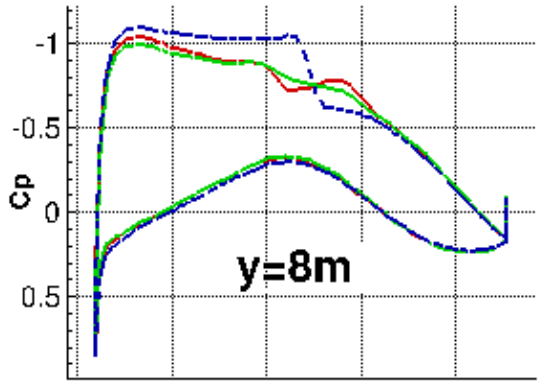

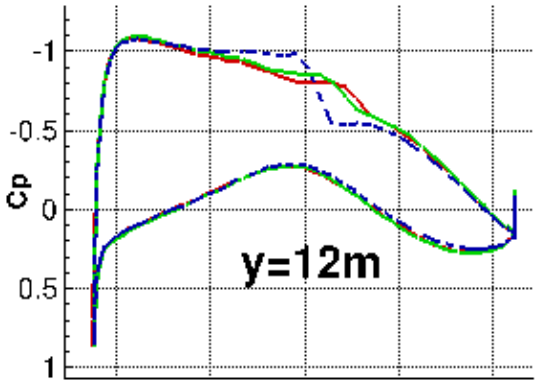

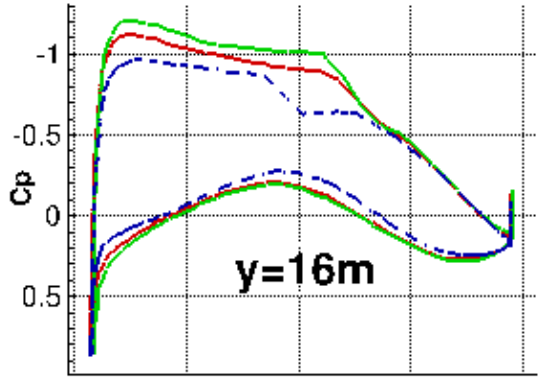

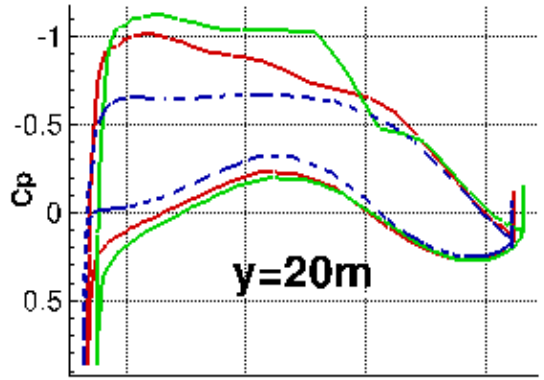

Prof. K.C. Giannakoglou, kgianna@mail.ntua.gr, Dr. V.G. Asouti, vasouti@mail.ntua.gr

Adjoint-based Pareto front

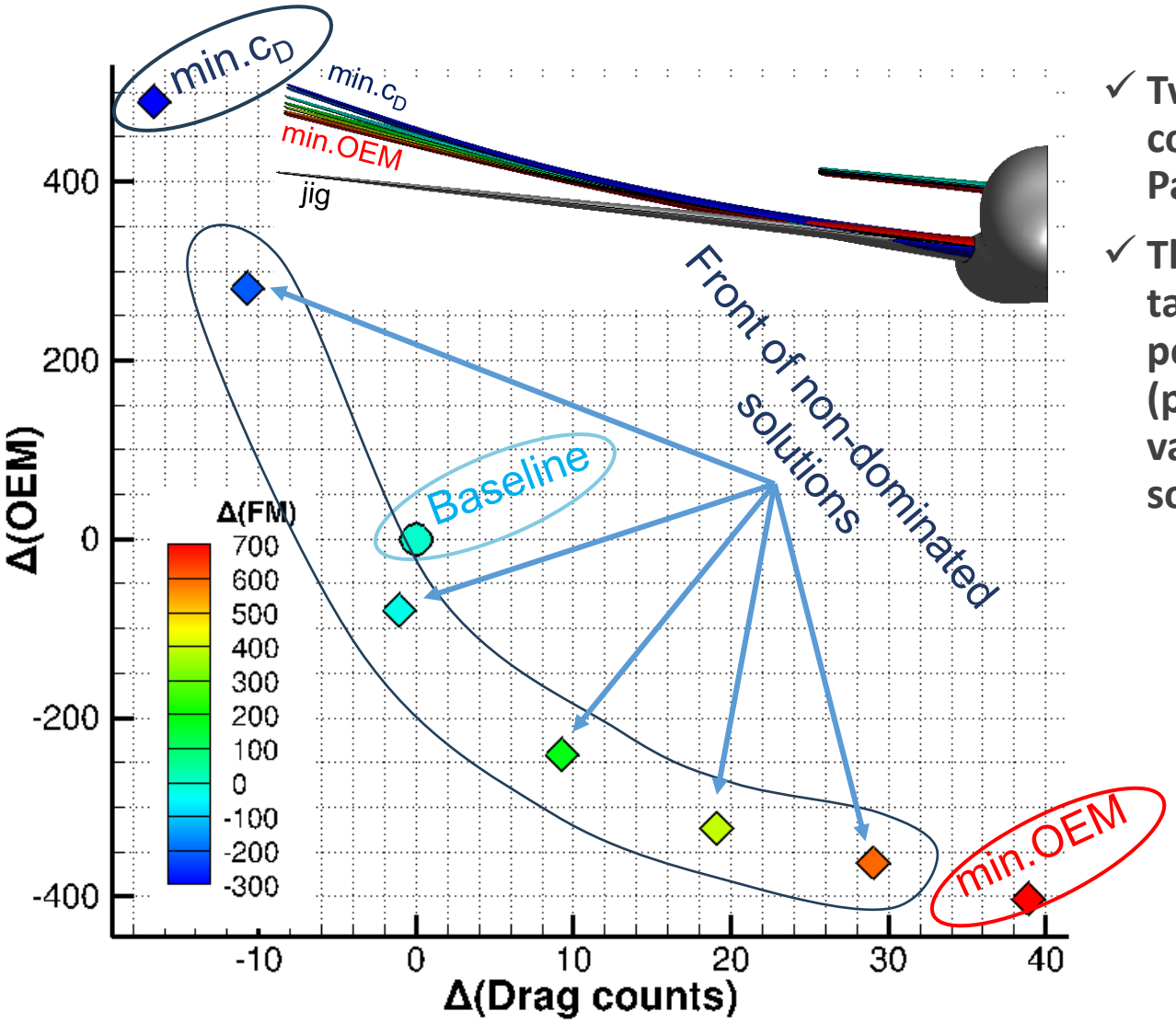

- ✓ Two ShpO minimising C_D & OEM at cruise conditions (same conditions, C_L=0.59) with fixed HTP = 0º, computing the Pareto front edges.
- ✓ Then, starting from the min. OEM solution, optimisation steps targeting different C_D values (sweeping the front!) were performed, resulting to the front of non-dominated solutions (points marked with rhombus) colored based on the fuel burn values evaluated from the Breguet expression. Min. C_D solution has the lowest fuel burn evaluation.

Funded by the European Union
NEXTAIR

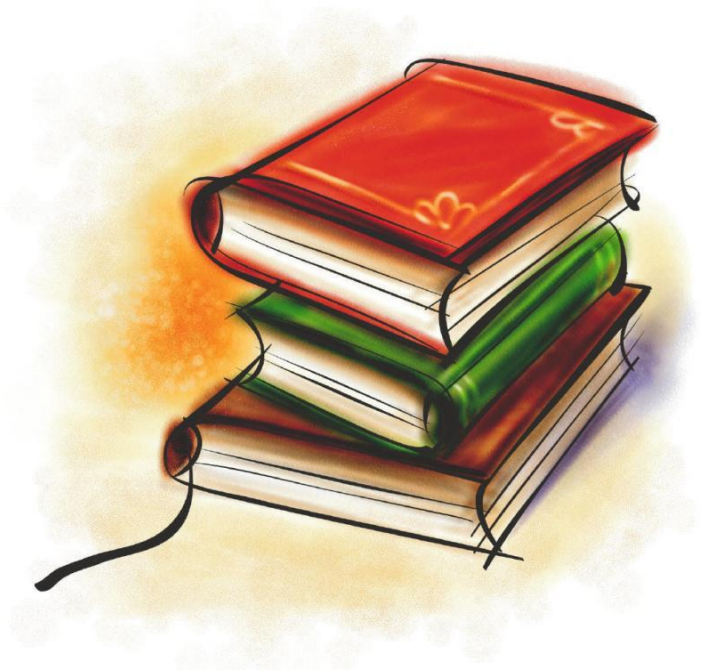

Other MDO problems: CFD - Electrochemistry

Proton Exchange Membrane Fuel Cell (PEMFC)

(some of the) Involved disciplines:

- **CFD (multiphase flow)**
- **Electrochemistry (electrochemical reactions)**
- **Materials science (porous domains with properties such as permeability, diffusivity, and conductivity)**

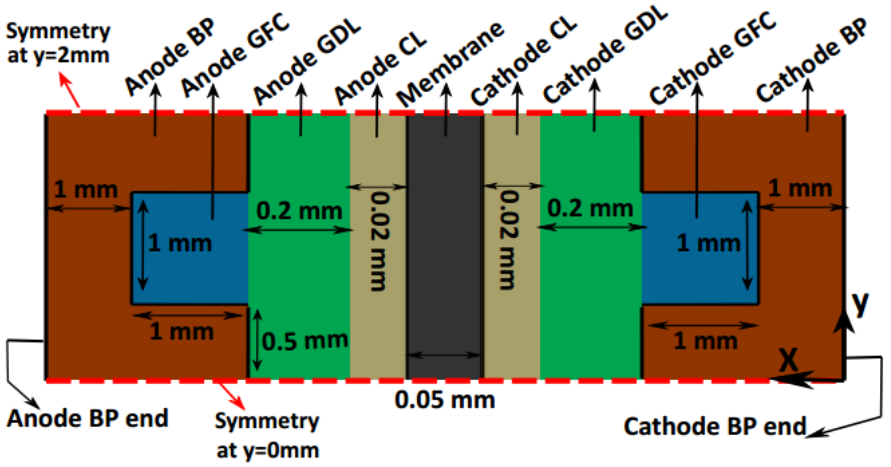

PEMFC components notation:

- **Membrane**
- **Catalyst Layer (CL)**
- **Gas Diffusion Layer (GDL)**
- **Gas Flow Channel (GFC)**
- **Bipolar Plates (BP)**

Proton Exchange Membrane Fuel Cell (PEMFC)

- **Mass and Momentum cons.**

$$\nabla\cdot\left(\frac{\rho_g\vec{U}_g\vec{U}_g}{\varepsilon^2(1-s)^2}\right)=-\nabla p_g+\nabla\cdot\left(\mu_g\nabla(\frac{\vec{U}_g}{\varepsilon(1-s)})\right)+\vec{S}_u,\ \vec{S}_u=-\frac{\mu_g\vec{U}_g}{K}\qquad\nabla\cdot\left(\rho_g\vec{U}_g\right)=S_m,\ S_m=\begin{cases}-S_{vl} & \text{, GDLs and GFCs,}\\ S_{H_2}-S_{vl} & \text{, anode CL,}\\ S_{O_2}+S_{wv} & \text{, cathode CL.}\end{cases}$$

- **Chemical species cons** (solved for H2, water vapor and O2) .

$$\nabla\cdot\left(\rho_g\vec{U}_g y_i\right)-\nabla\cdot\left(\rho_g D_i^{eff}\nabla y_i\right)=S_i,\ S_i=\begin{cases}S_{O_2}=\frac{-j_c}{4F}M_{O_2} & \text{, cathode CL,}\\ S_{H_2}=\frac{-j_a}{2F}M_{H_2} & \text{, anode CL,}\\ S_{wv}=-S_{vl} & \text{, anode CL,}\\ S_{wv}=-S_{vl}+\frac{j_c}{2F}M_{H_2O} & \text{, cathode CL.}\end{cases}$$

- **Liquid water**

$$\nabla\cdot(\rho_l\frac{K_l\mu_g}{K_g\mu_l}\vec{U}_g)-\nabla\cdot(\rho_l\frac{-K_0s^3}{\mu_l}\frac{\partial p_c}{\partial s}\nabla s)=S_{vl}$$

- **Electronic charge** $\nabla\cdot(\sigma_{ele}^{eff}\nabla\phi_{ele})=S_{ele}$

- **Protonic charge** $\nabla\cdot(\sigma_{ion}^{eff}\nabla\phi_{ion})=S_{ion}$

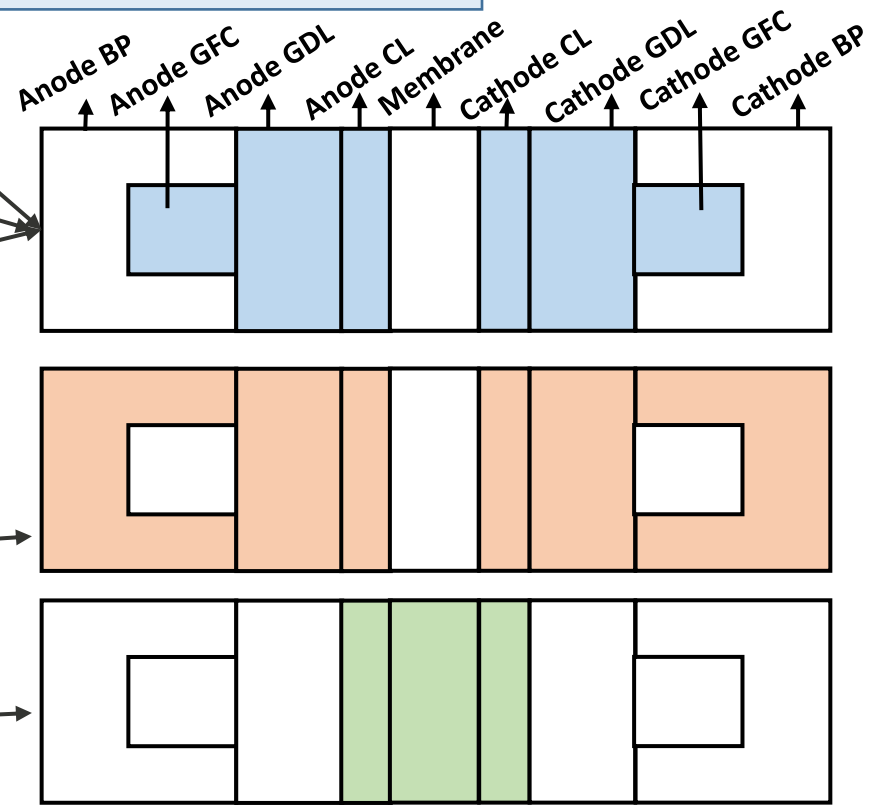

Proton Exchange Membrane Fuel Cell (PEMFC) – Solver

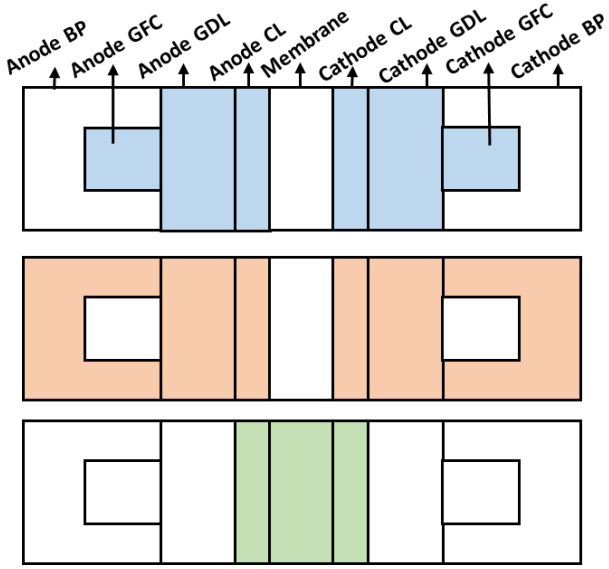

OpenFOAM-based solver, using the finite volume method and the SIMPLE algorithm.
Inner loop is necessary to make the liquid water equation converge.
Data mapping between different domains.

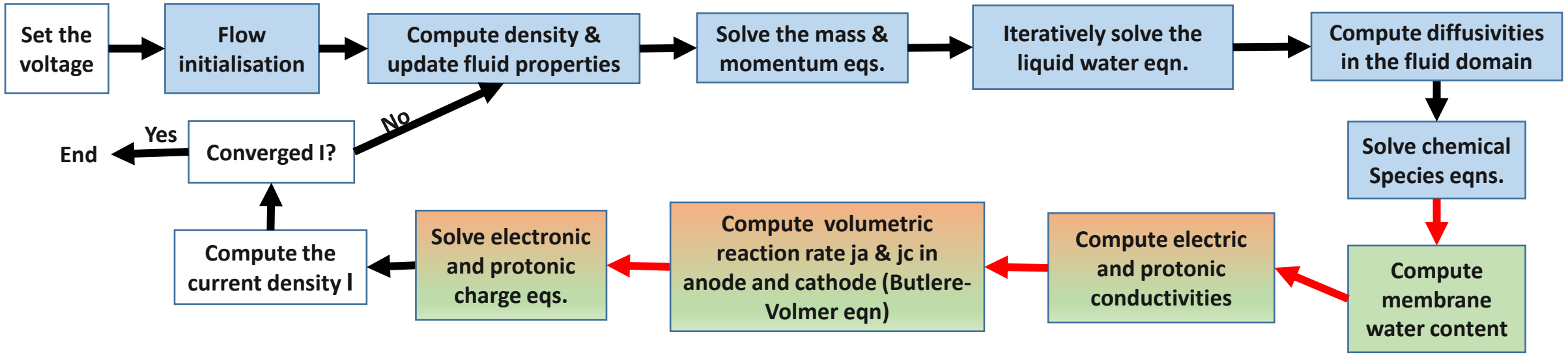

Optimisation of a PEMFC

Define the porosity distribution of the GDL (ε_{GDL}) and CL (ε_{CL}) of both the anode and the cathode for max. current density and min. H_2 consumption at constant voltage (0.6V).

10 design variables: 4 variables per side for the ε_{GDL} and one per side for the ε_{CL}

(μ, λ)= (10, 18) MAEA with PCA

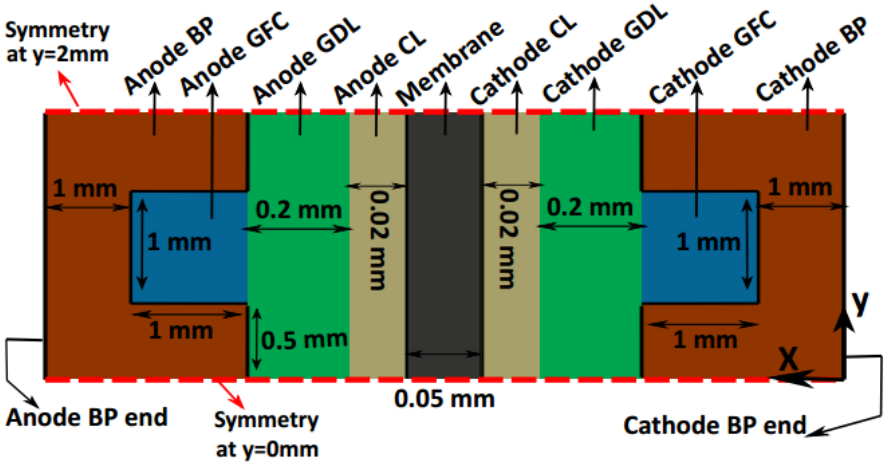

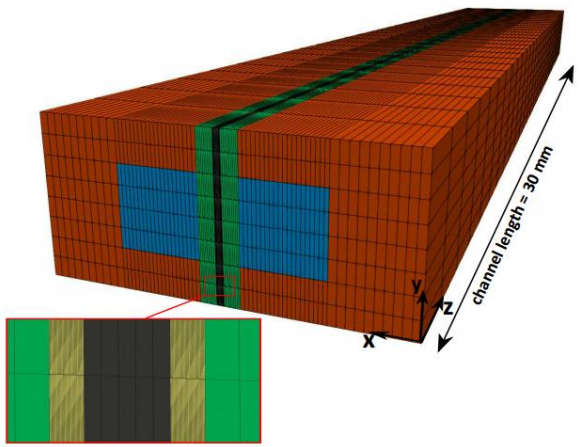

Optimisation of a PEMFC

Porosity distributions

Baseline (ε_{GDL}=0.55, ε_{CL}=0.475)

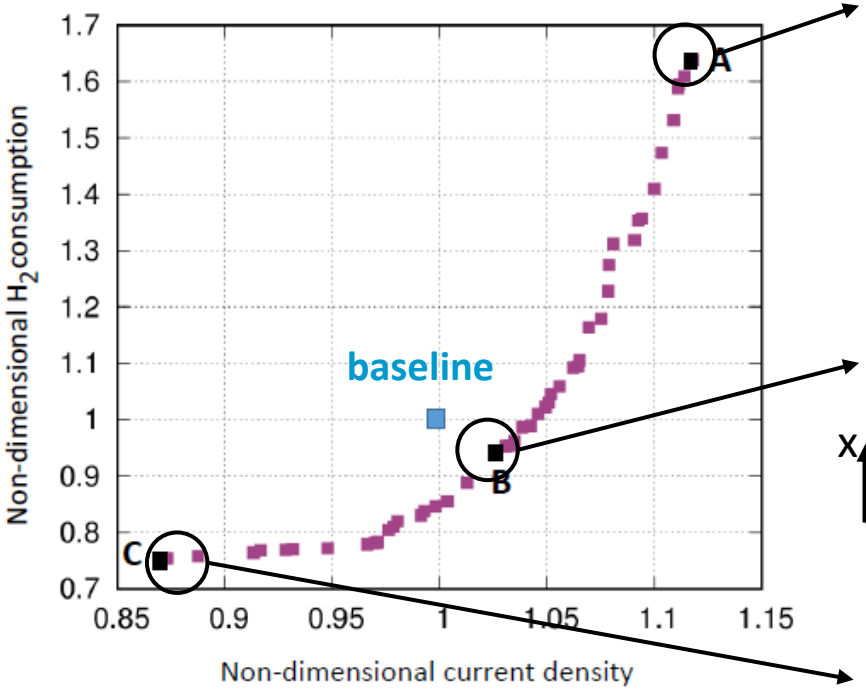

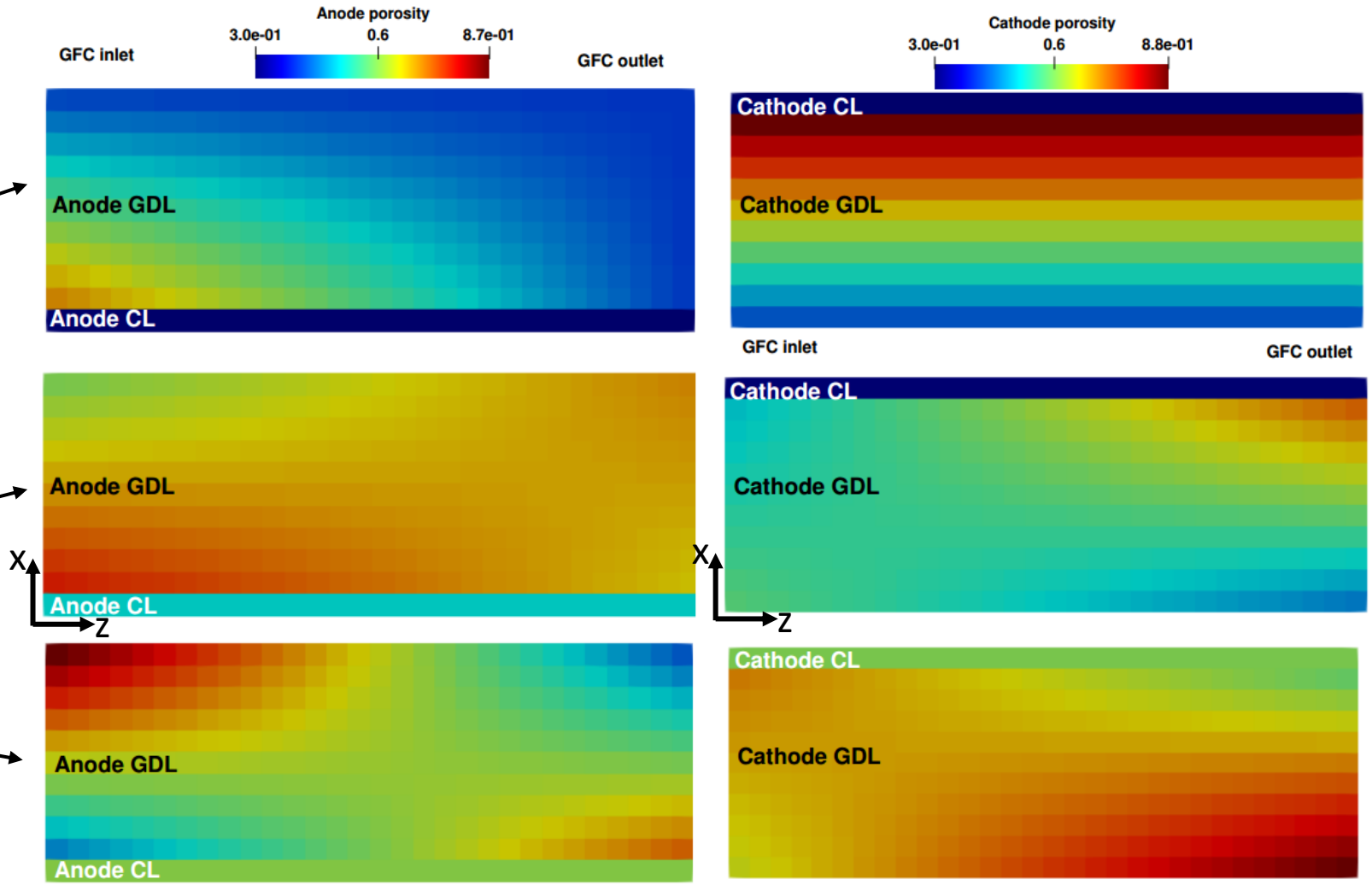

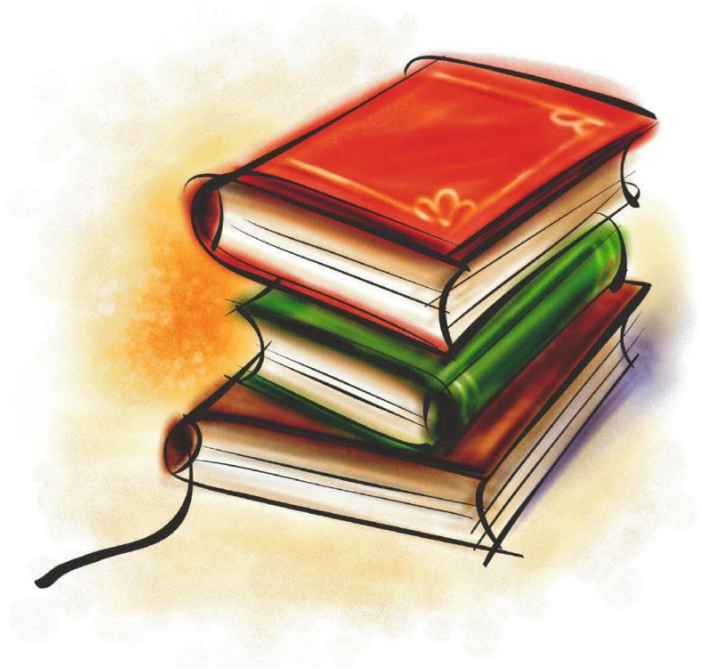

Aerothermal Optimisation

Adjoint-Based Conjugate Heat Transfer Optimisation

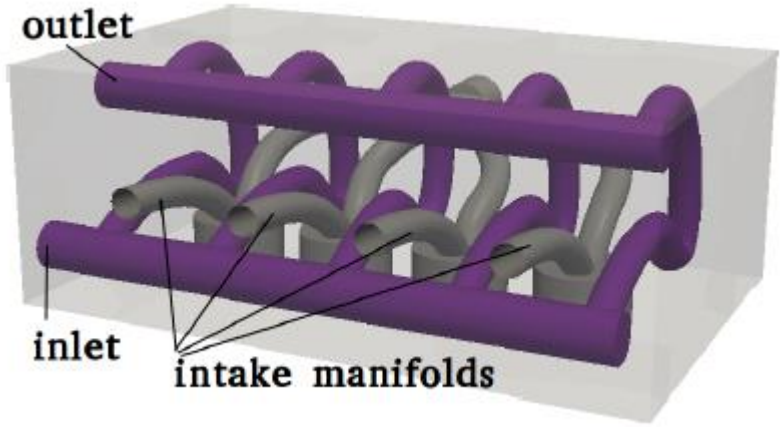

Cooled cylinder-head of a car engine.

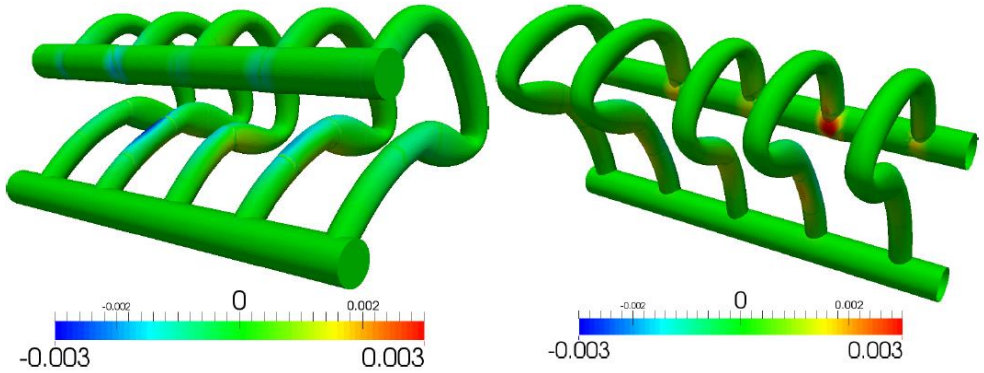

Computed normal displacement of the optimal shape.

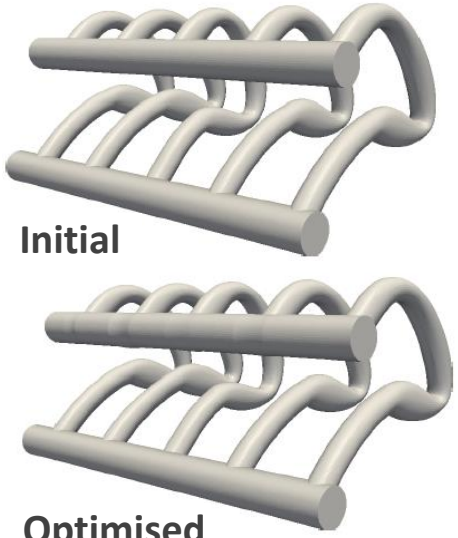

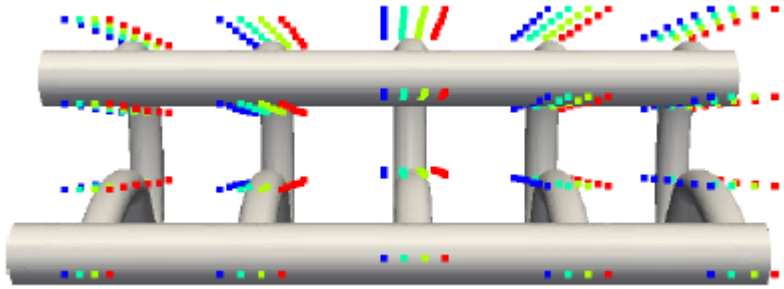

Parametrisation using Volumetric B-Splines

ShpO of the cooling channel (in **purple**) for minimizing both the max. temperature over the solid material block and the total pressure losses within the cooling channel.

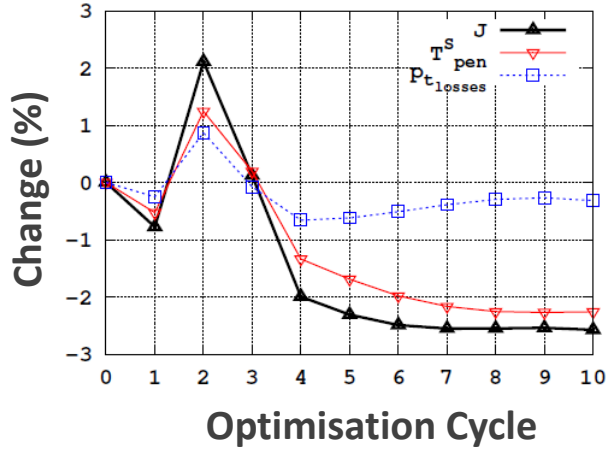

ShpO and TopO of **Conjugate Heat Transfer (CHT)** problems, based on the continuous adjoint method of the PCOpt/NTUA. This requires the development of the adjoint method or s/w for (a) the fluid domain, (b) the solid domain and (c) the **Fluid-Solid-Interface (FSI)**.

Aerothermal ShpO of an Internally Cooled Turbine Blade (1/4)

C3X turbine blade:

- **Parameter by a 7x3 volumetric NURBS control grid**
- **Control points at LE/TE are still**
- **The rest move in the pitch and stream-wise directions**
- **38 DoFs in total; circular cooling holes (fixed R).**

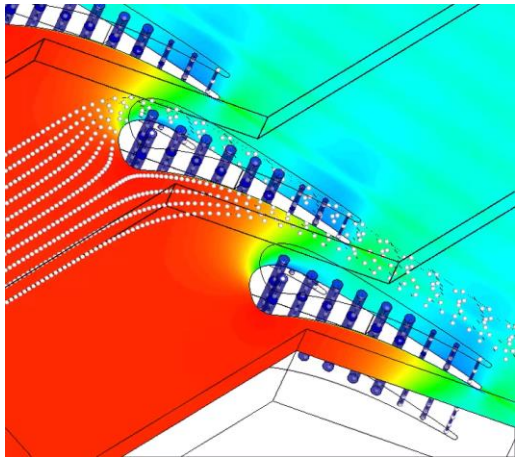

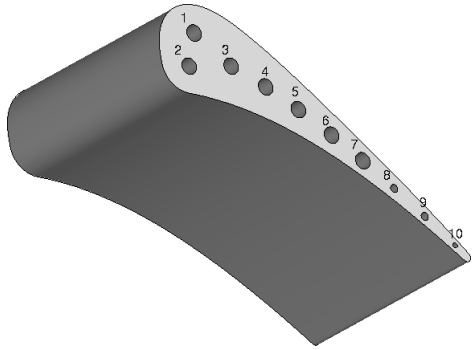

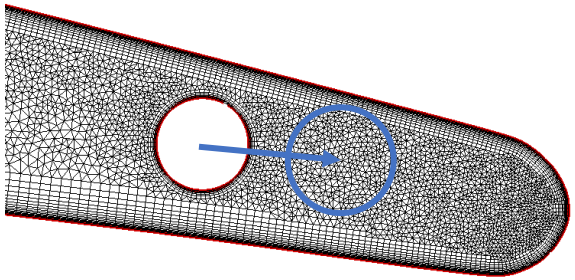

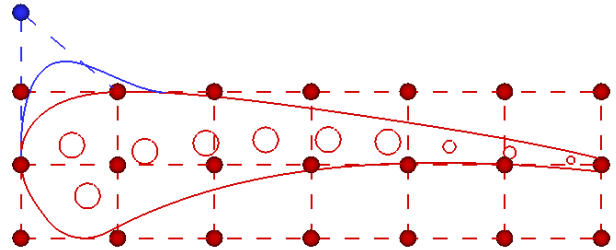

Aerothermal ShpO of an Internally Cooled Turbine Blade (2/4)

Objective functions:
- Total pressure drop
- Inlet capacity
- Flow turn
- Highest temperature

$$F_{aug} = F + \int_{\Omega^F} \Psi_n^{\mathrm{MF}} \mathrm{R}_n^{\mathrm{MF}} d\Omega^F + \int_{\Omega^F} \Psi_n^{\mathrm{TM}} \mathrm{R}_n^{\mathrm{TM}} d\Omega^F + \int_{\Omega^F} \Psi^{\mathrm{D}} \mathrm{R}^{\mathrm{D}} d\Omega^F + \int_{\Omega^S} \mathrm{T}_a \, \mathrm{R}^{\mathrm{S}} \, d\Omega^S$$

Fluid domain

Solid domain

Heat conduction eq.

Primal Fluid-Solid Conditions

$$\mathrm{T}^F = \mathrm{T}^S \;,\; k^F \frac{\partial \mathrm{T}^F}{\partial x_l} \mathrm{n}_l^F = -k^S \frac{\partial \mathrm{T}^S}{\partial x_l} \mathrm{n}_l^S$$

Adjoint Fluid-Solid Conditions

$$\Psi_5^{MF} = \mathrm{T}_a \;,\; k^F \frac{\partial \Psi_5^{MF}}{\partial x_l} \mathrm{n}_l^F = -k^S \frac{\partial \mathrm{T}_a}{\partial x_l} \mathrm{n}_l^S$$

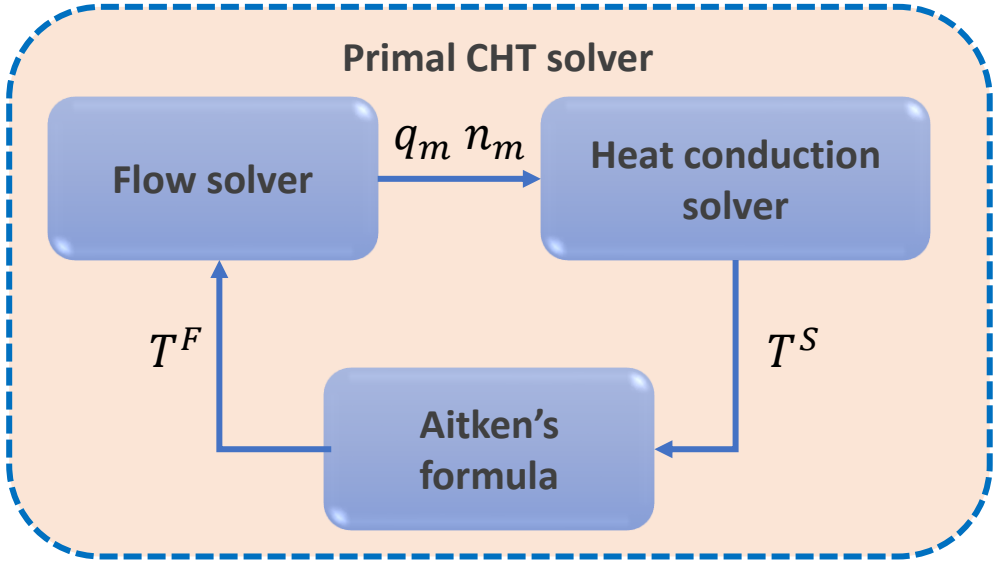

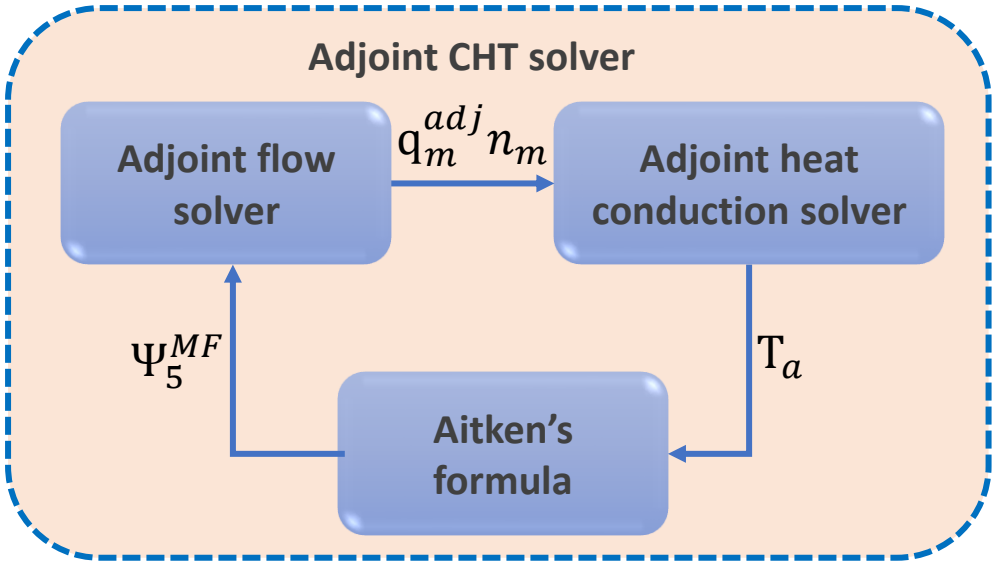

Aerothermal ShpO of an Internally Cooled Turbine Blade (3/4)

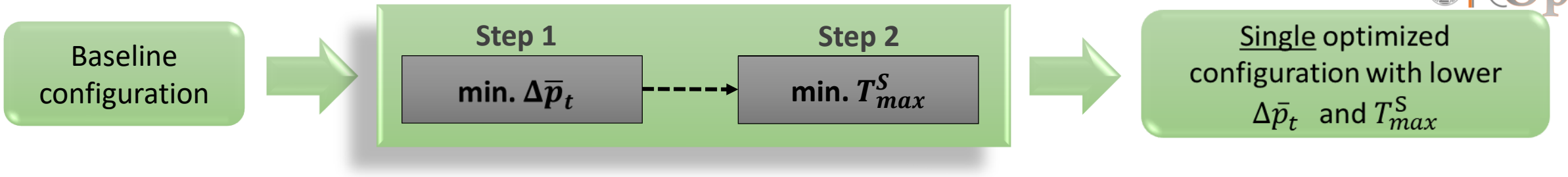

Step 1

- **Objective: Minimize $\Delta\bar{p}_t$.**
- **By changing the blade shape & circles' centers → controlled by the 7x3 morphing box.**
- **Flow constraints: The inlet capacity (φ^I) and hot gas flow turning $(\Delta\bar{\alpha})$ should change no more than ±0.1% from their datum values.**

→ **~21% lower $\Delta\bar{p}_t$**

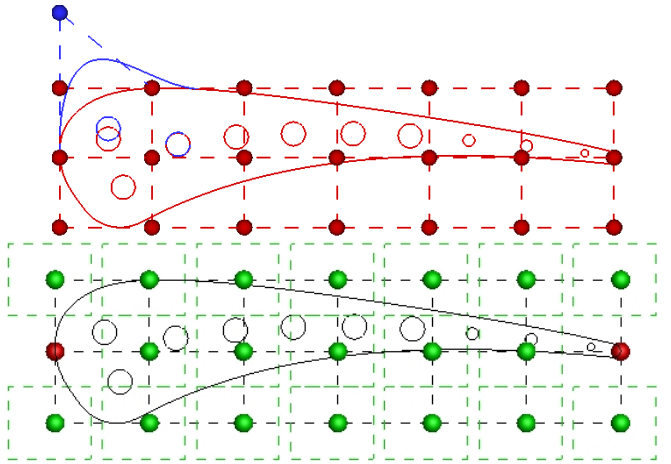

Step 2

- **Objective: Minimize T^S_{max}, with fixed blade shape.**
- **By changing the cooling hole positions → 10+10=20 DoFs.**
- **Geometric constraints: holes should not come closer than 0.3R to the blade contour.**

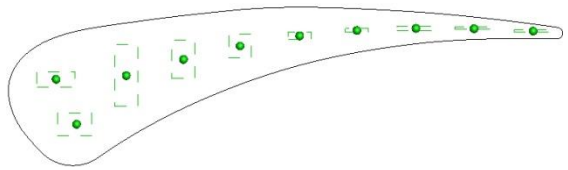

→ **~30K lower T^S_{max}**

Prof. K.C. Giannakoglou, kgianna@mail.ntua.gr, Dr. V.G. Asouti, vasouti@mail.ntua.gr

Aerothermal ShpO of an Internally Cooled Turbine Blade (4/4)

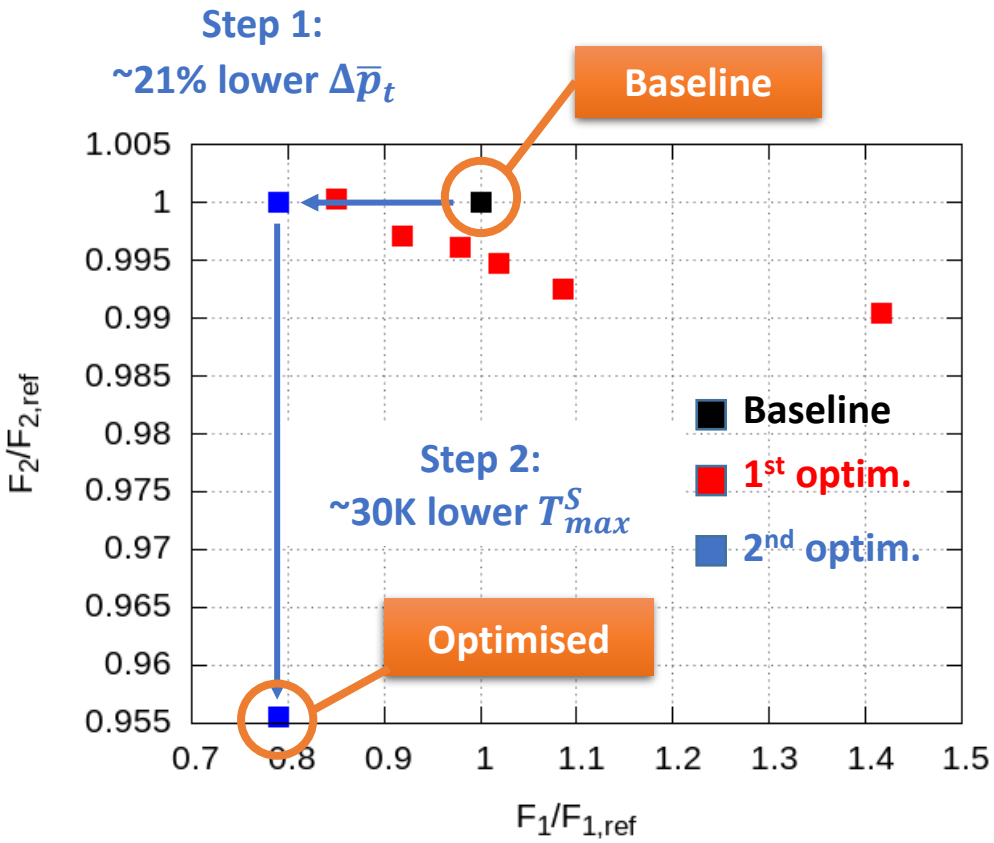

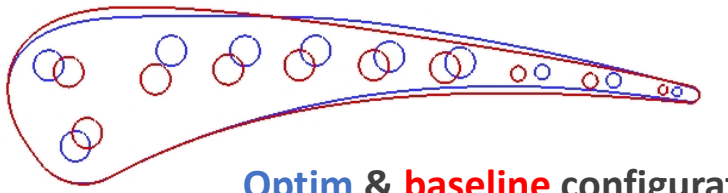

Optim & baseline configurations